MASTERARBEIT | MASTER'S THESIS

Titel | Title

Ecological, anthropogenic, and genomic drivers of population structure in the European spruce bark beetle (Ips typographus)

verfasst von | submitted by

Lisa Weidlich BSc

angestrebter akademischer Grad | in partial fulfilment of the requirements for the degree of

Master of Science (MSc)

Wien | Vienna, 2026

Studienkennzahl lt. Studienblatt | Degree programme code as it appears on the student record sheet:	UA 066 833
Studienrichtung lt. Studienblatt | Degree programme as it appears on the student record sheet:	Masterstudium Ecology and Ecosystems
Betreut von | Supervisor:	Kelly Swarts PhD

Abstract

The European spruce bark beetle (*Ips typographus*) is one of the most damaging forest pests in Central Europe, particularly to Norway spruce (*Picea abies*), a tree of major ecological and economic importance. While the ecological drivers of beetle outbreaks are well studied, the genetic processes shaping population structure, dispersal, and virulence remain less well understood. This thesis applies whole-genome sequencing to more than 700 beetles sampled across four European regions and time points to investigate the species' population structure, demographic patterns, and broader genomic characteristics. Overall genetic differentiation was low, consistent with high dispersal capacity, yet three genetic clusters were consistently observed. Localized genomic divergence, associated with putative structural variants — such as inversions in regions containing olfactory-related genes — may reflect behavioral mechanisms like assortative mating. Across populations, genetic signals suggest recent demographic expansion, with no consistent genomic differences linked to variation in forest management intensity. This study contributes a high-resolution genomic dataset for *I. typographus* and offers a foundation for future research on the behavioral and evolutionary dynamics influencing its outbreaks.

Zusammenfassung

Der Buchdrucker (*Ips typographus*) ist einer der bedeutendsten forstlichen Schädlinge Mitteleuropas und verursacht insbesondere an der ökologisch wie ökonomisch zentralen Gemeinen Fichte (*Picea abies*) erhebliche Schäden. Während ökologische Faktoren von Massenvermehrungen gut untersucht sind, sind die genetischen Prozesse hinter Populationsstruktur, Dispersionsverhalten und Virulenz bislang nur unzureichend charakterisiert. In dieser Studie wurden über 700 Käfer mittels Ganzgenomsequenzierung analysiert. Die Proben stammen aus vier europäischen Regionen und wurden zu unterschiedlichen Zeitpunkten erhoben, um Einblicke in die genetische Struktur, demografische Muster und genomischen Eigenschaften der Art zu gewinnen. Die insgesamt geringe genomische Differenzierung zwischen Populationen entspricht der bereits bekannten hohen Dispersionsfähigkeit von *I. typographus*. Dennoch konnten drei genetische Cluster identifiziert werden, die unabhängig von der geographischen Verteilung der Proben konsistent auftreten. Lokalisierte genomische Divergenzen, assoziiert mit putativen strukturellen Varianten wie Inversionen in olfaktorisch relevanten Genregionen, weisen auf potenzielle verhaltensbasierte Mechanismen wie assortative Paarung hin. Populationsübergreifende demografische Muster sprechen für eine rezente Expansion; ein Zusammenhang zwischen genomischer Variation und forstlicher Bewirtschaftungsintensität konnte nicht festgestellt werden. Diese Studie liefert einen hochauflösenden populationsgenomischen Datensatz für *I. typographus* und schafft eine Grundlage für weiterführende Untersuchungen zu den verhaltens- und evolutionsbiologischen Dynamiken von Massenvermehrungen.

Contents

1 Introduction

Bark beetles (Coleoptera: Curculionoidea: Scolytinae) comprise over 6,000 species. The majority colonize dying or dead trees, playing a crucial role in forest ecosystems where they accelerate decomposition and nutrient cycling, and create structurally diverse habitats that support a high diversity of saproxylic and sun-exposed species (Müller et al., 2008; Six & Wingfield, 2011; Stokland et al., 2012; Weed et al., 2013). While only around 1% of species can attack and subsequently kill their host, they are highly destructive tree pests (Ranger, 2016; Raffa et al., 2015). One such vulnerable host species is the Norway spruce (*Picea abies* [L.] Karst), which is among Europe's most economically important trees and is widely utilized for timber constructions, paper, and furniture (Caudullo et al., 2016). Its native habitat spans from Siberia to Fennoscandia, passing through the Baltic states and extending into the mountainous regions of Central Europe (de Vries et al., 2015; Farjon, 2017), thriving naturally in wet and cool environments (Honkaniemi et al., 2020). The species has experienced significant spread into various regions, including lower altitudes facilitated by human planting efforts, thanks to its valuable timber and ease of management (Johann et al., 2004; Honkaniemi et al., 2020). This expansion has led to the species' habitat extending into marginal and even non-native areas (von Teuffel et al., 2004). However, with climate change exacerbating conditions, particularly in the non-native regions, the trees' shallow root systems make them increasingly vulnerable to heat, drought, and subsequent bark beetle attacks (Pretzsch et al., 2013; Zang et al., 2014; Caudullo et al., 2016). While multiple bark beetle species are capable of infesting *Picea abies*, *Ips typographus* [L.], commonly referred to as European spruce bark beetle, stands out as the most destructive one due to its profound ecological and economic impact (Christiansen & Bakke, 1988; Grégoire & Evans, 2004; Raffa et al., 2015; Caudullo et al., 2016).

1.1 Live history

I. typographus typically begins flying in April, with males initiating flight after three to four consecutive days of warm temperatures. Flight activity requires a minimum temperature of 16.5°C, with optimal conditions between 22 and 26°C (Lobinger et al., 1994 & Wermelinger, 2004). During dispersal, beetles are attracted to potential host trees by tree kairomones — chemical compounds naturally emitted by trees for physiological functions but are exploited by beetles for host location — as well as visual cues. They primarily target *P. abies* but also attack *Larix* spp., *Pinus* spp., *Abies* spp., and *Pseudotsuga menziesii* (EFSA Panel on Plant Health

et al., 2017). This primary phase is followed by secondary attraction (Lehmanski et al., 2023), during which males and females aggregate in response to pheromones, especially 2-methyl-3-buten-2-ol and cis-verbenol, produced by pioneer males that have already located suitable hosts (Schlyter et al., 1987). This secondary phase typically begins within a few hours of the initial attack, facilitating a rapid mass colonization (Schlyter & Löfqvist, 1986).

Males bore through the bark, establishing mating chambers within the phloem after overcoming the tree defense (Sauvard et al., 2004). Up to three females may enter these chambers, each mating with the resident male (Wermelinger, 2004). The females then excavate vertical maternal tunnels for oviposition, typically depositing 80–100 eggs in small niches along both sides of the tunnel. Although only 25 to 60 offspring per female may reach adulthood under adverse conditions, the reproductive potential remains high. After hatching, larvae construct individual pupal tunnels perpendicular to the nuptial chamber, forming the characteristic feather-shaped gallery (Schebeck et al., 2023). In laboratory conditions, development from egg to adult takes 2-4 weeks at temperatures between 20 and 30°C (Wermelinger & Seifert, 2008). Depending on local climate and developmental stage, beetles may either emerge to colonize new hosts or remain to overwinter. Overwintering typically occurs under the bark of the natal tree or in the forest litter (Pettersen & Austara, 1975; Wermelinger, 2004).

1.2 Outbreak dynamics and drivers

Forest ecosystems heavily depend on the crucial services provided by bark beetles, including driving the nutrient cycle, altering stand structure, and facilitating successional processes (Hansen, 2014). Under endemic conditions characterized by low population densities, the beetles tend to favor trees that are physiologically weakened and exhibit compromised chemical defenses, yet still provide a relatively nutrient-rich environment conducive to brood development (Amman, 1972; Boone et al., 2011). However, stressed trees are relatively scarce under normal conditions, which can result in significant beetle mortality during dispersal (Raffa et al., 2016). Populations during these periods are constrained by a range of factors, including tree resistance, forest structure, weather conditions, competition, and natural antagonists (Raffa et al., 2008). During region-wide disturbances or climatic events such as windstorms, droughts, heatwaves, snow and ice damage, ample breeding material becomes available. This influx can initiate epidemic phases marked by notably high beetle densities, potentially persisting for several years (Hlásny et al., 2021). When reproductive rates rise significantly, beetles can exceed crucial thresh-

olds, overwhelming healthy, well-protected trees by aggregating in large numbers, thereby depleting the tree defense (Bakke et al., 1977; Boone et al., 2011; Franceschi et al., 2005). Strong trees not only exhibit superior chemical defenses but also provide a higher nutritional value. Consequently, successfully attacking healthy trees leads to enhanced brood production, facilitating strong positive feedback (Raffa et al., 2016; Boone et al., 2011). During epidemic phases, this intensified activity can damage Norway spruce stands extensively (Andrei & Ifrim, 2021). The equilibrium between suitable brood trees and beetle density is critical in understanding the beetle population's fluctuations, encompassing endemic and epidemic phases (Lehmanski et al., 2023).

Current outbreaks of *I. typographus* closely align with the distribution of *P. abies*, with significant infestations observed in Scandinavia, Eastern Europe, and Western Russia. Sporadic occurrences have been noted at higher elevations in Central Europe, particularly in the Alps and Carpathian Mountains (Soukhovolsky et al., 2022). Climate change is expected to exacerbate extreme weather events, such as storms and heightened snowfall (Stocker et al., 2014), potentially increasing the number of injured or dead trees. Additionally, drought conditions weaken standing trees, making them more susceptible to beetle infestation, thus providing a conducive breeding ground (Reed et al., 2018). This suggests that large, high-impact epidemic events are projected to become even more frequent and intense in the future (Kausrud et al., 2012). The influence of temperature and precipitation fluctuations on outbreak development has been highlighted in numerous studies, affecting both tree physiology and insect biology (Marini et al., 2017; Netherer et al., 2015; Faccoli, 2009). Rising temperature plays a multiscalar role in increasing beetle numbers. At higher temperatures beetle mortality during overwintering is decreased, meaning that more beetles can start a new generation in the following year (Safranyik, 1998; Faccoli, 2002). Earlier warm temperatures at the start of the season, combined with an extended warm period throughout the summer, accelerate beetle swarming and extend the period of activity. This scenario may therefore prompt shifts in their reproductive potential from uni- to bivoltinism or from bi- to trivoltinism, although the development of a third generation remains constrained by photoperiodic regulation during the summer (Faccoli, 2009; Jönsson et al., 2009; Schebeck et al., 2017; Jakoby et al., 2019; Romashkin et al., 2020).

1.3 Tree defense

P. abies mounts an array of defenses, including physical barriers such as thick bark, resin, and increased lignin deposition around the phloem, as well as induced

responses like enhanced resin flow and the synthesis of secondary metabolites such as terpenoids, phenolics, and alkaloids (Franceschi et al., 2005; Krokene, 2015).To overcome this multilayered defense, *I. typographus* relies on a combination of synchronized mass attacks — discussed in the previous paragraph — and microbial partners. Among these partners are fungal associates such as *Grosmannia*, *Ceratocystis*, and *Ophiostoma*, transported externally on the beetles' pronotum and elytra, which degrade host defense compounds and may also release volatiles that, alongside pheromones, could help guide conspecifics to suitable hosts (Lieutier et al., 2009; Wang et al., 2014; Kandasamy et al., 2016; Wadke et al., 2016). Through the interplay of mass attack and microbial activity, beetles undermine both physical and chemical defenses of *P. abies*, increasing colonization success and often leading to host mortality (Furniss et al., 1990; Lieutier et al., 2009).

1.4 Biological antagonists

Biotic antagonists, including protozoa, fungi, mites, and nematodes, play a significant role in pest control (Burjanadze et al., 2008). In addition to these microorganisms, predatory insects such as *Paromalus paralellepipedus* (Herbst), *Plegaderus vulneratus* (Panz.) (Col., Histeridae), and *Thanasimus* spp. (Zett.) (Col., Cleridae), as well as parasitoids like *Rhopalicus tutela* (Walk.), *Dinotiscus eupterus* (Walk.), and *Roptrocerus xylophagorum* (Ratz.) (Hym., Pteromalidae), have been documented for their roles in controlling outbreaks (Hilszczański et al., 2007). Birds, particularly woodpeckers, also contribute to population management. Despite the collective impact of these biotic antagonists, they often struggle to control epidemic outbreaks both effectively and rapidly enough, highlighting the need for further research and improved integrated pest management strategies (Pechacek, 1994).

1.5 Management strategies

Complementing these natural regulatory mechanisms, current anthropogenic management strategies utilize a combination of methods, including conventional chemical insecticides, traps baited with artificial aggregation pheromones, salvage logging, tree removal, and partial or complete debarking of wind-felled trees. Even when deployed at high densities, pheromone traps remove only a small fraction of the beetle population — typically between 3% and 10% — which makes them inadequate for suppressing active outbreaks (Weslien & Lindelöw, 1990; Lobinger & Skatulla, 1996). Moreover, this method can paradoxically attract beetles to areas that would not have been targeted otherwise (Kuhn et al. 2022). Salvage log-

ging and tree removal are employed in commercial forests and protected areas to safeguard timber production when beetle infestations are detected (Lindenmayer et al., 2012; Müller et al., 2019). Nonetheless, these practices are suboptimal as they deplete forest biomass. Debarking wind-felled trees is more effective in reducing beetle populations while preserving forest biomass. However, complete debarking negatively impacts non-target biodiversity, making partial debarking a more balanced approach (Hagge et al., 2019; Zielonka, 2006; Thorn et al., 2018). Trap trees, specifically logged to lure beetles away from the rest of the stand and subsequently remove them from the ecosystem, on the other hand, have proven more effective than pheromone traps (Lubojacky & Holusa, 2014). All these interventions need to be implemented before the beetles take flight to disrupt their reproduction cycle and eliminate the adults from the ecosystem. Recent studies have demonstrated that trained detection dogs and drone technology are promising tools for the early identification of bark beetle infestations. Detection dogs, in particular, have been shown to outperform human experts by locating recently attacked trees (Kautz et al., 2024; Vošvrdová et al., 2023). Nevertheless, manually managing outbreaks remains challenging, particularly in remote or rugged landscapes where the use of heavy machinery is impractical. Additionally, intensive management efforts can inadvertently harm natural antagonists and predators that play a crucial role in beetle population regulation. Disrupting these biocontrol agents may have unintended consequences, potentially exacerbating outbreaks rather than mitigating them (Weslien & Schroeder, 1999). A more sustainable approach involves shifting forest management practices away from monocultures of *P. abies*, which are particularly vulnerable to infestation, toward more diverse and resilient forest compositions. While these strategies are critical for mitigating beetle outbreaks, effective long-term management also requires a deeper understanding of the factors that drive population dynamics — including genetic mechanisms influencing dispersal, adaptation, and outbreak resilience.

1.6 Genetic research foundations and thesis objectives

Genetic research on *I. typographus* populations is crucial for addressing outbreak challenges and improving management strategies. By uncovering patterns in population size, genetic diversity, and demographic trends, such studies help predict outbreaks, trace infestation sources, and clarify ecological drivers of population fluctuations. Genetic insights also reveal dispersal patterns essential for designing interventions, such as buffer zones or targeted controls (Rollins et al., 2006; Porretta et al., 2007). Additionally, understanding genetic variation aids in identifying traits

linked to local adaptations and resilience, such as resistance to stressors and survival characteristics (Yu et al., 2013). This knowledge is increasingly valuable as climate changes impact forest ecosystems and pest behavior.

Historically, *I. typographus* genetics have been studied using limited representation markers, such as microsatellites and mitochondrial markers, to analyze population structure and diversity. Microsatellites proved useful for fine-scale structure (Sallé et al., 2007; Gugerli et al., 2008; Montano et al., 2016; Némethy et al., 2018), while mitochondrial markers revealed broader geographic patterns, including a division of European populations into northern and southern subpopulations, as well as a founder effect in Scandinavian regions (Mayer et al., 2015; Sallé et al., 2007). However, these methods lack the resolution needed to fully characterize genetic structure and adaptive variation, particularly as microsatellites cover limited genome regions and mitochondrial DNA reflects maternal inheritance alone.

A major advancement came with the publication of the *I. typographus* reference genome by Powell et al. (2021), organized into 272 contigs. This enabled more comprehensive whole-genome studies, including genome-wide markers used in RADseq and GBS approaches by Ellerstrand et al. (2022) and Müller et al. (2022), respectively. These studies revealed high genetic diversity and connectivity, but reduced-representation methods may have overlooked finer genetic structures due to incomplete genome coverage (Andrews et al., 2016; Elshire et al., 2011). More recently, Mykhailenko et al. (2024) conducted the first large-scale whole-genome sequencing study on *I. typographus*, highlighting the potential of high-resolution genomic approaches for understanding genetic differentiation and adaptation in forest pest species.

Building on these advancements, this thesis employs a Tn5-based whole-genome sequencing approach to generate high-resolution genomic data, enabling the detection of genetic variation, demographic processes, and structural variants such as inversions (Sanchis-Juan et al., 2018). This approach provides a more detailed view of population structure and adaptation compared to previous marker-based studies.

To build on these advancements, this thesis investigates the following research questions: (1) *How does genomic structure vary across space and time in* v *populations?* (2) *How do dispersal, demographic history, ecological factors, and forest management drive regional variation in I. typographus genetic diversity and outbreak dynamics?* (3) *How do structural genetic variants contribute to genetic differentiation within and between populations?*

2 Methods

2.1 Sampling design

2.1.1 Sampling regions

To capture multiple populations across Europe effectively, we implemented a comprehensive sampling design spanning four distinct regions, chosen to represent varying geographic scales and distances. The study utilized multiple transects within each location to ensure broad coverage while maintaining the feasibility of frequent monitoring (Figure 1). The sampling areas included 10 plots in Berchtesgaden National Park (BNP; Germany), 3 plots in Forchtenstein BOKU Lehrforst (FOR; Austria), 4 plots in Kalkalpen National Park (KAL; Austria), and 5 plots in Sumava National Park (SUM; Czech Republic), comprising elevations ranging from 706.98 to 1316.46 m. In BNP, two distinct locations, Watzmann and Klausbachtal, separated by an 8 km valley, were monitored to observe spatial variations within the park (Figure 1).

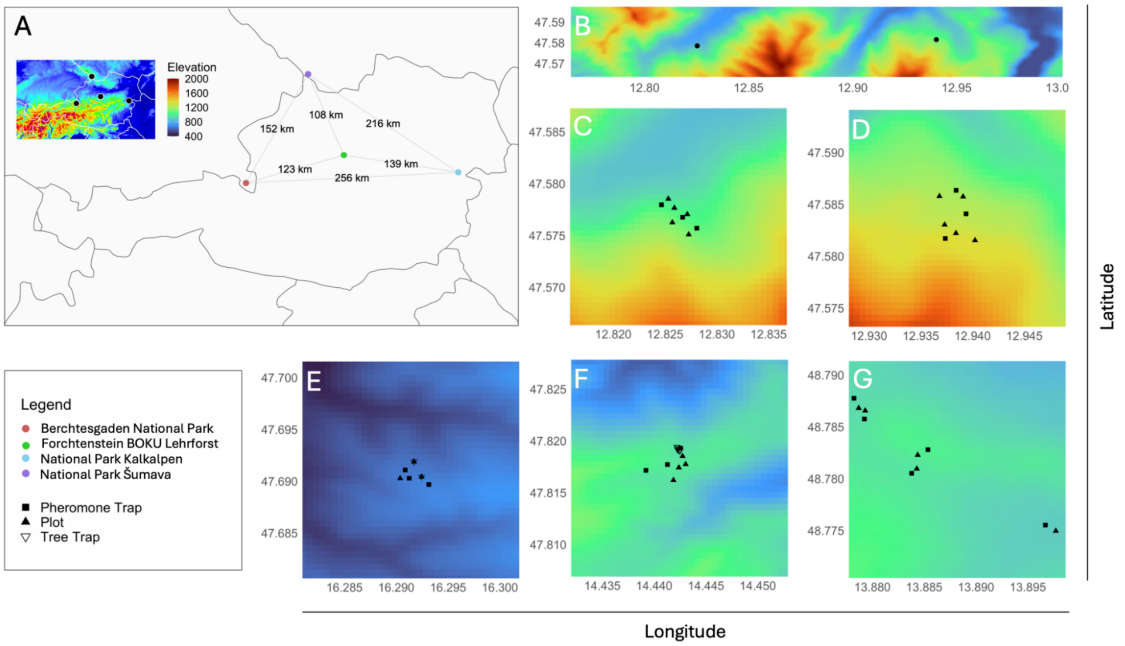

Figure 1: Overview of sampling design across Central Europe. Sampling was conducted in four Central European regions to capture both geographic distance and ecological variation in *Ips typographus* populations (A; inset shows topographic relief). Within Berchtesgaden National Park (Germany, B), two areas separated by a mountain ridge and valley — Klausbachtal (C) and Watzmann (D) — were monitored. Additional sites included Forchtenstein (Austria, E), Kalkalpen (Austria, F), and two clusters in Šumava (Czechia, G), enabling fine- and broad-scale comparisons across regions differing in elevation, forest management, and climate.

2.1.2 Plot design

To facilitate effective data collection, each plot was centered at a permanently marked point georeferenced with sub-meter accuracy. The plots were circular, up to 26 m, with diameters varying based on the number of trees in proximity to the center, accommodating up to 79 trees (Figure 2). Each tree within the plot was relatively mapped using a hypsometer from the centerpoint, and the diameter at breast height (DBH), tree height and canopy height were recorded for every individual. The plots were situated within *P. abies* stands, with only a few *Larix* individuals included. For monitoring purposes, all trees within these plots were tagged with aluminum tags to ensure accurate identification.

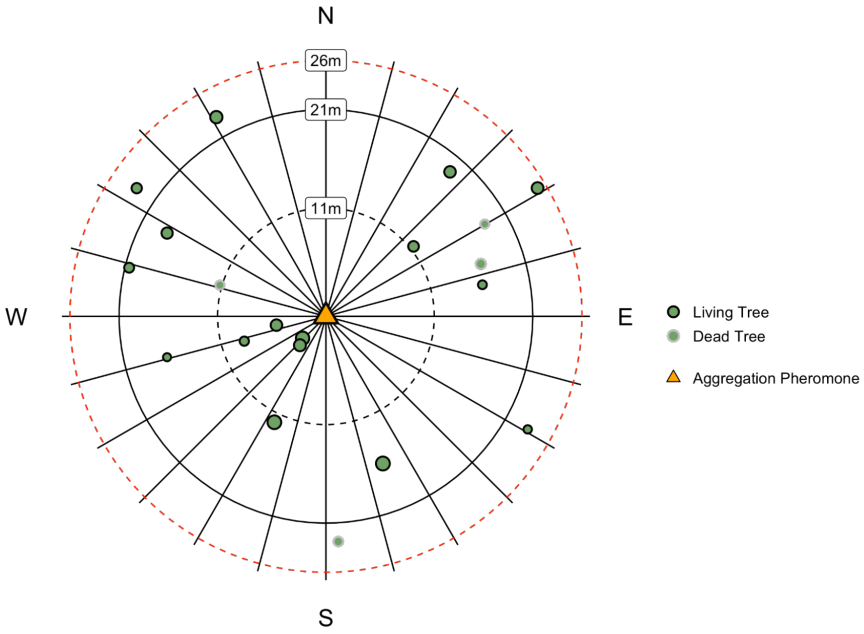

Figure 2: Example plot design. Trees within each circular plot were mapped by distance and orientation, distinguishing living and dead individuals. A subset of four plots in BNP was additionally baited with artificial aggregation pheromones, increasing the likelihood of infestation and enabling contrasts between baited and unbaited conditions.

2.1.3 Trap setup and sampling strategy

In 2020, plots were established within an active outbreak area in BNP that had been identified in the previous year by the Berchtesgaden National Park, and 80 tree traps were installed directly on the trunks of eight trees per plot. Additionally, six traps baited with artificial aggregation pheromone (Pheroprax®) were installed along transects between the established plots. In 2021, monitoring and trapping efforts were expanded to include not only BNP but also the FOR, KAL, and SUM regions. The use of pheromone traps increased to 17 across all four regions, with

six in BNP, three in FOR, three in KAL, and five in SUM. To account for the differences in the number of traps across regions, the total number of beetles collected by pheromone traps in each region was divided by the number of traps. This normalization allowed for a more accurate comparison of beetle activity between regions.

To further intensify sampling, Pheroprax® vials were also hung freely in the centers of plots 26, 28, 31, and 33 in BNP, each shielded from rain by a plastic cap, to artificially initiate beetle attacks. Additionally, nine trees were cut down in KAL on a clearing near the established plots to stimulate the production of natural kairomones, mimicking the condition of weakened trees and attracting beetles during the dying process. In FOR, two established trees were felled for the same purpose, one in plot 70 (18) and one in plot 71 (21). To prevent beetles from reproducing successfully in the trap trees, all felled trees were removed after four to five weeks. Additionally, naturally infested trees were sampled to monitor *I. typographus* populations. Figure 3 illustrates these different collection methods.

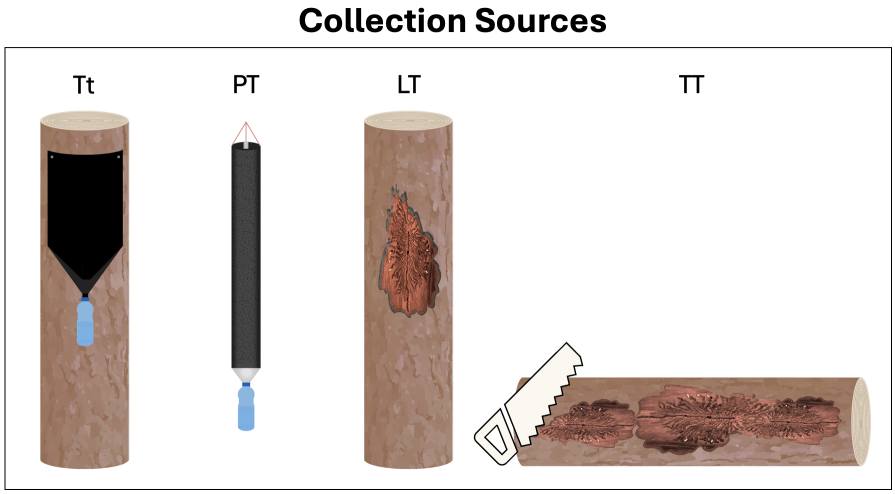

Figure 3: Collection sources. Beetles were collected from four sources: tree traps (Tt), pheromone traps (PT), naturally infested living trees (LT), and felled trap trees (TT). Using these complementary sources captured both naturally colonizing beetles and those attracted by artificial baits, enabling contrasts between natural infestation dynamics and experimentally induced conditions.

2.1.4 Monitoring

During each monitoring trip, beetles were hand-sampled from trap trees and galleries within living trees in the established plots and stored in Eppendorf tubes with 96% technical ethanol for preservation. Beetles captured in pheromone traps, which were pre-filled with the same ethanol and left outside for about two weeks, were also collected and preserved similarly. Ethanol in the pheromone traps was

replaced as soon as possible during monitoring trips to maintain preservation quality. In the lab, ethanol was replaced once, approximately two weeks after collection, to increase alcohol concentration and decrease water content for improved long-term storage. All samples were subsequently stored at -20°C until further analysis.

In 2020, monitoring at BNP was conducted bi-weekly from June 25 to August 27. In 2021, monitoring was extended to all four regions, with visits approximately every two weeks from May 4 to September 24, although logistical constraints sometimes prevented a perfect two-week interval in all locations (Figure 5, top row). Nevertheless, this detailed and structured approach allowed for thorough data collection and analysis across the diverse European landscapes. It enables multiple contrasts to be drawn: larger spatial scales between locations (BNP, FOR, KAL, SUM), smaller spatial scales across and within plots in these regions, temporal scale differences spanning two years and various points across one season, and variations in the sources from which beetles were collected (living infested trees, pheromone traps, trap trees and tree traps). These contrasts are important to highlight as they provide insights into the spatial and temporal dynamics of beetle populations, allowing for a better understanding of how beetle behavior and infestation patterns vary across different environments and conditions.

2.1.5 Quantification of beetles

Beetles extracted from trees were counted manually. In contrast, manual counting of beetles from pheromone traps was impractical for all samples due to the large number of individuals collected. To establish a reliable estimation method, five trap samples representing a broad range of beetle densities were selected. For each, the sample volume was recorded and the beetles manually counted. These volume-count pairs were used to fit a linear regression model, which showed that 99.6% of the variance in beetle counts could be explained by sample volume. The resulting model

$$y = 21.551x - 17.849, \quad R^2 = 0.996 \tag{1}$$

was subsequently used to estimate beetle abundance in the remaining trap samples based on their measured volumes, providing an efficient and accurate quantification approach.

2.2 Sample selection

Initially, a test dataset of 90 beetles was selected to assess the required sample size per source for comprehensive analysis in the full study. This dataset included 30 beetles originating from pheromone traps in BNP, FOR, and SUM in 2021. These samples underwent preliminary quality controls, including assessments of site and taxa coverage, depth, heterozygosity, and minor allele frequency, along with multi-dimensional scaling (MDS).

To determine the optimal number of beetles for sequencing, a bootstrapping analysis was conducted using pilot data in R version 4.0.2 to examine the relationship between sample size and the number of segregating sites (Figure 4). The results indicated that although 30 beetles did not capture the full diversity and no clear plateau was observed, the rate of increase in segregating sites began to slow. Therefore, a decision had to be made based on the trade-off between SNP gain, sample availability, and sequencing effort, and ∼30 beetles per source were considered a reasonable compromise. Additional samples were included based on this threshold to further improve the comprehensiveness of the analysis.

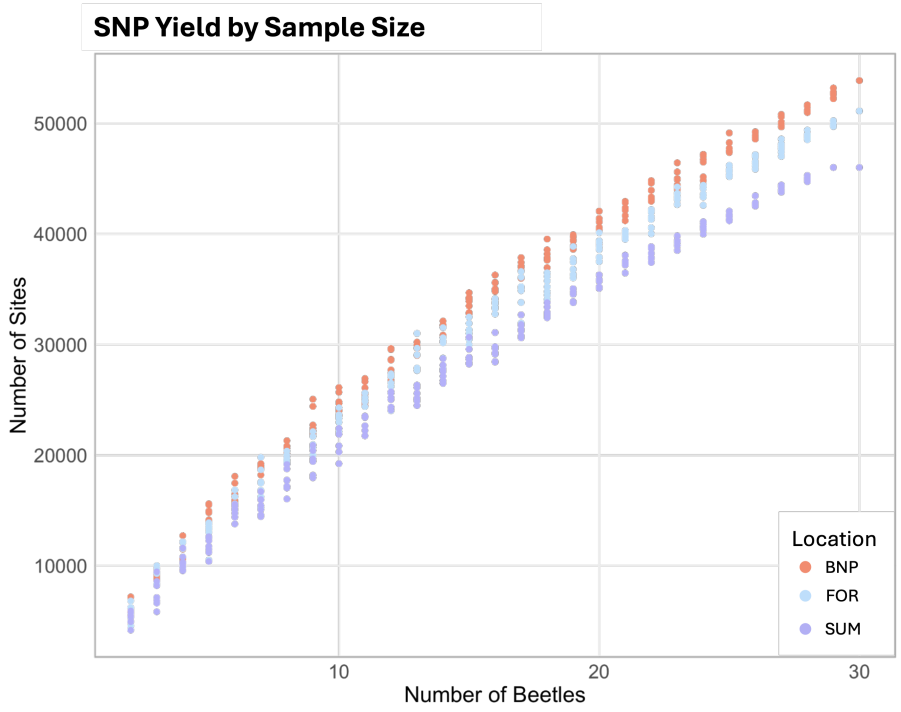

Figure 4: Bootstrapping-based assessment of sample size requirements. Pilot data from pheromone traps in BNP, FOR, and SUM showed that the number of segregating sites increased with additional individuals. Even though a clear plateau was not reached, a decision had to be made based on the trade-off between SNP gain, sample availability, and sequencing effort, with 30 individuals per source considered a reasonable compromise.

As shown in Figure 5F, 706 beetles were selected for the final sequencing set, distributed across the four sampled regions as follows: BNP (250), FOR (133), KAL (112), and SUM (200). Samples were drawn from pheromone traps (PT; 307), living trees (LT; 290), and trap trees (TT; 109). As indicated in Figure 5A–D, 27 beetles collected at BNP in 2020 originated from the second flight peak in August, as sampling began after the first flight peak that year. The remaining beetles were collected during the early and late 2021 flight peaks across all locations in May and August. To enhance analytical power for potential future host–beetle association analyses, all beetles collected from five selected trees were included (12–23 beetles per tree). These data were generated to support downstream studies and are not analyzed further in this thesis.

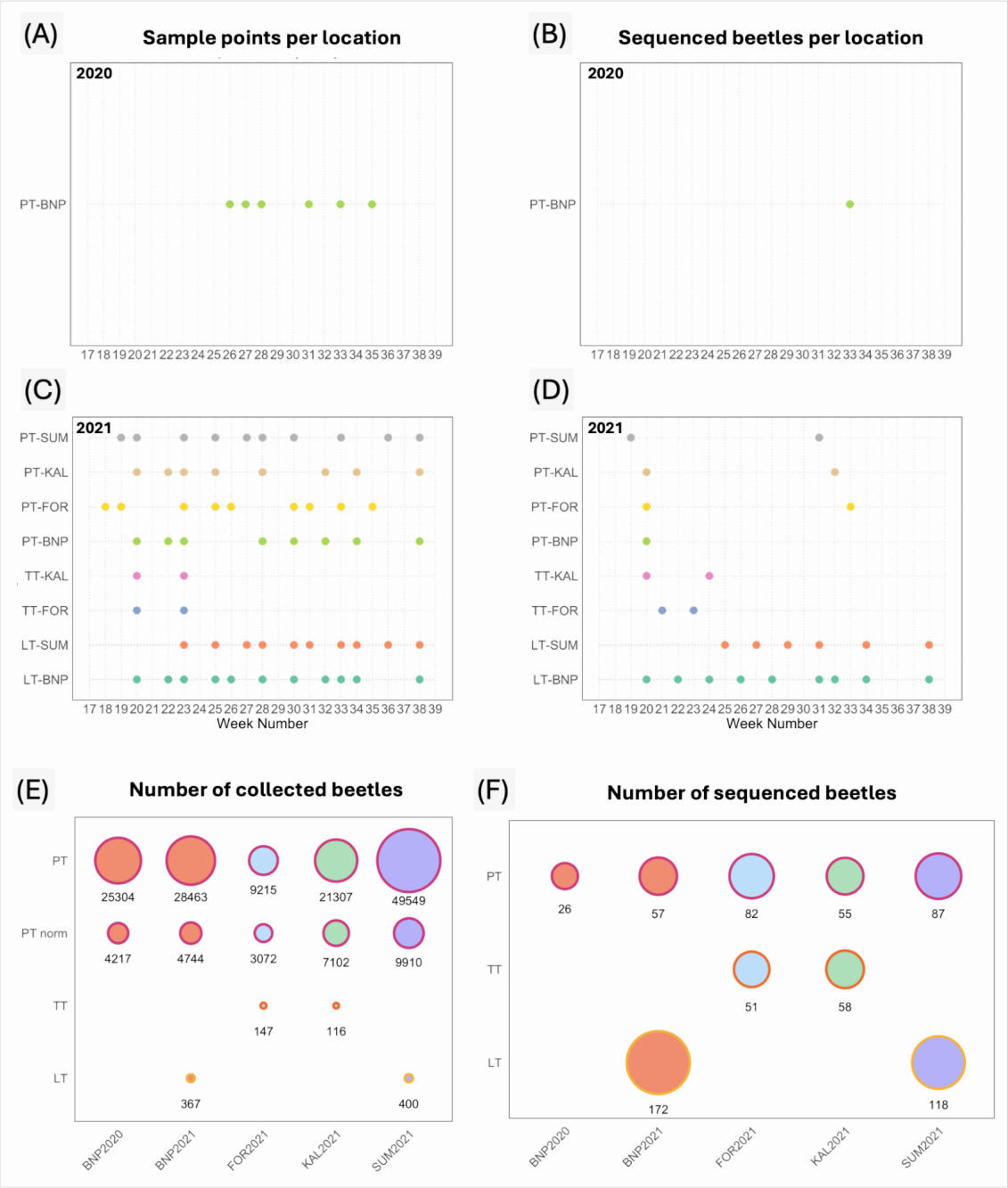

Figure 5: Sampling effort and final sequencing dataset. Plots A and C mark the weeks in which beetles were collected in 2020 and 2021 (by region–source); plots B and D show the corresponding weeks represented in the sequenced subset. Plot E summarizes totals collected per region and source, with PT norm indicating pheromone-trap counts normalized by the number of traps. Plot F shows the final sequencing set (n = 706) across pheromone traps (PT), trap trees (TT), and living trees (LT). This staged sampling across weeks, regions, and sources captures both flight peaks and enables temporal and source-based contrasts for the population-genetic analyses.

2.3 DNA extraction and library preparation

DNA extraction was conducted using an adapted protocol from Schäffer et al. (2010), with further optimizations based on multiple trials. A total of nine plates were processed: one in August 2021 and eight in October/November 2022. Samples were randomized with respect to time, space, and source, and distributed into Qiagen 96-well plates. Ethanol evaporated under a fume hood before the samples were lyophilized for approximately 12 hours. The samples were then ground twice using two 4 mm metal beads for 30 seconds at 30 Hz each, resulting in the beetles being largely pulverized.

The CTAB lysis buffer was prepared by combining 50 ml of 1M Tris-HCl (pH 8), 25 ml of 0.5M EDTA, 150 ml of 5M NaCl, 15 g of 3% CTAB, and ddH_2O to a total volume of 500 ml, followed by autoclaving for 15 minutes. RNAse solution was prepared by dissolving 100 mg of RNAse A powder (Sigma-Aldrich) in 1 ml of 1X TE buffer. For each 96-sample plate, 60 ml of premixed CTAB lysis buffer was prepared, along with 0.36 ml of RNAse, 0.06 ml of Proteinase K (Promega), and 0.60 ml of β-Mercaptoethanol (at 4°C).

In the extraction process, 500 µl of CTAB lysis buffer (RT) was added to each sample in order to break down cell membranes and release nucleic acids. The samples were shaken individually to ensure thorough mixing and incubated statically at 55°C for 15–24 hours for lysis. After incubation, samples were cooled to room temperature, followed by the addition of 500 µl of chloroform-isoamyl alcohol (RT), which facilitated phase separation by removing proteins and other contaminants. Samples were shaken thoroughly and then centrifuged at 4000 rpm for 1 hour at room temperature. The aqueous phase, which contains the purified nucleic acids, was carefully decanted and transferred to new tubes. DNA precipitation was initiated by adding 500 µl of cold (-20°C) isopropanol. The samples were stored at -20°C for 2–24 hours to enhance precipitation, followed by centrifugation at 4000 rpm for 1 hour at 4°C to collect the DNA pellet. The DNA pellet was washed separately to remove residual salts, proteins, and organic contaminants with 1 ml of 80% ethanol and 1 ml of 100% ethanol, both at -20°C, with each wash followed by centrifugation at 4000 rpm for 15 minutes at 4°C. The plates were dried overnight in a fume hood, and DNA was resuspended in 55 µl of ddH_2O overnight at 4°C, before performing a quality check on random samples. This included measuring DNA concentration using a Qubit™ dsDNA Quantification Assay Kit, and assessing quality with gel electrophoresis and a fragment analyzer. For storage, DNA samples intended for immediate use were kept at 4°C, while others were stored at -20°C until further analysis.

For DNA library preparation, a Tn5-based strategy was selected due to its high efficiency, minimal DNA input requirements, and suitability for whole-genome sequencing applications (Baym et al., 2015). The Tn5 transposase was obtained from Molecular Biology Service (MBS), and transposome assembly was carried out using oligonucleotides from Sigma-Aldrich. The assembly involved two separate reactions. In the first reaction, 3.5 µl of Oligo A (5′-TCGTCGGCAGCGTCAGATGTGTATAAGAGACAG-3) and 3.5 µl of Oligo Rev ([phos]CTGTCTCTTATACACATCT-3) were combined. In the second reaction, 3.5 µl of Oligo B (5′-GTCTCGTGGGCTCGGAGATGTGTATAAGAGACAG-3) and 3.5 µl of Oligo Rev were mixed. The annealing process for both reactions was performed in a thermocycler using the following program: 95 °C for 3 minutes (denaturation), 70 °C for 3 minutes, followed by a stepwise reduction of 1 °C per step at 30-second intervals for 44 cycles. The annealed oligonucleotides were then combined with 79 µl of 5X TAPS-DMF buffer, 5 µl of Tn5 transposase, and 0.9 µl of 0.1 M DTT, adjusting the final volume to approximately 100 µl. The reaction mixture was incubated at 37°C for 10 minutes, followed by 30 minutes at room temperature, and then stored at -20°C until use (ActiveMotif, 2023).

To ensure effective tagmentation, each batch of transposome was tested with multiple samples due to variability in performance across species and DNA quality. Optimal Tn5 transposome volumes were determined by testing different DNA concentrations with a 10 ng input and varying Tn5 volumes. The fragment analyzer assessed library quality by determining size distribution, which guided Tn5 volume selection to achieve a target size of ∼500 bp. Consequently, 1 µl Tn5 was used for the first six plates, while 0.5 µl was used for the final plate due to a fresh transposome batch.

Before proceeding with the final DNA library production, the concentration of each sample was quantified using a QuantiFluor system. Based on these concentrations, equimolar and randomized plates were prepared with the Xiril robot, resulting in plates with consistent concentrations of 2 ng/µl, although the volumes varied.

For tagmentation, the process by which DNA is simultaneously fragmented and tagged with sequencing adapters by the Tn5 transposase, each sample was aliquoted into 5 µl per well in new plates, which were then dried and resuspended in 3 µl of ddH_2O. Each sample, containing 10 ng of input DNA, was mixed with 7 µl of tagmentation buffer, comprising 5 µl of 2X TMA-DMF buffer, 1 µl of MQ H_2O, and 1 µl of Tn5 transposome. The 2X TMA-DMF buffer was prepared by mixing 20 mM Tris (hydroxymethyl)aminomethane, 10 mM $MgCl_2$, and 50% (vol/vol) dimethylformamide, with the pH adjusted to 7.6 using 100% acetic acid before the addition of dimethylformamide. The tagmentation solution was kept on ice before incuba-

tion at 55°C for 10 minutes. Following tagmentation, amplification was performed using PCR. For the PCR buffer 10 µl of 5X Phusion-like buffer, 0.4 µl of 100 mM dNTPs, 1 µl of Phusion-like polymerase (1 U per reaction), and 26.1 µl of H_2O were combined. These volumes are specified per sample for clarity; total volumes were scaled up as needed to prepare the master mix for all processed samples. To each tagmented sample, 37.5 µl of the prepared PCR buffer was added, along with 2.5 µl of unique Nextera adapters (XT1 – XT4; see Table 3), resulting in a final reaction volume of 50 µl per sample.

To minimize stochastic PCR error and increase library complexity, the 50 µl PCR reaction was split into two separate PCR plates, each containing 25 µl of the solution. PCR amplification was initiated with a denaturation step at 98°C for 5 minutes to ensure complete separation of DNA strands. This was followed by 8 cycles, each consisting of denaturation at 98°C for 10 seconds to maintain strand separation, annealing at 62°C for 30 seconds to facilitate primer binding, and extension at 72°C for 30 seconds to synthesize new DNA strands. A final extension step at 72°C for 5 minutes was included to ensure complete synthesis of all amplified products. Libraries were purified using 0.8× magnetic beads on a Bravo robot to remove adapters and strongly fragmented DNA. The purified DNA was subsequently resuspended in 10 mM Tris-HCl (pH 8.0). Additionally, a quality assessment was performed on a subset of randomly selected samples by determining DNA concentrations using a Qubit™ dsDNA Quantification Assay Kit and evaluating fragment distribution with the Fragment Analyzer.

Library pooling was conducted by combining 5 µl of each sample into a single pool per plate. Clean-up steps were performed to optimize the libraries for sequencing: a 0.5X right-side clean-up was used to remove fragments larger than 1000 bp, as these can interfere with Illumina sequencing, followed by a 2X capture to recover the remaining material. This approach was used for plates 1–4. For plates 5–7, a 0.9X clean-up was employed to remove adapters, as initial sequencing results suggested that the libraries were too small; thus, the right-side clean-up was omitted to retain potentially useful larger fragments. It should be noted that performing clean-up steps after pooling by volume rather than molarity may introduce biases in library representation, as individual library fragment size distributions and concentrations were not normalized prior to clean-up. Following these steps, all pooled libraries were then assessed for fragment distribution using the Fragment Analyzer before sequencing. For the final pooling, the concentration of each library was measured using Qubit™ and adjusted based on the DNA proportion within the desired size range as determined by Fragment Analyzer data. Volumes were calculated to ensure an equimolar representation of each library in the final pool, using their adjusted

molar concentrations. These volumes were then combined accordingly to form three final pools, which were then subjected to sequencing.

2.4 Sequencing

Illumina short-read sequencing was performed by the Next Generation Sequencing Facility at the Vienna BioCenter Core Facilities (VBCF), a member of the Vienna BioCenter (VBC), Austria. Libraries were sequenced on the NovaSeq S4 PE150 XP platform, generating paired-end reads of ∼150 bp with an intended depth of 8X. The sequencing was distributed across different runs: samples from plates 1-4 were sequenced using one full lane, while samples from plates 5-7 and the pilot plate were sequenced using half lanes. This approach ensured comprehensive coverage and optimized the sequencing process for each set of samples.

2.5 Preparation of genetic data

The sequencing data were initially demultiplexed by the in-house NGS facility to assign sequences to their corresponding samples. Once demultiplexed, the reads were processed and aligned using the Genome Analysis Toolkit (GATK) pipeline (McKenna et al., 2010). Specifically, the reads were aligned to the reference genome '`GCA_016097725.1/CZU_Ityp_1.0`' (Powell et al., 2021) using BWA-MEM (version 0.7.17). Variant calling was performed using GATK HaplotypeCaller (version 4.0.1.2), followed by joint genotyping and Phred quality score-based variant quality filtering with GATK GenotypeGVCFs (version 4.2.5.0) using GATK best practices with default settings. This initial step identified 31,762,283 SNPs.

Quality control measures were implemented by applying Phred score thresholds, with cutoffs assessed at 2.5%, 5%, 10%, 20%, and 30%. The difference in the proportion of variant calls between a Phred score of 10 and 20 was determined to be less than 5%, indicating minimal data loss at the higher threshold (Figure 6). Therefore, a Phred score cutoff of 20 was chosen, providing a 99% confidence level in the accuracy of variant calls while minimizing variant loss.

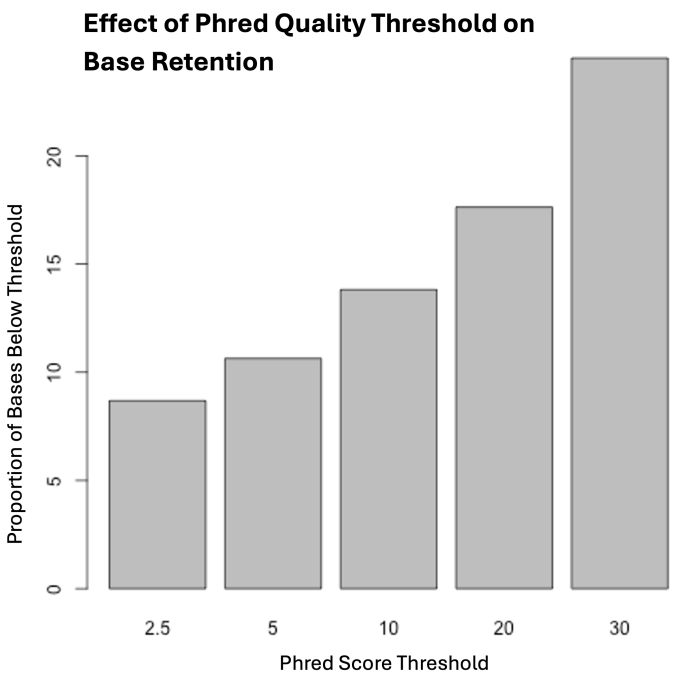

Figure 6: Impact of Phred quality thresholds on base retention. Higher cutoffs reduced data retention, but the difference in variant calls between thresholds of 10 and 20 was minor (<5%). A cutoff of 20 was therefore chosen as a balance between accuracy and variant recovery.

Further quality filtering of the variant dataset was carried out in TASSEL 5 (Bradbury et al., 2007) to ensure robust downstream analyses. To reduce the impact of excessive missing data, sites with genotypic information present in fewer than 20% of samples were removed, and taxa with more than 90% missing data were excluded. In addition, a minor allele frequency (MAF) threshold of 0.00001 was applied to ensure that only polymorphic sites were retained. The filtering process led to the exclusion of 11 samples with insufficient coverage and sequencing depth. After these steps, the final dataset consisted of 31,619,940 high-confidence SNPs. The same filtering criteria were also applied independently to subsets defined by sampling region and multidimensional scaling (MDS) groups to maintain consistency across analyses.

A custom plugin in the TASSEL 5 environment was also employed to generate a high-depth version of the dataset using a depth filter of 9–100X to accommodate analyses requiring depth-dependent metrics, such as heterozygosity calculations. The minimum threshold of 9X was selected to reduce the likelihood of allelic dropout and genotype misclassification. Under a binomial sampling model, the probability that a heterozygous site is miscalled as homozygous, due to all sequencing reads supporting only the reference or the alternate allele, is approximately 0.39% at 9X coverage. This threshold thus offers a practical balance between genotype

accuracy and data retention. To facilitate reference in subsequent sections, the dataset filtered for site and taxa coverage is hereafter referred to as the BaseSet, while the dataset with an additional high-depth filter (9–100X) is referred to as the HighDepthSet.

2.6 Data analysis

2.6.1 Assessment of size-selective infestation based on DBH

To determine whether tree diameter at breast height (DBH), measured at 1.3 m above ground level, significantly differed between beetle-infested and non-infested trees, data distributions were first assessed for normality using the Shapiro–Wilk test. As DBH values in both groups deviated significantly from normality ($p < 0.001$), group means were compared using Welch's two-sample t-test, which is robust to unequal variances and less sensitive to deviations from normality. To further assess whether the overall DBH distributions differed beyond central tendency, a two-sample Kolmogorov–Smirnov test was also applied.

2.6.2 Data quality assessment and visualization

R was used for all data visualizations and initial evaluations. Key SNP metrics were assessed across the BaseSet to ensure data quality and reliability, including taxon coverage and depth for genome completeness, and site coverage to evaluate data resolution. Mean and median values were also calculated to provide a more detailed summary of these metrics, offering a clearer understanding of the dataset's overall characteristics.

2.6.3 Sex classification and evaluation of collection source effects on sex ratio

Sex determination and subsequent analyses were performed in R. Individuals were classified by sex based on coverage analysis of contig 9, which has been linked to the X-chromosome by Mykhailenko et al. (2024). Sex was inferred using the XYp system, in which males carry heterozygous markers and females are homozygous (Smith, 1953). Normalized coverage values were calculated by determining the ratio of contig 9 coverage to total genomic coverage. The normalized values were used as input for a k-means clustering algorithm to classify individuals as male or female.

The threshold for classification was defined as the arithmetic mean of the two cluster centers (Figure 7).

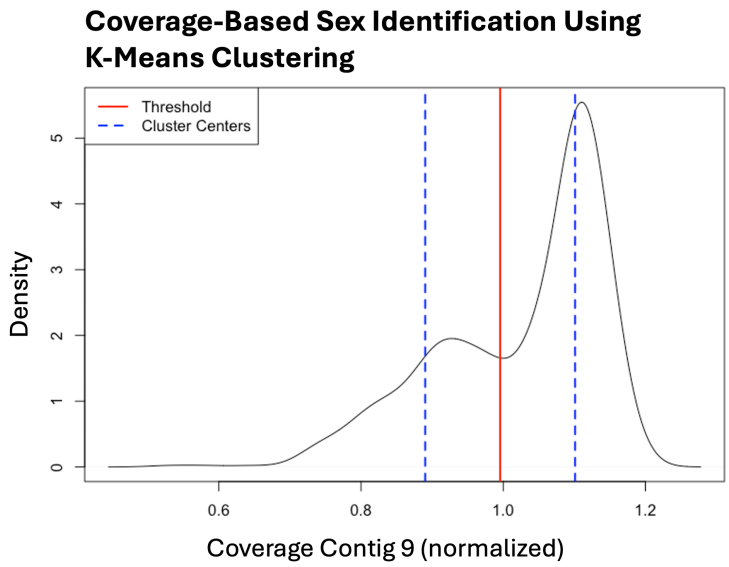

Figure 7: Coverage-based sex identification using k-means clustering. Normalized coverage on the sex-linked contig 9 showed a bimodal distribution corresponding to males and females. K-means clustering identified two cluster centers (dashed blue lines), and the centerpoint between them (red line) was used as the threshold for sex assignment.

After sex determination, a generalized linear model (GLM) under a logit model approximating a binomial response was employed to assess the effect of collection source (LivingTree, PheromoneTrap, TrapTree) on sex. Additionally, a binomial test was conducted to evaluate whether the proportion of females in pheromone traps significantly deviated from an equal sex distribution.

2.6.4 Genetic clustering and factor analysis

Genetic similarity among individuals was quantified by constructing an identity-by-state (IBS) distance matrix in TASSEL 5. IBS represents the proportion of shared alleles between pairs of individuals at genotyped loci, irrespective of their ancestral origin. It is calculated as the Hamming distance, defined as the number of shared alleles divided by the number of loci with genotype data available in both individuals. The resulting distance matrix was analyzed using metric multidimensional scaling (MDS) with the cmdscale() function from the stats package in R (version 4.0.2), projecting the data into a lower-dimensional space to isolate the variation that best explains the data, which can be interpreted as population structure. On the first coordinate, explaining 1.6% of the variation, three distinct genetic clusters were identified, which were treated as additional population groupings in downstream

analyses.

To identify which samples belonged to these visually defined genetic clusters, a custom R Shiny application was developed. The tool re-plots MDS coordinates and allows users to interactively select sample subsets by drawing polygons, using planar spatial intersection (via the sf and leaflet packages) to extract and export the corresponding sample names. The application is available on GitHub (GitHub repository).

This structure-informed approach also facilitated the evaluation of genetic relationships with respect to potential technical, spatial, and temporal sources of variation. Variables considered included quality control parameters (extraction plate, library plate, coverage, depth), spatio-temporal factors (region, collection source, plot, individual tree, elevation, date), and sex. Additionally, environmental variables such as mean, maximum, and minimum temperature, precipitation, and wind speed were derived from daily interpolated climate data obtained from the E-OBS dataset (version 25.0e, released in April 2022), available through the European Climate Assessment & Dataset platform (European Climate Assessment & Dataset, 2022).

In addition to the visual interpretation of the MDS plots, a statistical approach was employed to test associations between the genetic clusters and the above variables. Categorical variables, such as collection source, were analyzed using Chi-squared or Fisher's exact tests, with Fisher's exact applied when expected counts were <5 or distributions were uneven. For continuous variables that were not normally distributed, such as temperature, Kruskal–Wallis tests were performed. Given the 26 independent tests, a Bonferroni correction was applied to adjust the significance threshold, setting

$$\alpha = \frac{0.05}{n} \tag{2}$$

where n is the number of tests (Dunn, 1961). This controls the family-wise error rate at 5%.

2.6.5 Assessment of genetic variation and population structure

Genetic diversity and population structure were assessed using multiple metrics, each calculated independently per population. Observed heterozygosity (H_O), measuring the proportion of heterozygous genotypes within individuals, was calculated in TASSEL 5 as the proportion of heterozygous genotype calls per individual across

all SNPs in the HighDepthSet. Genome-wide individual values were then averaged across all individuals in a population to obtain population-level estimates.

Inbreeding coefficients (f) were estimated from the BaseSet using TASSEL 5 to compute a realized relationship matrix for each population. The population-level inbreeding coefficient was obtained as the mean of the diagonal elements of the kinship matrix minus 1, following Endelman and Jannink (2012), where the expected value of a diagonal element equals 1+f. This provides a population-level measure of excess homozygosity due to non-random mating or genetic subdivision.

Nucleotide diversity (π), the average number of nucleotide differences per site between any two DNA sequences, and Tajima's D, which compares π to the number of segregating sites to infer selection or demographic history (Tajima, 1989), were calculated from the BaseSet, representing the broader genomic dataset. Both metrics were estimated as overall population averages and using a sliding window approach (500 SNP windows, 250 SNP step size) in VCFtools v0.1.16. SNP density, defined as the number of SNPs per unit of covered genome sequence, was also computed from the BaseSet.

SNP counts were extracted using VCFtools version 0.1.16, while genome space — defined as the union of genomic regions covered across all individuals within a population — was determined from the original BAM files via depth analysis using Samtools version 1.10 (base quality ≥ 20, mapping quality ≥ 30) and unified with bedtools version 2.27.1.

Because SNP density and Tajima's D are sensitive to sample size — both through direct effects and indirectly via genome space coverage — a normalization procedure was applied to reduce biases and enable fair comparisons across populations. These adjustments address artificial differences introduced by sampling discrepancies and the underrepresentation of variable sites in smaller samples, as noted by Subramanian (2016). To correct for these effects, a regression analysis was conducted, revealing that a log-transformed relationship provided the best fit for both SNP density ($R^2 = 0.811$) and Tajima's D ($R^2 = 0.997$). The resulting log-transformed linear regression model was used to estimate predicted values for both measures:

$$y_i = \mu + \ln(X_{ij})\beta_j \tag{3}$$

where y_i is the normalized SNP density or Tajima's D for population i, μ is the intercept, representing the overall population baseline value, and β_j quantifies the effect of the natural log of sample size on the respective measure. Values were adjusted by calculating the residuals from the log-transformed regression model,

defined as the difference between the observed value and the value predicted for each population's sample size. These residuals represent the sample size–standardized values, capturing population-specific variation not explained by sampling differences while preserving the underlying biological signal.

2.6.6 Genome-wide F_{ST} scans to detect genetic differentiation

F_{ST} scans were performed to measure genetic differentiation between populations, analyzing contrasts within regional data, collection sources, and MDS-derived clusters. These scans employed sliding windows of 100, 500, and 1000 base pairs with half-step increments were employed using vcftools (version 0.1.16-foss-2018b-perl-5.28.0) to detect population structure across different scales. While smaller windows provide high-resolution insights into localized differentiation, larger windows help to capture broader, more robust patterns across the genome. The overlapping nature of half-step increments further enhanced the detection of true signals by smoothing out noise and improving precision. To minimize false positives, empirical null distributions were generated by randomly scrambling samples within each pairwise comparison for each window size, followed by applying F_{ST} scans to the randomized groups. These null distributions, assuming no population structure, were used to establish significance thresholds for F_{ST} values by calculating quantiles at $1 - \alpha$. Bonferroni corrections (Dunn, 1961) were applied to adjust for multiple comparisons.

Regions exhibiting significant differentiation were identified based on these thresholds, and genomic data were extracted from contigs displaying notable F_{ST} signal variations (contigs 13, 15, 43, 90). Individual MDS plots were generated for contigs with significant differentiation in the F_{ST} scans to assess their contribution to population clustering.

2.6.7 Identification of candidate genomic regions from F_{ST} analysis

Significant F_{ST} regions were identified, merged using bedtools merge, and corresponding sequences were extracted with bedtools getfasta. Gene annotation was conducted by intersecting these regions with an *I. typographus* genome annotation (GFF3 format, DOI: [10.6084/m9.figshare.14503065]) using bedtools intersect (v2.27.1). To ensure comprehensive gene coverage, extracted sequences were additionally verified against the NCBI nucleotide database using blastn (v2.12.0), retaining only high-similarity matches.

3 Results

3.1 Field monitoring and data collection

The monitoring efforts included nine sampling points in BNP (25.06.2021 - 24.09.2021), 10 in FOR (4.05.2021 - 6.09.2021), eight in KAL (19.05.2021 - 23.09.2021), and 10 in SUM (14.05.2021 - 22.09.2021). During these surveys, 22 Norway spruce stands were monitored, along with 15 pheromone traps and 10 trap trees. Phenotypic data were collected from 1,668 trees, of which 95 became infested, yielding 767 beetles sampled for genetic analysis. A total of 133,838 beetles were collected from pheromone traps across four regions: BNP 2020 (25,304 beetles), BNP 2021 (28,463 beetles) FOR (9,215 beetles), KAL (21,307 beetles), and SUM (49,549 beetles). Additionally, 263 beetles were obtained from trap trees in KAL (116 beetles) and FOR (147 beetles) (Figure 5E).

In 2020, plots were established in BNP within an active outbreak area identified the previous year, but no beetles were detected in living trees within these plots. By 2021, infestation was confirmed in BNP, affecting pheromone-baited plots 26, 28, 31, and 33, as well as unbaited plot 30, while no infestation was detected in the other unbaited BNP plots. In SUM, infestation was observed in unbaited plots 65 and 66. No infestation was detected in any monitored plots in FOR and KAL, nor were beetles found in tree traps across any of the study sites. In total, 45 trees became infested in BNP and 46 in SUM.

In 2021, the beetle populations across all regions showed distinct voltinism patterns, with two flight peaks observed between May–June and August–September, though the intensity of these peaks varied by location. In contrast, BNP in 2020 exhibited only a single flight peak between August and September, as monitoring began later that year. Within BNP in 2021, significant spatial variation was observed between the Watzmann and Klausbachtal areas. Nearly twice as many beetles were captured in Watzmann compared to Klausbachtal, indicating a higher population density. However, the beetle population in Watzmann appeared to be univoltine, with a single flight peak later in the season, while the population in Klausbachtal followed a bivoltine pattern, with two distinct flight peaks.

Based on beetle counts normalized by the number of pheromone traps in each region, SUM exhibited the highest beetle activity, followed by KAL, BNP, and FOR (Figure 5E).

3.2 Tree preference

The Kolmogorov–Smirnov (K-S) test indicated that the DBH distributions differed significantly between infested and non-infested trees ($D = 0.315$, $p < 1.1 \times 10^{-7}$), with infested trees showing a right-skewed distribution and generally larger diameters (median DBH: 30.7 cm vs. 23.2 cm; Figure 8). For comparison, Welch's t-test also detected a significant difference in mean DBH between the groups ($t = 6.84$, $df = 178.68$, $p < 1.2 \times 10^{-10}$), but because DBH was not normally distributed, the non-parametric K-S test provides a more appropriate assessment.

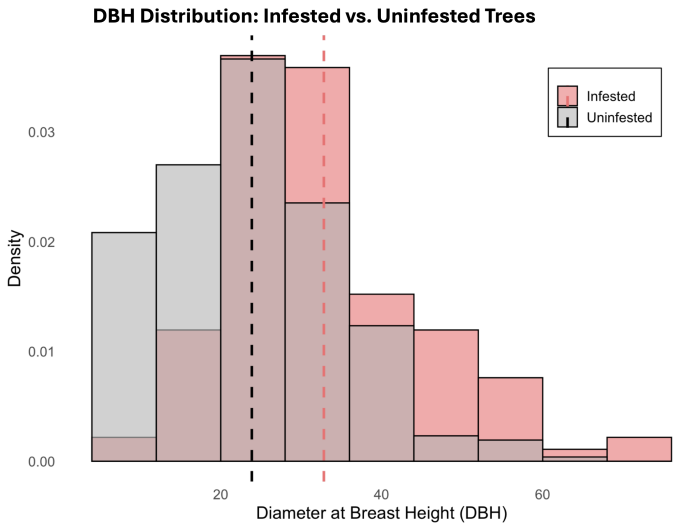

Figure 8: Diameter distributions of infested and uninfested trees. Infested trees had significantly (K-S test, $D = 0.315$, $p < 1.1 \times 10^{-7}$) larger diameters than uninfested trees, with a right-skewed distribution and higher median DBH (30.7 cm vs. 23.2 cm).

In BNP plots 26, 28, 31, and 33, which were treated with pheromone baits, infestations did not follow a symmetric radial pattern from the center. Some trees in close proximity to the pheromone sources were attacked, while others remained uninfested. The timing of infestations also varied across the plots, with attacks occurring at different points during the monitoring period. No clear consistent pattern in infestation timing or proximity to pheromone baits was observed across the plots (Figure 9).

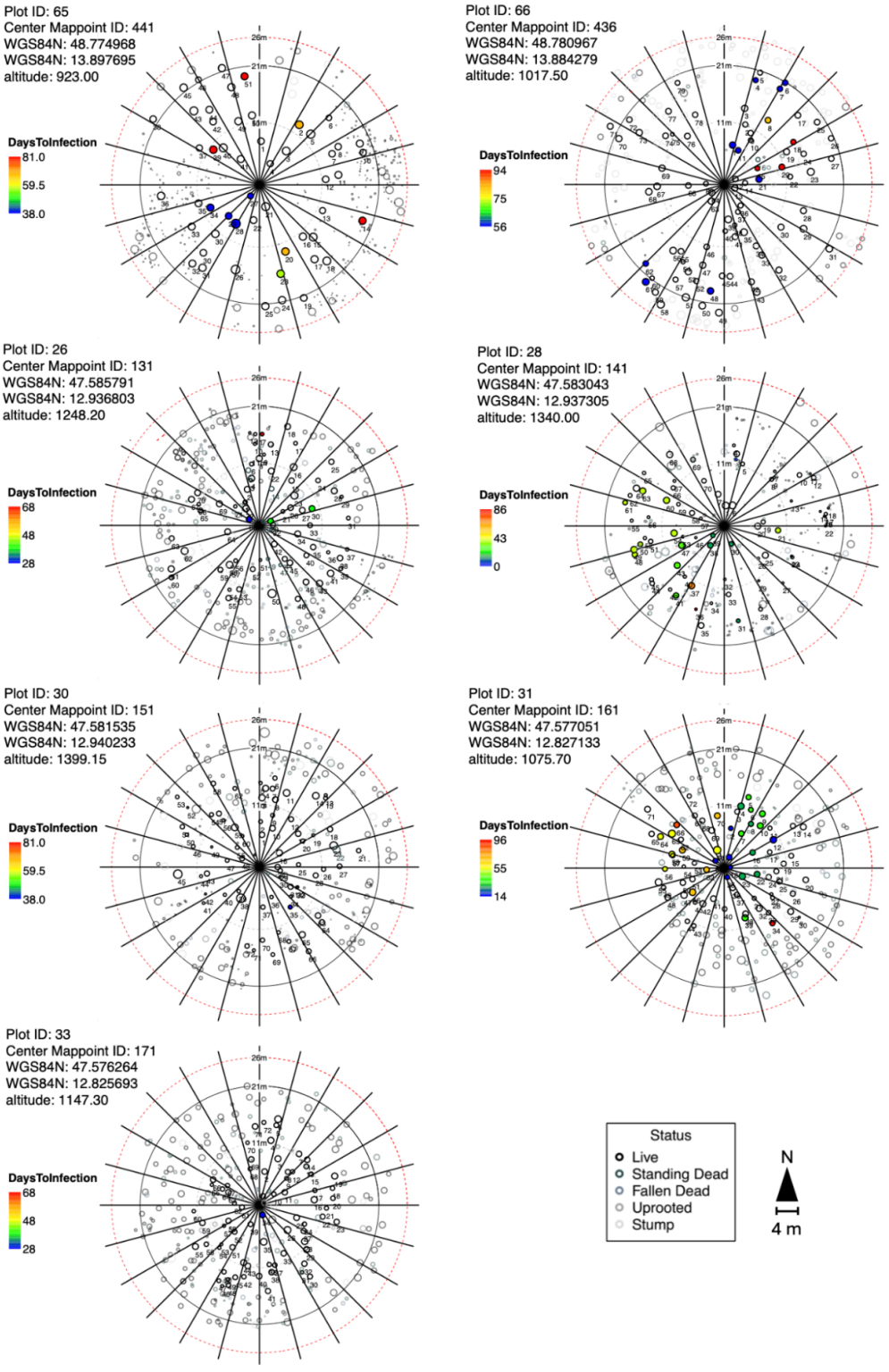

Figure 9: Spatial and temporal dynamics of infestations across plots. In baited plots, infestations did not spread symmetrically from pheromone sources, as some nearby trees remained uninfested while others farther away were attacked; across all plots, infestations occurred asynchronously, with no consistent relationship to bait proximity.

3.3 Genomic data quality evaluation and SNP filtering

The sequencing data yielded a median depth of 4.22X, reflecting an average coverage of each genomic position by approximately four reads. Genotype coverage was moderately high, with a median of 80.72% of taxa genotyped per SNP position and 77.40% of SNPs genotyped per taxon (Figure 10; Table 3). These metrics are generally adequate for SNP detection and most population genetic analyses, particularly given that approximately 28.2% of the genome consists of repetitive elements (Powell et al., 2021). To ensure more accurate estimations of genetic variation, genotype calls from the HighDepthSet were utilized specifically for heterozygosity analysis, as detailed in the Methods section.

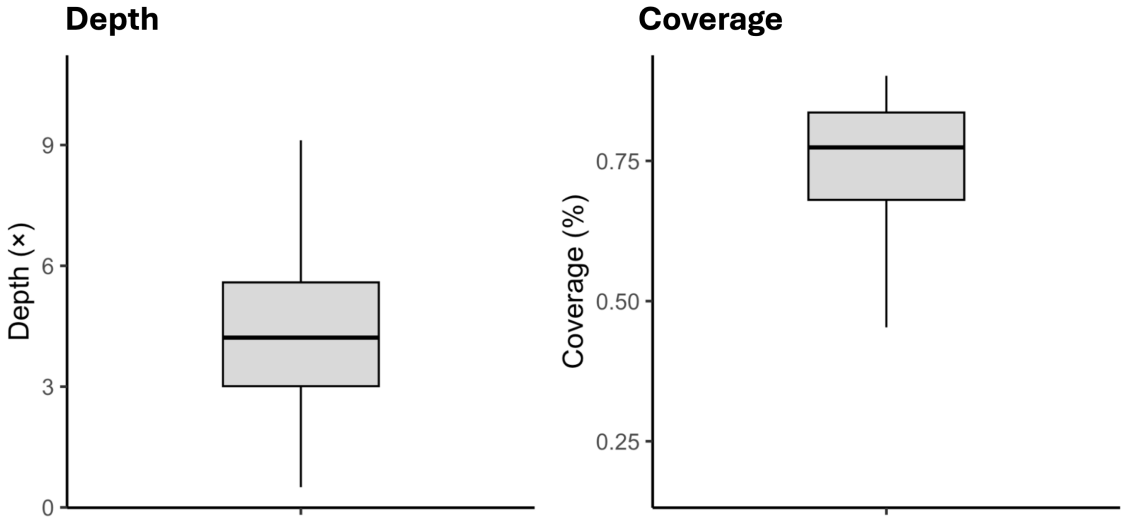

Figure 10: Assessment of sequencing depth and coverage. Boxplots show sequencing depth (left) and coverage (right). The dataset yielded a median depth of 4.2X, with ∼77% of SNPs genotyped per individual, providing sufficient quality for downstream population genetic analyses.

After filtering, the final dataset comprised 31,619,940 high-confidence SNPs across the retained samples. Eleven samples did not pass quality control due to insufficient coverage and sequencing depth, including five from BNP (all derived from living trees), one from KAL (living tree), and five from SUM (four living trees and one trap tree). A summary of SNP counts, coverage, and heterozygosity across filtering steps is provided in Table 1.

Table 1: Sequencing statistics Raw calls are SNPs after variant calling. *Coverage filtered* excludes poorly genotyped sites and individuals. *BaseSet (final)* applies an additional MAF filter to remove monomorphic sites, and *HighDepthSet* is a depth-filtered subset (9–100X) of the *BaseSet*.

Dataset	Number of SNPs	Mean taxon coverage (%)	Mean heterozygosity
Raw calls	31,762,283	77.4	–
Coverage filtered	31,697,503	77.4	0.027
BaseSet (final)	31,619,940	74.5	0.027
HighDepthSet	31,619,939	4.2	0.025

3.4 Female bias in pheromone trap collections

Of the 695 randomly selected and successfully sequenced beetles, 251 were identified as male (36.12%) and 444 as female (63.88%). A generalized linear model (GLM) revealed a significant effect of pheromone traps on sex, with males being significantly less likely to be collected in pheromone traps compared to LivingTree (Estimate = -1.38, $p < 0.001$). No significant difference was observed between TrapTree and LivingTree. Additionally, a binomial test confirmed that pheromone traps captured significantly more females than males, with 80.66% of individuals being female ($p < 2.2e\text{-}16$, 95% CI: [0.76, 0.85]).

3.5 Patterns of genetic variation and population differentiation

3.5.1 Genetic structure revealed by population clustering

Although the first two dimensions of the MDS explain only 1.6% and 1.4% of the genetic variance, respectively — indicating that the great majority of variation is widely shared across the dataset — the analysis reveals three distinct clusters (Figure 11). The final dataset comprised 695 beetles, which grouped into clusters of the following sizes: MDSGR1 (n = 62), MDSGR2 (n = 288), and MDSGR3 (n = 345).

Visual inspection of the MDS plot, with coloring by processing quality parameters (extraction plate, library plate, sequencing depth, and coverage), temporal factors (year and day of sampling), spatial variables (geographic region, plot, individual tree, altitude, and sampling source), environmental conditions (temperature, precipitation, wind speed, and humidity), and biological factors (sex and heterozy-

gosity), did not suggest any obvious association with the observed clustering (Figure 11).

Association between the MDS clusters and the explanatory variables were tested using Fisher's exact tests for categorical and Kruskal-Wallis tests for continuous variables. Before Bonferroni correction, altitude, longitude, sea level pressure, and sex showed nominal significance ($p < 0.05$). After correction, only Region (adjusted $p = 0.001$) and Relative Humidity (adjusted $p = 0.010$) remained significant. A Kruskal-Wallis test confirmed a strong correlation between these two variables, and post-hoc Dunn's tests revealed significant differences in humidity between all regions except BNP and SUM. The remaining variables showed no significant associations with MDS groupings after correction.

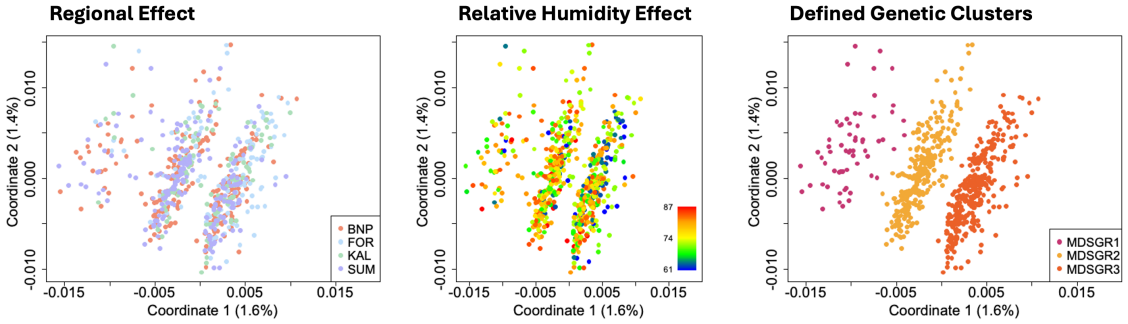

Figure 11: Multidimensional scaling (MDS) of genetic variation. MDS summarizes genetic relationships by projecting genetic distances (IBS) into two dimensions, where closer points represent greater similarity. The first two coordinates explain ~3% of the variance but reveal three distinct genetic clusters. Clustering is not explained by region (left) or median relative humidity (center). The right panel illustrates the three genetic clusters identified from the MDS analysis, which were used as the basis for subsequent analyses.

3.5.2 Genetic diversity and variation across populations

Since the analysis of the minor allele frequency (MAF) spectrum relies on a folded site frequency spectrum (SFS) (Figure 12), it is not possible to reliably disentangle selective from demographic processes. However, the predominance of rare alleles is more readily explained by demographic history, as selective signals are largely masked in folded spectra.

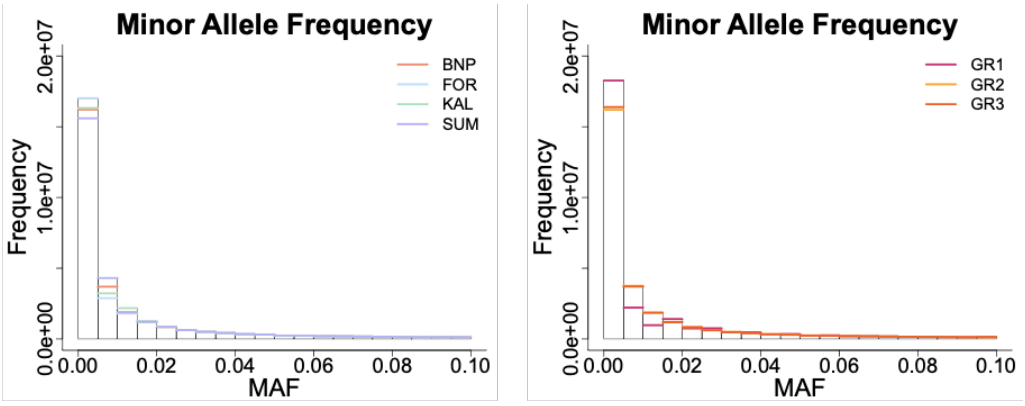

Figure 12: Folded site frequency spectrum (SFS) of minor allele frequencies (MAF) across (left) regional populations and (right) MDS-based genetic clusters. All groups show an excess of low-frequency alleles, with subtle differences among them, consistent with demographic expansion. The full SFS extends to MAF = 0.5, but only the range up to 0.1 is shown for clarity at the low-frequency end, as higher-frequency variants are rare and do not influence the comparative patterns.

The relative abundance of rare alleles varied among populations, with FOR showing the strongest excess, followed by KAL and BNP, and the weakest signal in SUM. In FOR, the pronounced excess of rare alleles, together with relatively high π and low f, points to recent expansion while maintaining high standing diversity. This pattern is consistent with frequent immigration and long-distance dispersal into an open landscape, which would increase diversity and dilute signals of inbreeding. KAL and BNP displayed similar SFS shapes but differed in diversity metrics: KAL had the lowest π and Ho, consistent with expansion from a smaller founder pool, whereas BNP combined high diversity with slightly elevated f, suggesting minor local structure despite substantial gene flow. SUM showed fewer rare alleles and a higher proportion of intermediate-frequency variants, along with intermediate π and H_O, indicative of a larger effective population size but a weaker expansion signal — possibly reflecting the aftermath of a major outbreak.

Consistent with this interpretation, the population-mean values of Tajima's D were uniformly negative (Table 2), confirming a genome-wide signal of demographic expansion across regions. The unmanaged populations (BNP and SUM) showed more negative values than the managed sites (KAL and FOR). This pattern suggests that expansion has been somewhat stronger or more recent in unmanaged forests, whereas managed populations exhibit weaker expansion signals, possibly reflecting reduced continuity of breeding substrate under management.

Table 2: Genetic diversity estimates. Values shown include sample size (N), adjusted SNP density, nucleotide diversity (π), adjusted Tajima's D, inbreeding coefficient (f), and observed heterozygosity (H_O). SNP density and Tajima's D were corrected for sample size effects using a log-transformed regression approach to allow unbiased comparisons across populations.

Population	**N**	**SNP Density**	$\boldsymbol{\pi}$	**Tajima's D**	$\boldsymbol{f}$	$\boldsymbol{H_O}$
BNP	250	0.15	0.06412	-1.164	0.017	0.026
FOR	133	0.14	0.06353	-1.130	0.005	0.024
KAL	112	0.18	0.06267	-1.134	0.007	0.023
SUM	200	0.13	0.06352	-1.150	0.002	0.025
MDSGR1	62	0.17	0.06271	-1.127	0.017	0.022
MDSGR2	288	0.19	0.06390	-1.151	0.002	0.027
MDSGR3	345	0.14	0.06294	-1.149	0.007	0.024

In addition to this consistent signal of demographic expansion, genetic diversity metrics (π, H_O) varied slightly among populations and between management types (Table 2). Unmanaged sites (BNP and SUM) showed generally higher or comparable diversity (π, H_O) than managed forests (FOR and KAL), whereas the latter had slightly higher Tajima's D values, consistent with weaker demographic expansion. The inbreeding coefficient (f) was low across all populations, indicating that the beetle populations are largely outbred and experience substantial gene flow. BNP exhibited the highest f values, while the remaining sites differed only marginally. When considering these remaining populations, f tended to be slightly higher in the managed forests (FOR and KAL) than in the unmanaged site SUM, consistent with expectations of somewhat reduced genetic mixing under management. However, given the small absolute differences and limited number of populations, no clear conclusion can be drawn, and forest management cannot be identified as a consistent driver of inbreeding levels.

Taken together, these metrics suggest that forest management may influence local population dynamics by altering the temporal stability and continuity of breeding substrate, resulting in weaker demographic expansion and slightly reduced diversity in managed areas. However, the magnitude of these differences remains small, indicating that high dispersal and recurrent outbreak events largely homogenize genetic variation at the regional scale.

Overall, all populations show evidence of ongoing demographic expansion, and unmanaged forests tend to display somewhat higher genetic diversity and stronger expansion signals. However, these trends are subtle and should be interpreted cautiously, as differences among populations are small and may partly reflect stochastic or regional demographic factors rather than management effects alone. These

contrasts likely reflect differences in habitat continuity, local outbreak stage, and dispersal dynamics rather than management alone.

The site frequency spectrum further revealed differences among genetic clusters, with the abundance of rare alleles following the order MDSGR1 > MDSGR3 > MDSGR2. MDSGR1 showed the strongest excess of rare alleles, but also the lowest π and H_O and the highest f. This points to expansion from a restricted base population, consistent with the founder-effect signal described above for KAL. MDSGR3 showed an intermediate pattern, combining a strong SFS skew with higher diversity (π, H_O) and lower f than MDSGR1, consistent with expansion from a larger base population. In contrast, MDSGR2 displayed the weakest excess of rare alleles in the SFS, but the highest π and HO together with the lowest f. This pattern reflects a large effective population size and extensive standing variation, where expansion signals are less pronounced. Importantly, these genetic patterns are mirrored by the relative sizes of the clusters (MDSGR1 < MDSGR3 < MDSGR2), which cannot be explained by sampling effort and therefore likely reflect biological differences in prevalence.

3.5.3 Genomic regions contributing to population differentiation

Genome-wide F_{ST} estimates were generally low (0–0.0007), indicating weak overall differentiation among populations. Sliding-window genome-wide F_{ST} patterns are shown in Figure 13. No significant differentiation was detected in regional or collection source comparisons, suggesting a high level of genetic homogeneity across these groups. In contrast, MDS-based population contrasts revealed distinct localized peaks of differentiation, primarily in contigs 13 and 43, which showed consistently elevated F_{ST} values across most sliding window analyses. Additional signals were detected in contigs 15 and 90. Although these appeared in fewer comparisons or window sizes, this does not necessarily diminish their biological relevance; rather, the pattern in contig 90, which was significant only in one window-size contrast, may reflect a narrow or localized region of differentiation captured under specific analytical resolutions.

The fact that significant differentiation was observed only when grouping individuals according to the genetic structure shown in the MDS plot — rather than by geographic or collection origin — suggests that these genomic regions contribute to intrinsic genetic divergence, most likely associated with structural variants such as chromosomal inversions — rather than with spatial or environmental factors. Importantly, such localized genomic regions are known to influence assortative mating, thereby enabling small portions of the genome to drive genome-wide patterns of

variation.

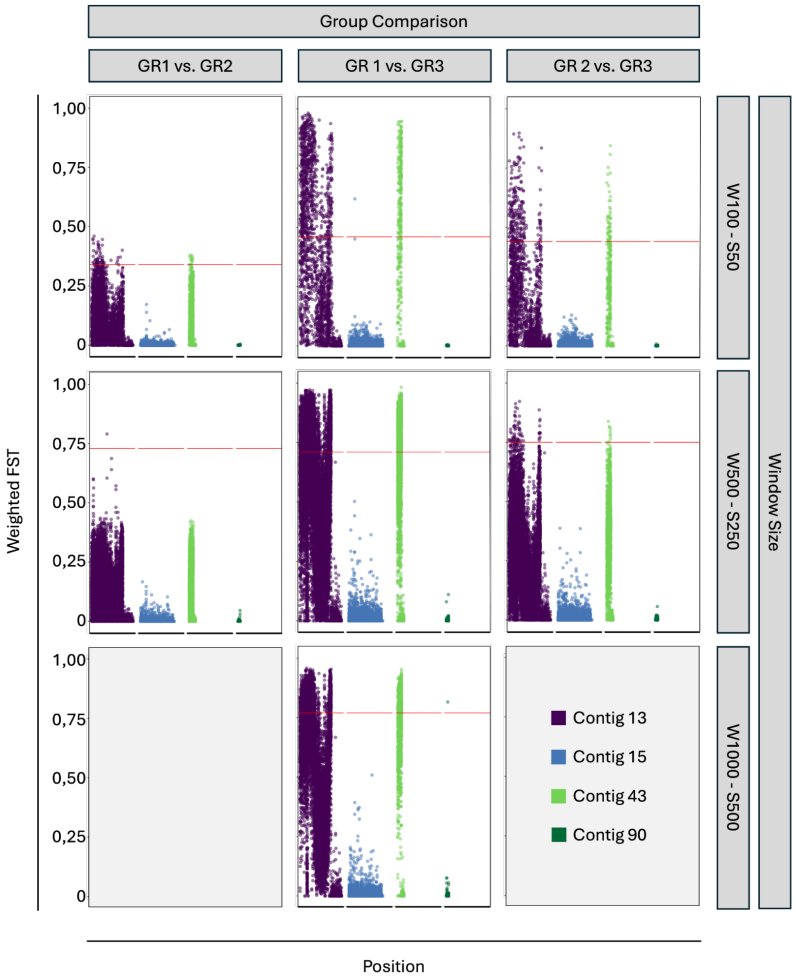

Figure 13: Genome wide FST scans across MDS groups. FST quantifies allele frequency differentiation between populations. Sliding window scans (100 bp, 500 bp, 1000 bp) balanced resolution and robustness. Strong peaks were detected in contigs 13 and 43, with weaker signals in contigs 15 and 90. No significant differentiation was observed in regional or sampling source comparisons.

Individual MDS analyses of the contigs identified from F_{ST} outlier regions (Figure 14) revealed distinct clustering patterns among the genetic groups. Contig 13 (∼6.00 Mb) showed three well-separated clusters that correspond closely to the overall population structure observed in the genome-wide MDS. Contig 43 (∼0.89 Mb) also displayed pronounced differentiation among groups, although its clustering pattern suggested additional substructure not captured in the global analysis. In contrast, contig 15 (∼4.90 Mb) exhibited clear within-contig clustering that did not align with the broader MDS grouping, indicating a potentially independent source of variation. Contig 90 (∼0.29 Mb) showed largely overlapping clusters, consistent with its weaker differentiation signal. No evidence of sex-related differentiation was detected in any contig, suggesting that the observed patterns are unrelated to

sex-linked variation.

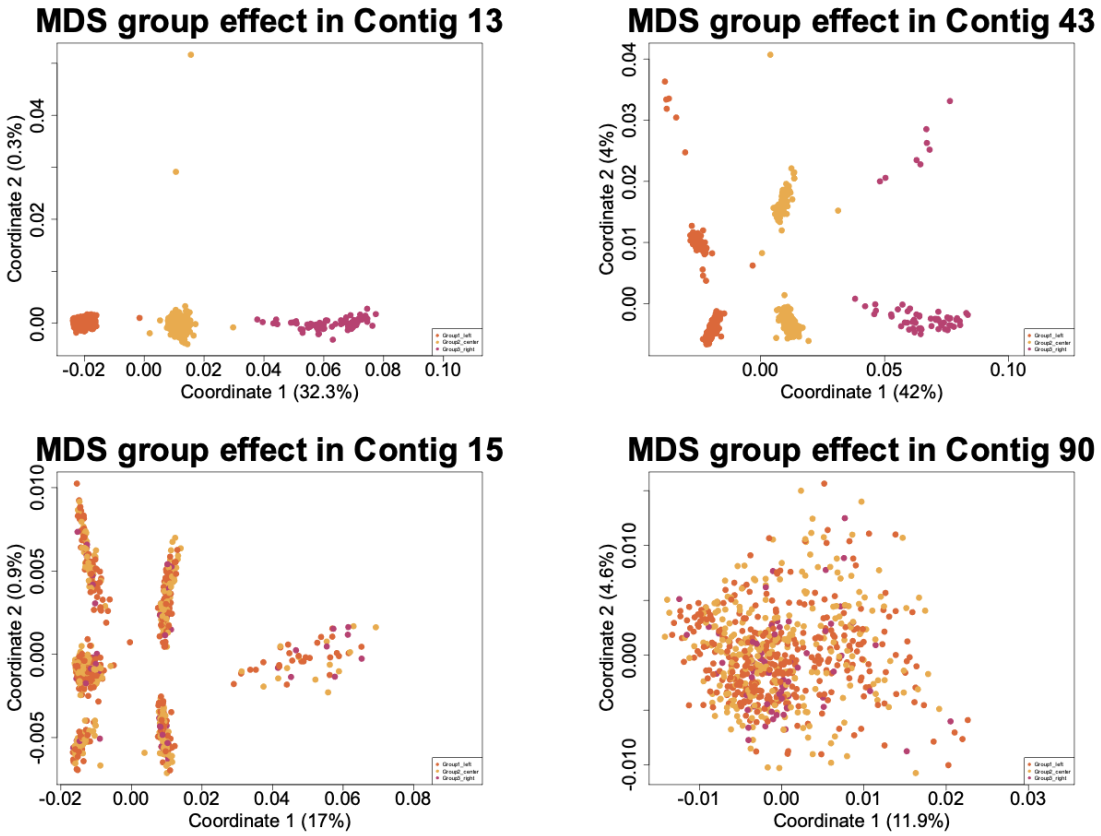

Figure 14: MDS clustering in candidate contigs. MDS plots of contigs highlighted by F_{ST} scans were used to test whether locus-specific differentiation underlies the genome-wide clustering. Contig 13 mirrored the three MDS groups, contig 43 showed additional sub-structuring, contig 15 displayed clustering unrelated to the overall structure, and contig 90 showed none.

3.5.4 Candidate regions revealing no gene matches

The gene annotation pipeline produced 432 unique entries, including features such as mRNA, exons, and untranslated regions (UTRs). Despite this, BLAST searches against the NCBI database did not identify any known genes within these regions.

4 Discussion

4.1 Ecological dynamics of pheromone attraction and host tree selection

While pheromone-baited traps clearly attracted *Ips typographus*, as indicated by the absence of infestation in unbaited plots within BNP, beetles did not always select the trees nearest to the pheromone sources. This suggests that pheromone attraction operates primarily at the stand level, whereas fine-scale host choice is influenced by additional cues.

One such cue was tree size. Infested trees had significantly greater diameter at breast height (DBH) than uninfested trees, confirming earlier findings that larger trees, with thicker bark and more phloem, provide more suitable breeding substrates (Schroeder & Eidmann, 1993; Schroeder et al., 1999; Takei et al., 2021). However, DBH alone did not fully predict infestation. Beetles also colonized intermediate trees and sometimes avoided large ones, indicating that further factors such as local beetle density, tree defense capacity, or micro-environmental conditions (Grodzki, 2022) contribute to host selection. These results refine existing knowledge by demonstrating that DBH is important, but not deterministic, when host choice occurs under the combined influence of pheromone attraction and local conditions. What remains unresolved is the relative contribution of tree defense physiology versus stand-level context in shaping final attack decisions.

A pronounced female bias in pheromone trap captures (64% female) was also observed, contrasting with the near 1:1 sex ratio in beetles collected from naturally infested trees. This provides clear evidence that trap catches do not necessarily reflect the operational sex ratio of attacking beetles. Such biases are consistent with sex-specific behaviors, where females are more strongly guided by aggregation pheromones, while males rely more on host volatiles (Heber et al., 2021; Zahradníková et al., 2024). The comparison between trap captures and natural infestations adds quantitative support to concerns that monitoring based solely on trap catches may overestimate female prevalence. Further work is needed to clarify how trap composition, environmental variation, and outbreak stage influence this bias, and how lures could be optimized to attract both sexes more evenly (Heber et al., 2021).

4.2 Present stability in voltinism patterns under expected climate change pressures

The voltinism patterns observed in 2021 are consistent with predictions based on altitudinal gradients and climatic conditions. Bivoltinism was recorded at lower elevations, including FOR (706 m) and SUM (995 m), where the warmer temperature regimes typically facilitate the occurrence of two generations per year. Bivoltinism was also observed at higher elevations, including BNP Klausbachtal (1091.16 m) and KAL (1023.60 m), despite the expectation that regions above 1000 meters would more commonly exhibit only 1.5 generations annually (Jakoby et al., 2019).

At the highest elevation, Watzmann in BNP (1313.46 m), univoltinism was observed, in line with the findings of Jakoby et al. (2019) that cooler temperatures above 1200 meters generally restrict populations to a single generation per year. Although climate change is expected to impact reproductive cycles by potentially altering voltinism patterns, no significant shifts have been detected in these regions to date. However, future changes remain possible as climate conditions evolve (Faccoli, 2009; Jönsson et al., 2009; Schebeck et al., 2017; Jakoby et al., 2019; Romashkin et al., 2020).

4.3 Population genetics and dynamics of *Ips typographus* in Central Europe

4.3.1 Genetic differentiation and connectivity in *Ips typographus*

This study provides a genomic assessment of *I. typographus* populations across Central Europe, revealing a largely panmictic structure with subtle genetic differentiation among regions. The minimal genome-wide differentiation observed (F_{ST} = 0–0.0007) suggests extensive gene flow, likely driven by the beetle's high dispersal capability, which enables connectivity across broad spatial scales. Low F_{ST} values reported in this study align with findings from Müller et al. (2022) (F_{ST} = 0.001) and Mykhailenko et al. (2024) (F_{ST} = 0.021).

Despite the identification of three genetic clusters (MDSGR1, MDSGR2, and MDSGR3), no differentiation was observed at fine scales, such as host or plot selection, nor across temporal scales, suggesting that local host associations and microhabitat preferences do not significantly influence genetic structure. This highlights that low-density marker sets are insufficient to detect trait-linked diversity, whereas high-resolution genome-wide data are required to pinpoint specific loci involved

in local adaptation. Genome scans using resequencing data provided meaningful signals, enabling the identification of loci underlying genome-wide differentiation. Genome–environment association (GEA) analyses could test for signatures of local adaptation to climatic or ecological variables, while genome-wide association studies (GWAS) could link genomic variation to specific phenotypic traits such as host or mate preference. Functional genomic methods, including transcriptomics or expression profiling, would then provide a means to validate candidate genes and clarify their biological roles.

Differentiation was only detected at the regional level, indicating that broad-scale environmental or ecological factors drive population divergence. While statistical analyses found correlations between genetic structure, region, and relative humidity, these factors did not fully explain the observed clustering in the MDS plot. The first two coordinates explained only 3% of the variance, reinforcing the idea that high dispersal and gene flow dilute genetic structuring in this species. The subtle clustering observed may reflect processes such as local adaptation to environmental or ecological factors, including host tree availability, climatic variation, or even mate choice. Structural variants may play a role in facilitating these processes by maintaining adaptive allelic combinations.

Further supporting the high levels of gene flow inferred from F_{ST} and MDS, low levels of inbreeding (f) suggest that genetic drift has a limited impact on the populations. This aligns with expectations for a highly dispersive species, where frequent outcrossing prevents the accumulation of homozygosity and preserves genetic diversity. The low f values observed in this study are consistent with Müller et al. (2022), further reinforcing the conclusion that *I. typographus* populations are well-connected across Central Europe.

4.3.2 Structural barriers to gene flow: the impact of inversions

Genome-wide F_{ST} analysis revealed significant genetic differentiation in specific genomic regions, particularly in contigs 13 and 43, suggesting the presence of structural variants like inversions, which can reduce recombination and maintain genetic differentiation by restricting gene flow. Such variants can play a crucial role in shaping population structure by preserving locally adapted genetic combinations despite high dispersal potential (Wellenreuther & Bernatchez, 2018).

Mykhailenko et al. (2024) confirmed that contig 13 harbors an inversion (Inv13) associated with olfactory receptor genes (ItypOR23 and ItypOR27), which are critical for interactions with fungal symbionts. Significant latitudinal variation in the fre-

quency of this inversion suggests its role in local adaptation, particularly in olfactory sensing. Johny et al. (2025) further demonstrated that functional polymorphisms in ItypOR33 alter receptor function, influencing beetle responses to semiochemicals and driving differentiation shaped by ecological rather than geographic factors. These findings highlight how genetic variation in olfactory perception may contribute to host selection, communication, and outbreak potential in *I. typographus*.

Strong F_{ST} signals in contig 43, together with distinct clustering in contig-specific MDS, indicate that this region contributes disproportionately to the genetic structure observed among MDS groups. While an inversion in this contig has not yet been confirmed, its strong signal suggests it may harbor structural variation influencing differentiation. In contrast, contig 15, another confirmed inversion, exhibited weaker signals, possibly due to fixation or a lesser role in current population dynamics (Mykhailenko et al., 2024).

These structural variants likely contribute to maintaining genetic structure, as shown by individual MDS plots that reveal clear genetic clusters for contigs 13 and 43, aligning with the overall population structure. The persistence of genetic differentiation in MDSGR1, despite the potential for gene flow, suggests that factors beyond genetic drift — such as behavioral or ecological differences — may be maintaining its distinctiveness. Differences in reproductive timing, host tree preference, or microhabitat specialization could limit genetic exchange between these groups.

Understanding the significance of these structural variants is crucial, as they can facilitate local adaptation by preserving advantageous allele combinations and maintaining genetic differences, even in overlapping geographic ranges with ongoing gene flow (Wellenreuther & Bernatchez, 2018). These variants may also influence assortative mating, potentially explaining their persistence despite gene flow between regions (Wellenreuther et al., 2019). Given the involvement of olfactory genes, these structural changes likely contribute to adaptations such as host tree selection, symbiont interactions, and pheromone communication — all vital to the beetle's survival and population dynamics (Mykhailenko et al., 2024).

4.3.3 Demographic expansion outweighs management effects on genetic variation

Genetic diversity patterns across populations indicate a largely panmictic structure shaped predominantly by demographic expansion and high dispersal, but with subtle regional differences. While all populations exhibit clear signals of demographic growth, variation in Tajima's D and diversity metrics (π, H_O, and f) among

sites suggests that expansion has been somewhat stronger or more recent in unmanaged forests (BNP, SUM) than in managed stands (FOR, KAL). This may reflect reduced temporal continuity of breeding substrate in managed landscapes rather than a fundamental barrier to gene flow. Overall, demographic processes associated with outbreak cycles appear to play a stronger role than forest management in shaping genome-wide variation.

All populations showed signatures of demographic expansion, consistent with the boom phases that follow increases in breeding material. However, the strength and character of this signal differed across regions. FOR showed evidence of recent expansion while maintaining high diversity, a pattern consistent with strong immigration and long-distance dispersal into an open landscape. KAL displayed a contrasting signal of expansion from a smaller founder pool, indicating founder effects that may arise when outbreaks originate from a limited number of colonizers. BNP combined high overall diversity with slightly elevated inbreeding, suggesting subtle restrictions to gene flow despite its unmanaged status. SUM, by contrast, exhibited the weakest expansion signal, likely reflecting a demographic slowdown after a major outbreak had already subsided.

These contrasts highlight how demographic signatures can vary with local outbreak dynamics: dispersal and immigration buffer genetic diversity in some regions, while restricted colonization events or declining outbreaks leave founder-effect or contraction-like signatures in others. Although slight differences between managed and unmanaged forests were detected, they remain minor compared to the influence of demographic processes. Thus, high dispersal, outbreak-driven expansions, and the persistence of multiple chromosomal lineages dominate the genetic landscape of *I. typographus* in Central Europe, underscoring the demographic resilience of this species across management contexts.

4.3.4 Understanding genetic drivers of population cycles can improve targeted control measures

Genome-wide resequencing revealed that chromosomal inversions, particularly on contigs 13 and 43, contribute to persistent genetic structure in *I. typographus* by suppressing recombination and maintaining distinct haplotypic backgrounds. Within the same geographic range, three genetic clusters were consistently identified (MDSGR1: 62 individuals; MDSGR2: 288 individuals; MDSGR3: 345 individuals). These groups most likely represent assortatively mating subpopulations whose divergence originates from localized inversion polymorphisms. Because these structural variants restrict recombination, they facilitate the accumulation of linked

functional differences that can influence mating compatibility, thereby enabling a small portion of the genome to drive genome-wide differentiation. The unequal representation of the three groups therefore reflects differences in the frequencies-and evolutionary trajectories-of the underlying inversion-associated haplotypes. Consequently, each group likely maintains its own effective population size, shaped by the balance of mutation, drift, selection, and restricted gene flow among haplotypes. Genetic patterns observed among groups — such as slightly lower nucleotide diversity and heterozygosity, along with marginally higher f in MDSGR1 compared to MDSGR2 and MDSGR3 — are consistent with expectations for a rarer or more recently derived inversion, where reduced recombination limits the accumulation of variation, even though the magnitude of these differences is modest. Conversely, the higher diversity and SNP density observed in MDSGR2 may reflect an older inversion that has persisted longer, allowing mutations to accumulate. MDSGR3, the largest group, shows intermediate values, suggesting a more stable arrangement with diversity maintained either by higher connectivity or moderate inversion age.

These findings highlight the complexity of *I. typographus* population dynamics, where multiple chromosomal lineages co-occur and vary in frequency. Further research into behavioral and ecological differences between these groups could provide insight into the mechanisms maintaining these genetic structures despite ongoing expansion.

4.4 Biases and methodological constraints

While the genomic data presented here provide robust insights into demographic history, several methodological factors influence absolute estimates of genetic diversity and must be considered when comparing across studies. Levels of nucleotide diversity (π) in this study ranged from 0.0627 to 0.0641, considerably higher than values reported in previous whole-genome studies. For example, Mykhailenko et al. (2024) estimated π between 0.0055 and 0.0066 across populations separated by over 2000 km, nearly an order of magnitude lower than observed here. Such contrasts most likely reflect methodological rather than biological causes. The present study used Tn5 transposase–based library preparation, which can introduce biases in GC-rich regions and preferentially capture mutable loci, potentially inflating nucleotide diversity estimates (Kozarewa et al., 2009; Head et al., 2014). In contrast, Mykhailenko et al. (2024) employed enzymatic fragmentation (NEBNext Ultra II FS), which reduces such biases and may yield lower π estimates. Differences in sequencing depth, genome coverage, and variant calling thresholds could also contribute.

Observed heterozygosity (H_O) in this study (0.022–0.027) was substantially lower than values reported from genotyping-by-sequencing (GBS) data. Müller et al. (2022), for example, reported heterozygosity of 0.245 and 0.258 in two German populations. Such discrepancies again most likely reflect methodological effects: GBS captures a different subset of the genome and applies distinct SNP detection thresholds.

A further limitation of this study was the lower-than-intended sequencing depth. While the target was 8X, the achieved mean depth was only ∼4X, primarily due to ineffective size selection during library preparation. Because adapter fragments (137 bp) were not excluded during size calibration, ∼40% of reads contained adapter sequences, resulting in a substantial loss of usable data. Pooling libraries by volume rather than molarity may have further contributed to uneven coverage across individuals. Although ∼4X coverage was sufficient for broad population-level metrics (π, Tajima's D, F_{ST}, MDS; Ferretti et al., 2013), reduced depth inevitably increases missingness and biases genotype calls toward the reference allele. These biases particularly affect heterozygosity and individual-level inbreeding estimates, whereas population-level averages are less strongly impacted. Depth-based filtering reduced potential errors, but may also have unevenly excluded regions of lower mappability.

Taken together, these considerations highlight that while relative comparisons among populations within this dataset are robust, absolute estimates of π, H_O, and f should be interpreted cautiously, especially when compared to values obtained with different sequencing methods. For future studies, careful fragment size calibration that accounts for adapter length, combined with molarity-based pooling to balance coverage among individuals, is recommended to improve sequencing efficiency (Harismendy & Frazer, 2009; Duntsch et al., 2021).

5 Conclusion

This study provides a genome-wide perspective on *Ips typographus* populations across Central Europe, revealing a largely panmictic structure with only weak regional differentiation. Genetic variation is shaped predominantly by demographic expansion and the recurrent boom–bust dynamics typical of bark beetle outbreaks, while high dispersal maintains extensive connectivity among populations.

Relative to the effects of natural demographic processes, forest management did not generate strong or consistent genome-wide differences between managed and unmanaged stands. Nonetheless, subtle shifts in genomic diversity metrics in managed forests suggest that interventions could influence local population stability

and expansion intensity.

Beyond these broad-scale patterns, signals of genomic differentiation associated with structural variants indicate that local adaptation may persist despite high gene flow. Such variants could maintain ecological or behavioral differentiation among lineages, influencing traits like host use, symbiotic and intraspecific pheromone preferences, dispersal, or reproductive timing.

Together, these findings depict *I. typographus* as a species in which pervasive gene flow and recurrent demographic expansion dominate genomic patterns, while structural variants preserve localized islands of differentiation. These contrasting processes highlight a system where widespread connectivity coexists with pockets of ecological or behavioral divergence. Understanding how these elements interact across landscapes will be essential for predicting population dynamics and refining management strategies in an era of accelerating environmental change.

References

Active Motif. (2023). pA-Tn5 Loading Protocol. Retrieved May 12, 2024, from https://www.activemotif.com/documents/2261.pdf

Amman, G. D. (1972). Mountain pine beetle brood production in relation to thickness of lodgepole pine phloem. *Journal of Economic Entomology*, *65*(1), 138–140.

Andrei, S., & Ifrim, I. L. (2021). Ips infestation–a global problem for coniferous in the face of climate change. *Scientific Study & Research. Chemistry & Chemical Engineering, Biotechnology, Food Industry*, *22*(2), 245–261.

Andrews, K. R., Good, J. M., Miller, M. R., Luikart, G., & Hohenlohe, P. A. (2016). Harnessing the power of radseq for ecological and evolutionary genomics. *Nature Reviews Genetics*, *17*(2), 81–92.

Bakke, A., Frøyen, P., & Skattebøl, L. (1977). Field response to a new pheromonal compound isolated from *Ips typographus* [Please add journal, volume and pages]. *Unspecified journal*.

Baym, M., Kryazhimskiy, S., Lieberman, T. D., Chung, H., Desai, M. M., & Kishony, R. (2015). Inexpensive multiplexed library preparation for megabase-sized genomes. *PLOS ONE*, *10*(5), e0128036.

Boone, C. K., Aukema, B. H., Bohlmann, J., Carroll, A. L., & Raffa, K. F. (2011). Efficacy of tree defense physiology varies with bark beetle population density: A basis for positive feedback in eruptive species. *Canadian Journal of Forest Research*, *41*(6), 1174–1188.

Bradbury, P. J., Zhang, Z., Kroon, D. E., Casstevens, T. M., Ramdoss, Y., & Buckler, E. S. (2007). Tassel: Software for association mapping of complex traits in diverse samples. *Bioinformatics*, *23*(19), 2633–2635.

Burjanadze, M., Moser, J. C., Zimmermann, G., & Kleespies, R. G. (2008). Antagonists of the spruce bark beetle *Ips typographus* l. (coleoptera: Scolytidae) of german and georgian populations. *IOBC-WPRS Bulletin*, *31*, 245–250.

Caudullo, G., Tinner, W., & de Rigo, D. (2016). *Picea abies* in europe: Distribution, habitat, usage and threats [Add editor, pages and publisher if required]. *European Atlas of Forest Tree Species*.

Christiansen, E., & Bakke, A. (1988). The spruce bark beetle of eurasia. In A. A. Berryman (Ed.), *Dynamics of forest insect populations: Patterns, causes, implications* (pp. 479–503). Springer.

de Vries, S. M. G., Alan, M., Bozzano, M., Burianek, V., Collin, E., Cottrell, J., Ivankovic, M., Kelleher, C. T., Koskela, J., Rotach, P., & Vietto, L. (2015). *Pan-european strategy for genetic conservation of forest trees and establish-*

ment of a core network of dynamic conservation units. European Forest Genetic Resources Programme (EUFORGEN), Bioversity International.

Dunn, O. J. (1961). Multiple comparisons among means. *Journal of the American Statistical Association*, *56*(293), 52–64.

Duntsch, L., Whibley, A., Brekke, P., Ewen, J. G., & Santure, A. W. (2021). Genomic data of different resolutions reveal consistent inbreeding estimates but contrasting homozygosity landscapes for the threatened aotearoa new zealand hihi. *Molecular Ecology*, *30*(23), 6006–6020.

EFSA Panel on Plant Health. (2017). Pest categorisation of ips cembrae. *EFSA Journal*, *15*, 5039.

Ellerstrand, S. J., Choudhury, S., Svensson, K., Andersson, M. N., Kirkeby, C., Powell, D., Schlyter, F., Jönsson, A. M., Brydegaard, M., Hansson, B., & Runemark, A. (2022). Weak population genetic structure in eurasian spruce bark beetle over large regional scales in sweden. *Ecology and Evolution*, *12*(7), e9078.

Elshire, R. J., Glaubitz, J. C., Sun, Q., Poland, J. A., Kawamoto, K., Buckler, E. S., & Mitchell, S. E. (2011). A robust, simple genotyping-by-sequencing (gbs) approach for high diversity species. *PLOS ONE*, *6*(5), e19379.

Endelman, J. B., & Jannink, J. L. (2012). Shrinkage estimation of the realized relationship matrix. *G3: Genes—Genomes—Genetics*, *2*(11), 1405–1413.

European Climate Assessment and Dataset (ECA&D). (2022). E-obs: Daily gridded observational dataset. version 25.0e.

Faccoli, M. (2002). Winter mortality in sub-corticolous populations of *Ips typographus* (coleoptera, scolytidae) and its parasitoids in the south-eastern alps. *Anzeiger für Schädlingskunde / Journal of Pest Science*, *75*, 62–68.

Faccoli, M. (2009). Effect of weather on *Ips typographus* (coleoptera curculionidae) phenology, voltinism, and associated spruce mortality in the southeastern alps. *Environmental Entomology*, *38*(2), 307–316.

Farjon, A. (2017). *Picea abies* [Accessed 12 May 2024].

Ferretti, L., Ramos-Onsins, S. E., & Pérez-Enciso, M. (2013). Population genomics from pool sequencing. *Molecular Ecology*, *22*(22), 5561–5576.

Franceschi, V. R., Krokene, P., Christiansen, E., & Krekling, T. (2005). Anatomical and chemical defenses of conifer bark against bark beetles and other pests. *New Phytologist*, *167*(2), 353–376.

Furniss, M. M., Solheim, H., & Christiansen, E. (1990). Transmission of blue-stain fungi by *Ips typographus* (coleoptera: Scolytidae) in norway spruce. *Annals of the Entomological Society of America*, *83*(4), 712–716.

Grégoire, J. C., & Evans, H. F. (2004). Damage and control of bawbilt organisms: An overview. In *Bark and wood boring insects in living trees in europe, a synthesis* (pp. 19–37). Springer.

Grodzki, W. (2022). Do *Ips typographus* (l.) beetles prefer the thickest trees? a retrospective study from polish mountains. *Sylwan*, *166*(06).

Gugerli, F., Gall, R., Meier, F., & Wermelinger, B. (2008). Pronounced fluctuations of spruce bark beetle (scolytinae: *Ips typographus*) populations do not invoke genetic differentiation. *Forest Ecology and Management*, *256*(3), 405–409.

Hagge, J., Müller, J., Bässler, C., Biebl, S. S., Brandl, R., Drexler, M., Gruppe, A., Hotes, S., Hothorn, T., Langhammer, P., & Stark, H. (2019). Deadwood retention in forests lowers short-term browsing pressure on silver fir saplings by overabundant deer. *Forest Ecology and Management*, *451*, 117531.

Hansen, E. M. (2014). Forest development and carbon dynamics after mountain pine beetle outbreaks. *Forest Science*, *60*(3), 476–488.

Harismendy, O., & Frazer, K. A. (2009). Method for improving sequence coverage uniformity of targeted genomic intervals amplified by lr-pcr using illumina ga sequencing-by-synthesis technology. *BioTechniques*, *46*(3), 229–231.

Head, S. R., Komori, H. K., LaMere, S. A., Whisenant, T., Van Nieuwerburgh, F., Salomon, D. R., & Ordoukhanian, P. (2014). Library construction for next-generation sequencing: Overviews and challenges. *BioTechniques*, *56*(2), 61–77.

Heber, T., Helbig, C. E., Osmers, S., & Müller, M. G. (2021). Evaluation of attractant composition, application rate, and trap type for potential mass trapping of *Ips typographus* (l.) *Forests*, *12*(12), 1727.

Hilszczański, J., Gibb, H., & Bystrowski, C. (2007). Insect natural enemies of *Ips typographus* (l.) (coleoptera, scolytinae) in managed and unmanaged stands of mixed lowland forest in poland. *Journal of Pest Science*, *80*, 99–107.

Hlásny, T., König, L., Krokene, P., Lindner, M., Montagné-Huck, C., Müller, J., Qin, H., Raffa, K. F., Schelhaas, M. J., Svoboda, M., & Viiri, H. (2021). Bark beetle outbreaks in europe: State of knowledge and ways forward for management. *Current Forestry Reports*, *7*, 138–165.

Honkaniemi, J., Rammer, W., & Seidl, R. (2020). Norway spruce at the trailing edge: The effect of landscape configuration and composition on climate resilience. *Landscape Ecology*, *35*(3), 591–606.

Jakoby, O., Lischke, H., & Wermelinger, B. (2019). Climate change alters elevational phenology patterns of the european spruce bark beetle (*Ips typographus*). *Global Change Biology*, *25*(12), 4048–4063.

Johann, E., Agnoletti, M., Axelsson, A. L., Bürgi, M., Östlund, L., Rochel, X., Schmidt, U. E., Schuler, A., Skovsgaard, J. P., & Winiwarter, V. (2004).

History of secondary norway spruce forests in europe. In *Norway spruce conversion* (pp. 25–62). Brill.

Johny, J., Diallo, S., NadachowskaBrzyska, K., Moliterno, A. A. C., Roy, A., Kalinová, B., GroßeWilde, E., & Schlyter, F. (2025). Not all bark beetles smell the same: Population-level functional olfactory polymorphisms in *Ips typographus* pheromone receptor itypor33. *Molecular Ecology*, e17693.

Jönsson, A. M., Appelberg, G., Harding, S., & Bärring, L. (2009). Spatio-temporal impact of climate change on the activity and voltinism of the spruce bark beetle, *Ips typographus*. *Global Change Biology*, *15*(2), 486–499.

Kandasamy, D., Gershenzon, J., & Hammerbacher, A. (2016). Volatile organic compounds emitted by fungal associates of conifer bark beetles and their potential in bark beetle control. *Journal of Chemical Ecology*, *42*(9), 952–969.

Kausrud, K., Økland, B., Skarpaas, O., Grégoire, J. C., Erbilgin, N., & Stenseth, N. C. (2012). Population dynamics in changing environments: The case of an eruptive forest pest species. *Biological Reviews*, *87*(1), 34–51.

Kautz, M., Feurer, J., & Adler, P. (2024). Early detection of bark beetle (*Ips typographus*) infestations by remote sensing–a critical review of recent research. *Forest Ecology and Management*, *556*, 121595.

Kozarewa, I., Ning, Z., Quail, M. A., Sanders, M. J., Berriman, M., & Turner, D. J. (2009). Amplification-free illumina sequencing-library preparation facilitates improved mapping and assembly of (g+c)-biased genomes. *Nature Methods*, *6*(4), 291–295.

Krokene, P. (2015). Conifer defense and resistance to bark beetles. In F. E. Vega & R. W. Hofstetter (Eds.), *Bark beetles* (pp. 177–207). Academic Press.

Kuhn, A., Hautier, L., & San Martin, G. (2022). Do pheromone traps help to reduce new attacks of *Ips typographus* at the local scale after a sanitary cut? *PeerJ*, *10*, e14093.

Lehmanski, L. M., Kandasamy, D., Andersson, M. N., Netherer, S., Alves, E. G., Huang, J., & Hartmann, H. (2023). Addressing a century-old hypothesis–do pioneer beetles of *Ips typographus* use volatile cues to find suitable host trees? *New Phytologist*, *238*(5), 1762–1770.

Lieutier, F., Yart, A., & Salle, A. (2009). Stimulation of tree defenses by ophiostomatoid fungi can explain attack success of bark beetles on conifers. *Annals of Forest Science*, *66*(8), 801.

Lindenmayer, D. B., Burton, P. J., & Franklin, J. F. (2012). *Salvage logging and its ecological consequences*. Island Press.

Lobinger, G. (1994). Die lufttemperatur als limitierender faktor für die schwärmaktivitat zweier rindenbrütender fichtenborkenkäferarten, *Ips typographus* l.

und *Pityogenes chalcographus* l. (col., scolytidae). *Anzeiger für Schädlingskunde, Pflanzenschutz, Umweltschutz*, *67*(1), 14–17.

Lobinger, G. V., & Skatulla, U. (1996). Untersuchungen zum einfluss von sonnenlicht auf das schwärmverhalten von borkenkäfern. *Anzeiger für Schädlingskunde, Pflanzenschutz, Umweltschutz*, *69*(8), 183–185.

Lubojacký, J., & Holuša, J. (2014). Attraction of *Ips typographus* (coleoptera: Curculionidae) beetles by lure-baited insecticide-treated tripod trap logs and trap trees. *International Journal of Pest Management*, *60*(3), 153–159.

Marini, L., Økland, B., Jönsson, A. M., Bentz, B., Carroll, A., Forster, B., Grégoire, J. C., Hurling, R., Nageleisen, L. M., Netherer, S., & Ravn, H. P. (2017). Climate drivers of bark beetle outbreak dynamics in norway spruce forests. *Ecography*, *40*(12), 1426–1435.

Mayer, F., Piel, F. B., Cassel-Lundhagen, A., Kirichenko, N., Grumiau, L., Økland, B., Bertheau, C., Grégoire, J. C., & Mardulyn, P. (2015). Comparative multilocus phylogeography of two palaearctic spruce bark beetles: Influence of contrasting ecological strategies on genetic variation. *Molecular Ecology*, *24*(6), 1292–1310.

McKenna, A., Hanna, M., Banks, E., Sivachenko, A., Cibulskis, K., Kernytsky, A., Garimella, K., Altshuler, D., Gabriel, S., Daly, M., & DePristo, M. A. (2010). The genome analysis toolkit: A mapreduce framework for analyzing next-generation dna sequencing data. *Genome Research*, *20*(9), 1297–1303.

Montano, V., Bertheau, C., Doležal, P., Krumböck, S., Okrouhlík, J., et al. (2016). How differential management strategies affect *Ips typographus* l. dispersal. *Forest Ecology and Management*, *360*, 195–204.

Müller, J., Bußler, H., Goßner, M., Rettelbach, T., & Duelli, P. (2008). The european spruce bark beetle *Ips typographus* in a national park: From pest to keystone species. *Biodiversity and Conservation*, *17*, 2979–3001.

Müller, J., Noss, R. F., Thorn, S., Bässler, C., Leverkus, A. B., & Lindenmayer, D. (2019). Increasing disturbance demands new policies to conserve intact forest. *Conservation Letters*, *12*(1), e12449.

Müller, M., Niesar, M., Berens, I., & Gailing, O. (2022). Genotyping by sequencing reveals lack of local genetic structure between two german *Ips typographus* l. populations. *Forestry Research*, *2*(1).

Mykhailenko, A., Zieliński, P., Bednarz, A., Schlyter, F., Andersson, M. N., Antunes, B., Borowski, Z., Krokene, P., Melin, M., Morales-García, J., et al. (2024). Complex genomic landscape of inversion polymorphism in europe's most destructive forest pest. *Genome Biology and Evolution*, *16*(12), evae263.

Némethy, M., Mihálik, D., Steifetten, Ø., Rošteková, V., Mrkvová, M., Janiga, M., & Kraic, J. (2018). Genetic differentiation between local populations of *Ips ty-*

pographus in the high tatra mountains range. *Scandinavian Journal of Forest Research*, *33*(3), 215–221.

Netherer, S., Matthews, B., Katzensteiner, K., Blackwell, E., Henschke, P., Hietz, P., Pennerstorfer, J., Rosner, S., Kikuta, S., Schume, H., & Schopf, A. (2015). Do water-limiting conditions predispose norway spruce to bark beetle attack? *New Phytologist*, *205*(3), 1128–1141.

Pechacek, P. (1994). Reaktion des dreizehenspechts auf eine borkenkäfergradation. *Allgemeine Forstzeitschrift*, *49*, 661.

Pettersen, H., & Austara, O. E. (1975). Overwintering conditions for *Ips typographus* l. (col., scolytidae) [Please add journal, volume and pages]. *Unspecified journal*.

Porretta, D., Canestrelli, D., Bellini, R., Celli, G., & Urbanelli, S. (2007). Improving insect pest management through population genetic data: A case study of the mosquito *Ochlerotatus caspius* (pallas). *Journal of Applied Ecology*, *44*(3), 682–691.

Powell, D., Große-Wilde, E., Krokene, P., Roy, A., Chakraborty, A., Löfstedt, C., Vogel, H., Andersson, M. N., & Schlyter, F. (2021). A highly-contiguous genome assembly of the eurasian spruce bark beetle, *Ips typographus*, provides insight into a major forest pest. *Communications Biology*, *4*(1), 1059.

Pretzsch, H., Schütze, G., & Uhl, E. (2013). Resistance of european tree species to drought stress in mixed versus pure forests: Evidence of stress release by inter-specific facilitation. *Plant Biology*, *15*(3), 483–495.

Raffa, K. F., Andersson, M. N., & Schlyter, F. (2016). Host selection by bark beetles: Playing the odds in a high-stakes game. In *Advances in insect physiology* (pp. 1–74, Vol. 50). Academic Press.

Raffa, K. F., Aukema, B. H., Bentz, B. J., Carroll, A. L., Hicke, J. A., Turner, M. G., & Romme, W. H. (2008). Cross-scale drivers of natural disturbances prone to anthropogenic amplification: The dynamics of bark beetle eruptions. *BioScience*, *58*(6), 501–517.

Raffa, K. F., Grégoire, J. C., & Lindgren, B. S. (2015). Natural history and ecology of bark beetles. In F. E. Vega & R. W. Hofstetter (Eds.), *Bark beetles* (pp. 1–40). Academic Press.

Ranger, C. M. (2016). Bark beetles: Biology and ecology of native and invasive species [Book review or section; please clarify if needed]. In *Bark beetles: Biology and ecology of native and invasive species* (pp. 196–198).

Reed, D. E., Ewers, B. E., Pendall, E., Frank, J., & Kelly, R. (2018). Bark beetle-induced tree mortality alters stand energy budgets due to water budget changes. *Theoretical and Applied Climatology*, *131*, 153–165.

Rollins, L. A., Woolnough, A. P., & Sherwin, W. B. (2006). Population genetic tools for pest management: A review. *Wildlife Research*, *33*(4), 251–261.

Romashkin, I., Neuvonen, S., & Tikkanen, O. P. (2020). Northward shift in temperature sum isoclines may favour *Ips typographus* outbreaks in european russia. *Agricultural and Forest Entomology*, *22*(3), 238–249.

Safranyik, L. (1998). Mortality of mountain pine beetle larvae, *dendroctonus ponderosae* (coleoptera: Scolytidae) in logs of lodgepole pine (*pinus contorta* var. *latifolia*) at constant low temperatures. *Journal of the Entomological Society of British Columbia*, *95*, 81–88.

Sallé, A., Arthofer, W., Lieutier, F., Stauffer, C., & Kerdelhue, C. (2007). Phylogeography of a host-specific insect: Genetic structure of *Ips typographus* in europe does not reflect past fragmentation of its host. *Biological Journal of the Linnean Society*, *90*(2), 239–246.

Sanchis-Juan, A., Stephens, J., French, C. E., Gleadall, N., Mégy, K., Penkett, C., Shamardina, O., Stirrups, K., Delon, I., Dewhurst, E., et al. (2018). Complex structural variants in mendelian disorders: Identification and breakpoint resolution using short- and long-read genome sequencing. *Genome Medicine*, *10*, 1–10.

Sauvard, D. (2004). General biology of bark beetles. In *Bark and wood boring insects in living trees in europe, a synthesis* (pp. 63–88). Springer.

Schäffer, S., Koblmüller, S., Pfingstl, T., Sturmbauer, C., & Krisper, G. (2010). Contrasting mitochondrial dna diversity estimates in austrian *Scutovertex minutus* and *S. sculptus* (acari, oribatida, brachypylina, scutoverticidae). *Pedobiologia*, *53*(3), 203–211.

Schebeck, M., Hansen, E. M., Schopf, A., Ragland, G. J., Stauffer, C., & Bentz, B. J. (2017). Diapause and overwintering of two spruce bark beetle species. *Physiological Entomology*, *42*(3), 200–210.

Schebeck, M., Schopf, A., Ragland, G. J., Stauffer, C., & Biedermann, P. H. (2023). Evolutionary ecology of the bark beetles *Ips typographus* and *Pityogenes chalcographus*. *Bulletin of Entomological Research*, *113*(1), 1–10.

Schlyter, F., Birgersson, G., Byers, J. A., Löfqvist, J., & Bergström, G. (1987). Field response of spruce bark beetle, *Ips typographus*, to aggregation pheromone candidates. *Journal of Chemical Ecology*, *13*, 701–716.

Schlyter, F., & Löfqvist, J. (1986). Response of walking spruce bark beetles *Ips typographus* to pheromone produced in different attack phases. *Entomologia Experimentalis et Applicata*, *41*(3), 219–230.

Schroeder, L. M., & Eidmann, H. H. (1993). Attacks of bark- and wood-boring coleoptera on snow-broken conifers over a two-year period. *Scandinavian Journal of Forest Research*, *8*(1-4), 257–265.

Schroeder, L. M., Weslien, J., Lindelöw, Å., & Lindhe, A. (1999). Attacks by bark- and wood-boring coleoptera on mechanically created high stumps of norway spruce in the two years following cutting. *Forest Ecology and Management*, *123*(1), 21–30.

Six, D. L., & Wingfield, M. J. (2011). The role of phytopathogenicity in bark beetle–fungus symbioses: A challenge to the classic paradigm. *Annual Review of Entomology*, *56*(1), 255–272.

Smith, S. G. (1953). Chromosome numbers of coleoptera. *Heredity*, *7*(1), 31–48.

Soukhovolsky, V., Kovalev, A., Tarasova, O., Modlinger, R., Křenová, Z., Mezei, P., Škvarenina, J., Rožnovský, J., Korolyova, N., Majdák, A., & Jakuš, R. (2022). Wind damage and temperature effect on tree mortality caused by *Ips typographus* l.: Phase transition model. *Forests*, *13*(2), 180.

Stocker, T. F., Qin, D., Plattner, G. K., Tignor, M. M., Allen, S. K., Boschung, J., Nauels, A., Xia, Y., Bex, V., & Midgley, P. M. (2014). *Climate change 2013: The physical science basis. contribution of working group i to the fifth assessment report of the ipcc*. Cambridge University Press.

Stokland, J. N., Siitonen, J., & Jonsson, B. G. (2012). *Biodiversity in dead wood*. Cambridge University Press.

Subramanian, S. (2016). The effects of sample size on population genomic analyses–implications for the tests of neutrality. *BMC Genomics*, *17*, 1–13.

Tajima, F. (1989). The effect of change in population size on dna polymorphism. *Genetics*, *123*(3), 597–601.

Takei, S. Y., Köbayashi, K., & Takagi, E. (2021). Distribution pattern of entry holes of the tree-killing bark beetle *Polygraphus proximus*. *PLOS ONE*, *16*(2), e0246812.

Thorn, S., Bässler, C., Brandl, R., Burton, P. J., Cahall, R., Campbell, J. L., Castro, J., Choi, C., Cobb, T., Donato, D. C., et al. (2018). Impacts of salvage logging on biodiversity: A meta-analysis. *Journal of Applied Ecology*, *55*(1), 279–289.

von Teuffel, K., Heinrich, B., & Baumgarten, M. (2004). Present distribution of secondary norway spruce in europe. In *Norway spruce conversion* (pp. 63–96). Brill.

Vošvrdová, N., Johansson, A., Turčáni, M., Jakuš, R., Tyšer, D., Schlyter, F., & Modlinger, R. (2023). Dogs trained to recognise a bark beetle pheromone locate recently attacked spruces better than human experts. *Forest Ecology and Management*, *528*, 120626.

Wadke, N., Kandasamy, D., Vogel, H., Lah, L., Wingfield, B. D., Paetz, C., Wright, L. P., Gershenzon, J., & Hammerbacher, A. (2016). The bark-beetle-associated fungus, *Endoconidiophora polonica*, utilizes the phenolic defense compounds of its host as a carbon source. *Plant Physiology*, *171*(2), 914–931.

Wang, Y., Lim, L., Madilao, L., Lah, L., Bohlmann, J., & Breuil, C. (2014). Gene discovery for enzymes involved in limonene modification or utilization by the mountain pine beetle-associated pathogen *Grosmannia clavigera*. *Applied and Environmental Microbiology*, *80*(15), 4566–4576.

Weed, A. S., Ayres, M. P., & Hicke, J. A. (2013). Consequences of climate change for biotic disturbances in north american forests. *Ecological Monographs*, *83*(4), 441–470.

Wellenreuther, M., & Bernatchez, L. (2018). Eco-evolutionary genomics of chromosomal inversions. *Trends in Ecology & Evolution*, *33*(6), 427–440.

Wellenreuther, M., Mérot, C., Berdan, E., & Bernatchez, L. (2019). Going beyond snps: The role of structural genomic variants in adaptive evolution and species diversification. *Molecular Ecology*, *28*(6), 1203–1209.

Wermelinger, B. (2004). Ecology and management of the spruce bark beetle *Ips typographus*–a review of recent research. *Forest Ecology and Management*, *202*(1-3), 67–82.

Wermelinger, B., & Seifert, M. (1998). Temperature-dependent reproduction of the spruce bark beetle *Ips typographus*, and analysis of the potential population growth. *Ecological Entomology*, *24*(1), 103–110.

Weslien, J., & Lindelöw, Å. (1990). Recapture of marked spruce bark beetles (*Ips typographus*) in pheromone traps using area-wide mass trapping. *Canadian Journal of Forest Research*, *20*(11), 1786–1790.

Weslien, J., & Schroeder, L. M. (1999). Population levels of bark beetles and associated insects in managed and unmanaged spruce stands. *Forest Ecology and Management*, *115*(2-3), 267–275.

Yu, N., Christiaens, O., Liu, J., Niu, J., Cappelle, K., Caccia, S., Huvenne, H., & Smagghe, G. (2013). Delivery of dsrna for rnai in insects: An overview and future directions. *Insect Science*, *20*(1), 4–14.

Zahradníková, M., Dostál, J., & Zahradník, P. (2024). The sex ratio of spruce bark beetles–*Ips typographus* (coleoptera: Curculionidae: Scolytinae) captured in different types of traps. *Journal of Forest Science*, *70*(12), 603–609.

Zang, C., Hartl-Meier, C., Dittmar, C., Rothe, A., & Menzel, A. (2014). Patterns of drought tolerance in major european temperate forest trees: Climatic drivers and levels of variability. *Global Change Biology*, *20*(12), 3767–3779.

Zielonka, T. (2006). When does dead wood turn into a substrate for spruce replacement? *Journal of Vegetation Science*, *17*(6), 739–746.

Appendix A: Supplementary table

Table 3: Sample-specific adapter and barcode assignments used for demultiplexing. Columns include numeric ID, sample name, collection source (CS), P5 and P7 adapter identifiers (adapter_p5, adapter_p7) with corresponding barcode sequences (tag_p5_5to3, tag_p7_5to3), and sequencing metrics (coverage and depth). Sample names encode region (BNP, FOR, KAL, or SUM), sampling date (YYYYMMDD), source identifier (tree ID or trap ID), optional replicate letter, and a unique internal sample ID.

ID	sample	CS	adapter_p5	tag_p5_5to3	adapter_p7	tag_p7_5to3	cov	depth
0	BNP20200815_194_24657	PT	XT1_UDN5075	GATGGATGTA	XT1_UDN7075	CTCTGCAGCG	0.71	2.98
1	BNP20200815_194_24713	PT	XT4_UDN5290	AGAGCACTAG	XT4_UDN7290	CCGGACCACA	0.74	3.66
2	BNP20200815_194_24818	PT	XT3_UDN5215	CAGAGTGATA	XT3_UDN7215	ATTCTAAGCG	0.59	2.48
3	BNP20200815_201_24323	PT	XT4_UDN5382	CAAGTTCATA	XT4_UDN7382	TCGTGGTTGA	0.58	2.42
4	BNP20200815_201_24376	PT	XT2_UDN5176	GATAAGCTCT	XT2_UDN7176	TGTTAGAAGG	0.51	1.63
5	BNP20200815_201_24378	PT	XT1_UDN5020	CGCACATGGC	XT1_UDN7020	GATAGGCCGA	0.83	5.5
6	BNP20200815_201_24589	PT	XT3_UDN5218	GTGACCTTGA	XT3_UDN£7218	AATAGAGCAA	0.52	2.06
7	BNP20200815_201_24590	PT	XT4_UDN5370	TGGAGGTAAT	XT4_UDN7370	CACTCGCACT	0.6	2.2
8	BNP20200815_201_24607	PT	XT3_UDN5257	CTCTGTATA£C	XT3_UDN7257	AGATTGTTAC	0.74	3.96
9	BNP20200815_202_24517	PT	XT2_UDN5129	CGAAGGTTAA	XT2_UDN7129	CGCGCCTAGA	0.82	5.83
10	BNP20200815_202_24634	PT	XT1_UDN5094	GATTAAGGTG	XT1_UDN7094	TCATAGATTG	0.83	5.06
11	BNP20200815_202_24689	PT	XT3_UDN5259	GGTAACGCAG	XT3_UDN7259	AACGGTATGA	0.82	6.24
12	BNP20200815_202_24813	PT	XT3_UDN5282	CGGCAAGCTC	XT3_UDN7282	GGCGAATTCT	0.86	6.21
13	BNP20200815_202_24975	PT	XT3_UDN5209	AATACGACAT	XT3_UDN7209	ATAGTCTAGC	0.61	2.19
14	BNP20200815_202_24998	PT	XT4_UDN5335	CTCTGACGTG	XT4_UDN7335	CCGGAATCAT	0.64	2.36
15	BNP20200815_203_24439	PT	XT4_UDN5379	TACACGCTCC	XT4_UDN7379	CAGTATCAAT	0.77	4.06
16	BNP20200815_203_24631	PT	XT3_UDN5272	TCGCGTATAA	XT3_UDN7272	AGCTGTTATA	0.83	5.39
17	BNP20200815_203_24791	PT	XT3_UDN5239	CACGTTAGGC	XT3_UDN7239	ACTCTTCCTT	0.85	6.22
18	BNP20200815_203_24930	PT	XT3_UDN5220	AACATACCTA	XT3_UDN7220	GCGTACTTAG	0.77	4.28
19	BNP20200815_203_24991	PT	XT3_UDN5203	TTAATAGACC	XT3_UDN7203	GTAGCATACT	0.57	2.15
20	BNP20200815_204_24317	PT	XT4_UDN5314	GTTGTACTCA	XT4_UDN7314	AGCGTGAATG	0.81	4.89
21	BNP20200815_204_24495	PT	XT4_UDN5347	TGGCACGACC	XT4_UDN7347	TGTGTAAGCT	0.67	2.42
22	BNP20200815_204_24641	PT	XT2_UDN5181	AATTGGCGGA	XT2_UDN7181	TGTTCGCATT	0.8	4.53
23	BNP20200815_204_24890	PT	XT2_UDN5157	AGATATGGCG	XT2_UDN7157	CGCAATCTAG	0.74	3.53
24	BNP20200815_204_24901	PT	XT2_UDN5108	ATGTCGTGGT	XT2_UDN7108	CATGAGTACT	0.73	3.01
25	BNP20200815_204_24905	PT	XT2_UDN5138	CGGTCCGATA	XT2_UDN7138	AATATTGGCC	0.81	5.06
26	BNP20210521_28030_A_25063	LT	XT1_UDN5039	GCTGTAGGAA	XT1_UDN7039	CAATCGGCTG	0.81	4.62
27	BNP20210521_28038_A_24392	LT	XT1_UDN5051	ACTGTTGTGA	XT1_UDN7051	CCTGTCTGTC	0.86	6.65
28	BNP20210521_28038_A_24992	LT	XT1_UDN5015	GAATGCACGA	XT1_UDN7015	TCCATTGCCG	0.83	5.33
29	BNP20210521_28038_B_24815	LT	XT2_UDN5138	CGGTCCGATA	XT2_UDN7138	AATATTGGCC	0.74	3.41
30	BNP20210521_28038_C_24548	LT	XT2_UDN5141	GATAACAAGT	XT2_UDN7141	GGCCAATAAG	0.82	4.74
31	BNP20210521_28038_D_24947	LT	XT1_UDN5077	CGTTGCTTAC	XT1_UDN7077	TCTGGTATCC	0.89	7.99
32	BNP20210521_28038_E_24924	LT	XT1_UDN5048	TAACAATAGG	XT1_UDN7048	CAGTGGCACT	0.8	4.45
33	BNP20210521_28038_F_24602	LT	XT3_UDN5226	GACCGGAGAT	XT3_UDN7226	AGATATGGCG	0.8	4.81
34	BNP20210521_28038_G_24423	LT	XT2_UDN5192	GAGTTGTACT	XT2_UDN7192	GTGTTACCGG	0.85	5.89
35	BNP20210521_28038_H_24767	LT	XT1_UDN5076	ACGGCCGTCA	XT1_UDN7076	CTGACTCTAC	0.8	4.36
36	BNP20210521_28038_I_24477	LT	XT1_UDN5014	CGGCTCTACT	XT1_UDN7014	GAAGCGGCAC	0.77	4.24
37	BNP20210521_28039_A_24763	LT	XT4_UDN5291	ACTCTACAGG	XT4_UDN7291	GACTTAGAAG	0.61	2.15
38	BNP20210521_31001_A_24545	LT	XT4_UDN5299	TATCATGAGA	XT4_UDN7299	AGTGAGTGAA	0.69	2.85
39	BNP20210521_31001_B_25017	LT	XT1_UDN5080	CAAGCATCCG	XT1_UDN7080	GGCAAGCCAG	0.89	7.29
40	BNP20210521_31001_C_24461	LT	XT2_UDN5100	GCACTACAAC	XT2_UDN7100	TCTCCATTGA	0.88	8.19
41	BNP20210521_31001_D_24432	LT	XT2_UDN5097	CCTGATACAA	XT2_UDN7097	CTGACCGGCA	0.65	2.51
42	BNP20210521_31001_E_24932	LT	XT1_UDN5055	CTTAACCACT	XT1_UDN7055	CTGAGGAATA	0.87	6.49
43	BNP20210521_31001_G_24870	LT	XT1_UDN5025	GGCGAGATGG	XT1_UDN7025	AACCATAGAA	0.82	5.07
44	BNP20210521_31001_H_24485	LT	XT1_UDN5030	CTTATGGAAT	XT1_UDN7030	CCACCAGGCA	0.79	4.65

ID	sample	CS	adapter_p5	tag_p5_5to3	adapter_p7	tag_p7_5to3	cov	depth
45	BNP20210521_31001_I_25025	LT	XT1_UDN5045	CCATAAGGTT	XT1_UDN7045	CGTTATTCTA	0.89	7.63
46	BNP20210521_31001_J_24954	LT	XT2_UDN5125	CTCGTGCGTT	XT2_UDN7125	TCCACGGCCT	0.85	5.83
47	BNP20210521_31002_A_24943	LT	XT3_UDN5274	CTAGTCCGGA	XT3_UDN7274	AATAGGCCTC	0.45	1.25
48	BNP20210521_31012_A_24694	LT	XT1_UDN5047	CGGTGGCGAA	XT1_UDN7047	GTCCTGGATA	0.82	4.85
49	BNP20210521_31018_A_24819	LT	XT3_UDN5258	GCAACAGGTG	XT3_UDN7258	TCTACCGCTG	0.75	3.16
50	BNP20210521_31035_A_24598	LT	XT2_UDN5119	CTCCGTGCTG	XT2_UDN7119	AATTGGCGGA	0.88	7.83
51	BNP20210521_31060_A_24369	LT	XT3_UDN5273	GAGTGTGCCG	XT3_UDN7273	GTATCATTGG	0.82	4.92
52	BNP20210521_202_24381	PT	XT2_UDN5108	ATGTCGTGGT	XT2_UDN7108	CATGAGTACT	0.8	4.36
53	BNP20210521_202_24422	PT	XT3_UDN5278	CCGTGGCCTT	XT3_UDN7278	ACTTGTCCAC	0.85	6.37
54	BNP20210521_202_24467	PT	XT3_UDN5215	CAGAGTGATA	XT3_UDN7215	ATTCTAAGCG	0.72	2.98
55	BNP20210521_202_24617	PT	XT3_UDN5283	TCTTGGCTAT	XT3_UDN7283	AGTGGTCAGG	0.81	5.53
56	BNP20210521_202_24630	PT	XT2_UDN5114	GTTAATCTGA	XT2_UDN7114	TCCAATTCTA	0.8	4.95
57	BNP20210521_202_24663	PT	XT3_UDN5199	GGACCAACAG	XT3_UDN7199	CAGTCGTGCG	0.79	3.6
58	BNP20210521_202_24709	PT	XT3_UDN5200	AATGTATTGC	XT3_UDN7200	GTCTAACCTC	0.82	4.93
59	BNP20210521_202_24796	PT	XT3_UDN5227	CGTTCAGCCT	XT3_UDN7227	AATATGAAGC	0.77	3.72
60	BNP20210521_202_24810	PT	XT3_UDN5279	GGATATATCC	XT3_UDN7279	TGTACTTGTT	0.75	3.8
61	BNP20210521_202_24984	PT	XT3_UDN5287	TGGCTCGCAG	XT3_UDN7287	AGAAGCCAAT	0.87	7.11
62	BNP20210521_203_24546	PT	XT3_UDN5216	TGCTAACTAT	XT3_UDN7216	AGCGCTTCGG	0.76	3.74
63	BNP20210521_203_24690	PT	XT3_UDN5241	CTTCGAAGGA	XT3_UDN7241	TCCGCGTTCA	0.83	5.79
64	BNP20210521_203_24702	PT	XT2_UDN5154	CGCCTTCTGA	XT2_UDN7154	AACTCCGAAC	0.76	4.6
65	BNP20210521_203_24749	PT	XT3_UDN5220	AACATACCTA	XT3_UDN7220	GCGTACTTAG	0.76	3.66
66	BNP20210521_203_24856	PT	XT3_UDN5263	TTGAGCCTAA	XT3_UDN7263	ATACTGTGTG	0.77	5.31
67	BNP20210521_203_24869	PT	XT3_UDN5288	AACTAACGTT	XT3_UDN7288	TAATCGGTAC	0.79	4.84
68	BNP20210521_203_25024	PT	XT1_UDN5007	TGGAACAGTA	XT1_UDN7007	CTAGTGCTCT	0.68	3.31
69	BNP20210521_205_24386	PT	XT2_UDN5173	TCCTATTAGC	XT2_UDN7173	AGCGGTGGAC	0.83	5.35
70	BNP20210521_205_24400	PT	XT3_UDN5195	AGATTGTTAC	XT3_UDN7195	GTCTCGTGAA	0.54	2.48
71	BNP20210521_205_24401	PT	XT2_UDN5117	CCGAACGTTG	XT2_UDN7117	TCGGTCACGG	0.84	5.13
72	BNP20210521_205_24405	PT	XT2_UDN5112	CCAACAACAT	XT2_UDN7112	GTAGCCATCA	0.68	2.79
73	BNP20210521_205_24412	PT	XT4_UDN5341	CGTATAATCA	XT4_UDN7341	ATCGTCGCTC	0.63	2.27
74	BNP20210521_205_24489	PT	XT3_UDN5228	TTACTTCCTC	XT3_UDN7228	TAGCGCTAGT	0.26	0.7
75	BNP20210521_205_24659	PT	XT4_UDN5383	AATCCTTAGG	XT4_UDN7383	CAAGTTCATA	0.87	7.24
76	BNP20210521_205_24741	PT	XT4_UDN5294	TGTGCTAACA	XT4_UDN7294	CGTGTATCTT	0.8	4.28
77	BNP20210521_205_24851	PT	XT2_UDN5107	ATCTTACTGT	XT2_UDN7107	TATTGCGTTC	0.7	3.3
78	BNP20210521_205_25038	PT	XT3_UDN5267	GCTACATTAG	XT3_UDN7267	TCGCCGGTTA	0.85	6.28
79	BNP20210604_26068_A_25039	LT	XT2_UDN5111	TGTTGTTCGT	XT2_UDN7111	CCTTGTTAAT	0.88	7.9
80	BNP20210604_28030_A_24948	LT	XT4_UDN5372	CTATACGCGG	XT4_UDN7372	ATAGACCGTT	0.86	6.73
81	BNP20210604_28038_A_24899	LT	XT2_UDN5123	TAGGTTCTCT	XT2_UDN7123	TTCCTGTACG	0.34	1.87
82	BNP20210604_28038_B_24445	LT	XT2_UDN5104	CCACGACACG	XT2_UDN7104	TTAATAGACC	0.84	5.79
83	BNP20210604_28038_C_24940	LT	XT1_UDN5066	AATTGCTGCG	XT1_UDN7066	ATACCAACGC	0.86	6.56
84	BNP20210604_28039_A_24366	LT	XT4_UDN5314	GTTGTACTCA	XT4_UDN7314	AGCGTGAATG	0.84	5.52
85	BNP20210604_28043_A_24881	LT	XT4_UDN5360	AAGGCCACCT	XT4_UDN7360	ATCCTTGTCG	0.8	4.4
86	BNP20210604_28047_A_24632	LT	XT1_UDN5037	GATCACCGCG	XT1_UDN7037	TGTAATCGAC	0.79	4.4
87	BNP20210604_31001_A_24962	LT	XT1_UDN5040	CGCACTAATG	XT1_UDN7040	TATGTAGTCA	0.83	5.09
88	BNP20210604_31001_B_24846	LT	XT1_UDN5093	TATGTGCAAT	XT1_UDN7093	ACATATCCAG	0.79	4.36
89	BNP20210604_31001_C_24469	LT	XT2_UDN5097	CCTGATACAA	XT2_UDN7097	CTGACCGGCA	0.88	8.14
90	BNP20210604_31001_C_24494	LT	XT2_UDN5136	ACGCTAATTA	XT2_UDN7136	TGGTGCCTGG	0.66	2.72
91	BNP20210604_31002_A_24365	LT	XT3_UDN5246	TACGCACGTA	XT3_UDN7246	AGTGGATAAT	0.88	7.93
92	BNP20210604_31004_A_24518	LT	XT4_UDN5307	TGCTGGACAT	XT4_UDN7307	GTGCTAGGTG	0.81	4.53
93	BNP20210604_31007_A_24664	LT	XT2_UDN5164	AGGATAAGTT	XT2_UDN7164	CTGGTACACG	0.88	7.57
94	BNP20210604_31016_A_24710	LT	XT2_UDN5151	ACAGAGGCCA	XT2_UDN7151	CCTGATACAA	0.86	7.22
95	BNP20210604_31018_A_24803	LT	XT3_UDN5261	AGCCGGAACA	XT3_UDN7261	CTAATTCGCT	0.4	1.01
96	BNP20210604_31022_A_24821	LT	XT1_UDN5034	ACTAGCCGTG	XT1_UDN7034	CAGCCGCGTA	0.79	4.16
97	BNP20210604_31023_A_24679	LT	XT3_UDN5230	GCTACTATCT	XT3_UDN7230	CAGATACCAC	0.74	3.35
98	BNP20210604_31035_A_24693	LT	XT3_UDN5253	GACGTTCGCG	XT3_UDN7253	GGTATTGAGA	0.81	4.39
99	BNP20210604_31060_A_24929	LT	XT4_UDN5376	AGTATACGGA	XT4_UDN7376	GGACGTCTTG	0.71	3.13
100	BNP20210604_33034_A_24373	LT	XT3_UDN5280	CACCTCTTGG	XT3_UDN7280	CACTTAATCT	0.75	3.35
101	BNP20210615_26020_A_24715	LT	XT4_UDN5349	CAGTAGTTGT	XT4_UDN7349	TCGACTTAAG	0.51	1.6

ID	sample	CS	adapter_p5	tag_p5_5to3	adapter_p7	tag_p7_5to3	cov	depth
102	BNP20210615_26030_A_24554	LT	XT2_UDN5112	CCAACAACAT	XT2_UDN7112	GTAGCCATCA	0.82	6.3
103	BNP20210615_26068_A_24939	LT	XT2_UDN5135	TGAGACAGCG	XT2_UDN7135	ACAGAGGCCA	0.78	5.81
104	BNP20210615_28022_A_24972	LT	XT4_UDN5322	TCATCCTCTT	XT4_UDN7322	TGCCTACGAG	0.79	4.31
105	BNP20210615_28030_A_24455	LT	XT4_UDN5346	TTCCGACATT	XT4_UDN7346	TTCCTCCTTA	0.86	6.4
106	BNP20210615_28038_B_24696	LT	XT3_UDN5261	AGCCGGAACA	XT3_UDN7261	CTAATTCGCT	0.82	5.3
107	BNP20210615_28038_B_24986	LT	XT2_UDN5121	GGTTATGCTA	XT2_UDN7121	TAGGTTCTCT	0.7	3.29
108	BNP20210615_28038_C_25048	LT	XT3_UDN5284	ACGGAATGCG	XT3_UDN7284	CATTCCAGCT	0.68	3.5
109	BNP20210615_28038_D_24396	LT	XT1_UDN5046	ATCTCTACCA	XT1_UDN7046	AGATCCATTA	0.87	6.3
110	BNP20210615_28038_E_25001	LT	XT1_UDN5074	TGTTAGAAGG	XT1_UDN7074	TTCATAAGGT	0.72	2.86
111	BNP20210615_28039_A_24654	LT	XT4_UDN5334	TCTCACGCGT	XT4_UDN7334	ACCAGTCATT	0.61	2.22
112	BNP20210615_28041_A_24444	LT	XT2_UDN5147	GACCGCTGTG	XT2_UDN7147	TAAGGAACGT	0.76	5.09
113	BNP20210615_28043_A_24600	LT	XT1_UDN5012	GTGTGGCGCT	XT1_UDN7012	GAGTCATAGG	0.82	5.05
114	BNP20210615_28047_A_24639	LT	XT4_UDN5367	GTGGCGAGAC	XT4_UDN7367	CGCCATACCT	0.74	3.21
115	BNP20210615_28048_G_24723	LT	XT3_UDN5260	ACCGCGCAAT	XT3_UDN7260	CAATGGCGCC	0.75	4.02
116	BNP20210615_28049_A_24834	LT	XT3_UDN5254	CATTCAACAA	XT3_UDN7254	CAAGATGCTT	0.82	4.73
117	BNP20210615_28050_A_24474	LT	XT3_UDN5200	AATGTATTGC	XT3_UDN7200	GTCTAACCTC	0.75	3.31
118	BNP20210615_28054_A_24361	LT	XT4_UDN5327	GTCACGGTGT	XT4_UDN7327	TTGGATTCAA	0.62	2.18
119	BNP20210615_28060_A_24449	LT	XT4_UDN5342	ATGACAGAAC	XT4_UDN7342	GGTGCGTTCG	0.79	3.96
120	BNP20210615_28061_A_24860	LT	XT3_UDN5207	ACGAGACTGA	XT3_UDN7207	CCGCATATTC	0.84	5.94
121	BNP20210615_28063_A_24433	LT	XT4_UDN5342	ATGACAGAAC	XT4_UDN7342	GGTGCGTTCG	0.77	4.04
122	BNP20210615_28064_A_24845	LT	XT1_UDN5018	CTAATGATGG	XT1_UDN7018	AGAGGCAACC	0.85	5.94
123	BNP20210615_28066_B_25041	LT	XT2_UDN5142	AGTTATCACA	XT2_UDN7142	CAGTAGTTGT	0.8	4.44
125	BNP20210615_31001_A_24528	LT	XT3_UDN5251	TGCGGTGTTG	XT3_UDN7251	ATTAATACGC	0.42	1.12
126	BNP20210615_31001_B_24393	LT	XT1_UDN5061	AGGCATGTAG	XT1_UDN7061	TGGCTAATCA	0.74	3.58
127	BNP20210615_31001_C_24900	LT	XT2_UDN5177	GAGATGTCGA	XT2_UDN7177	TATATTCGAG	0.81	5.22
128	BNP20210615_31001_D_24516	LT	XT2_UDN5102	TCCACGGCCT	XT2_UDN7102	CAGGCGCCAT	0.87	7.05
129	BNP20210615_31001_D_24877	LT	XT1_UDN5024	CTAACTGTAA	XT1_UDN7024	TTCTACATAC	0.89	7.5
130	BNP20210615_31004_B_24917	LT	XT2_UDN5103	TTGTAGTGTA	XT2_UDN7103	ACATAACGGA	0.6	2.54
131	BNP20210615_31005_G_24936	LT	XT3_UDN5265	CCTCGCAACC	XT3_UDN7265	CGAGGCGGTA	0.61	1.92
132	BNP20210615_31007_B_24658	LT	XT1_UDN5042	AGTGGTCAGG	XT1_UDN7042	GTCTAATGGC	0.85	5.58
133	BNP20210615_31009_E_24742	LT	XT1_UDN5095	ATGTAGACAA	XT1_UDN7095	GTATTCCACC	0.84	5.61
134	BNP20210615_31010_A_25034	LT	XT4_UDN5289	TAGAGTTGGA	XT4_UDN7289	GGAATTGTTC	0.61	2.15
135	BNP20210615_31016_A_24697	LT	XT4_UDN5298	TTAGGCTTAC	XT4_UDN7298	CTCGACTCCT	0.86	6.83
136	BNP20210615_31018_D_24419	LT	XT4_UDN5304	TACGGCGAAG	XT4_UDN7304	AACGGAGCGG	0.69	2.68
137	BNP20210615_31022_A_24492	LT	XT1_UDN5010	ACCAGCGACA	XT1_UDN7010	AGTCAGACGA	0.81	4.63
138	BNP20210615_31023_E_24353	LT	XT2_UDN5118	TAACCGCCGA	XT2_UDN7118	GAACAAGTAT	0.81	4.69
139	BNP20210615_31035_A_24967	LT	XT4_UDN5337	AAGGCCTTGG	XT4_UDN7337	CCACCTTACA	0.71	2.98
140	BNP20210615_31039_A_24420	LT	XT3_UDN5242	GTAGAGTCAG	XT3_UDN7242	AGGTTGCAGG	0.72	2.66
141	BNP20210615_33034_A_24651	LT	XT4_UDN5324	AACGAGCCAG	XT4_UDN7324	CACCTCTTGG	0.83	5.37
142	BNP20210701_31005_A_24542	LT	XT4_UDN5349	CAGTAGTTGT	XT4_UDN7349	TCGACTTAAG	0.87	7.58
143	BNP20210701_31008_A_24559	LT	XT3_UDN5270	GTACTGGCGT	XT3_UDN7270	AGGATAAGTT	0.71	2.93
144	BNP20210701_31016_A_24468	LT	XT1_UDN5091	GGCCATCATA	XT1_UDN7091	TCAGAAGGCG	0.77	3.73
145	BNP20210701_31018_A_24497	LT	XT4_UDN5317	CACTTAATCT	XT4_UDN7317	GGAGATTAGT	0.56	1.76
146	BNP20210701_31022_A_24752	LT	XT4_UDN5302	CGGATTATAT	XT4_UDN7302	GGACCTCAAT	0.77	3.94
147	BNP20210701_31024_A_24529	LT	XT4_UDN5355	TCGATACTAG	XT4_UDN7355	AGCGCGGTGA	0.84	5.02
148	BNP20210701_31064_A_24770	LT	XT4_UDN5382	CAAGTTCATA	XT4_UDN7382	TCGTGGTTGA	0.25	0.71
149	BNP20210702_28008_A_24961	LT	XT3_UDN5214	GCCGTCTGTT	XT3_UDN7214	TCGCGTATAA	0.86	6.65
150	BNP20210702_28037_A_24515	LT	XT2_UDN5162	TCCTGACCGT	XT2_UDN7162	ACACCGTTAA	0.88	8.43
151	BNP20210702_28038_A_24555	LT	XT2_UDN5142	AGTTATCACA	XT2_UDN7142	CAGTAGTTGT	0.87	7.2
152	BNP20210702_28038_A_24997	LT	XT4_UDN5368	GCCAGATCCA	XT4_UDN7368	GCAGGCTGGA	0.75	3.41
153	BNP20210702_28038_B_24390	LT	XT1_UDN5067	TTACAATTCC	XT1_UDN7067	AGGATGTGCT	0.81	4.6
154	BNP20210702_28038_B_25040	LT	XT1_UDN5087	GATACCTCCT	XT1_UDN7087	CCTCTACATG	0.86	5.8
155	BNP20210702_28041_A_25003	LT	XT4_UDN5336	TCGAATGGAA	XT4_UDN7336	TTGAGCCTAA	0.89	7.79
156	BNP20210702_28043_A_24956	LT	XT4_UDN5301	GAATTGAGTG	XT4_UDN7301	GCTCTCGTTG	0.72	2.89
157	BNP20210702_28047_A_24773	LT	XT3_UDN5193	AACACGTGGA	XT3_UDN7193	TATCATGAGA	0.78	3.67
158	BNP20210702_28048_A_24425	LT	XT4_UDN5311	ATACACAGAG	XT4_UDN7311	TGCACGAGAA	0.83	4.69
159	BNP20210702_28049_A_25047	LT	XT2_UDN5140	CGGTTATTAG	XT2_UDN7140	CCTTCACGTA	0.4	2.58

ID	sample	CS	adapter_p5	tag_p5_5to3	adapter_p7	tag_p7_5to3	cov	depth
160	BNP20210702_28050_A_24360	LT	XT3_UDN5212	TAAGACCTAT	XT3_UDN7212	GTGCGGTAAG	0.79	4.06
161	BNP20210702_28058_A_25022	LT	XT3_UDN5240	TGGTGAGTCT	XT3_UDN7240	GTCTCCTTCC	0.7	2.93
162	BNP20210702_28060_A_24362	LT	XT4_UDN5316	AGTCCGAGGA	XT4_UDN7316	TGTACCGAAT	0.68	2.5
163	BNP20210702_28061_A_24983	LT	XT4_UDN5328	GGTGTACAAG	XT4_UDN7328	ACTAGCCGTG	0.82	4.68
164	BNP20210702_28064_A_24510	LT	XT4_UDN5375	TCTCAGTACA	XT4_UDN7375	ACTGAATAGA	0.87	7.2
165	BNP20210702_28066_A_24583	LT	XT2_UDN5160	TGGCGGTCCA	XT2_UDN7160	GCTCCGTCAC	0.82	5.22
166	BNP20210714_31001_A_24797	LT	XT3_UDN5225	AGTACCTATA	XT3_UDN7225	GCTTCCACTA	0.84	5.63
167	BNP20210714_31004_A_24838	LT	XT3_UDN5221	CCATGTGTAG	XT3_UDN7221	TACCGAACTA	0.81	5.14
168	BNP20210714_31005_A_24348	LT	XT2_UDN5144	CATGTAGAGG	XT2_UDN7144	CAATTGGATT	0.68	2.99
169	BNP20210714_31007_A_24914	LT	XT3_UDN5214	GCCGTCTGTT	XT3_UDN7214	TCGCGTATAA	0.8	4.01
170	BNP20210714_31008_A_24364	LT	XT4_UDN5373	GTTGCAGTTG	XT4_UDN7373	TGAACGCAAC	0.66	2.41
171	BNP20210714_31009_A_24682	LT	XT4_UDN5330	TAATACGGAG	XT4_UDN7330	GAAGCTAGCT	0.87	6.65
172	BNP20210714_31010_A_24758	LT	XT2_UDN5153	TATTCCTCAG	XT2_UDN7153	TTCAGCGTGG	0.73	4.08
173	BNP20210714_31022_A_24784	LT	XT4_UDN5361	CTGTGAGCTA	XT4_UDN7361	GAAGGTACAC	0.88	8.15
174	BNP20210714_31023_A_24918	LT	XT4_UDN5319	GCGACTCGAT	XT4_UDN7319	TAGGTCGTTG	0.87	6.81
175	BNP20210714_31024_A_24789	LT	XT3_UDN5256	TTGAGGACGG	XT3_UDN7256	TTATCTTGCA	0.82	4.44
176	BNP20210714_31052_A_25011	LT	XT3_UDN5276	CCTAGAGTAT	XT3_UDN7276	TCCTAGGAAG	0.81	5.48
177	BNP20210714_31064_A_24907	LT	XT3_UDN5249	CAGCGGACAA	XT3_UDN7249	TGCTGGACAT	0.83	5.27
178	BNP20210716_28037_A_24840	LT	XT4_UDN5356	TACCACAATG	XT4_UDN7356	CAAGGCTATC	0.89	8.62
179	BNP20210716_28038_A_24774	LT	XT1_UDN5029	TCCGACCTCG	XT1_UDN7029	GCCGCACTCT	0.87	7.27
180	BNP20210716_28047_A_24822	LT	XT3_UDN5237	GTCACCACAG	XT3_UDN7237	TAAGACCTAT	0.88	7.38
181	BNP20210716_28048_A_24638	LT	XT4_UDN5353	GACTATATGT	XT4_UDN7353	GTGTGATATC	0.57	1.9
182	BNP20210716_28050_A_24968	LT	XT3_UDN5252	ACATAACGGA	XT3_UDN7252	TAGTCACAAC	0.64	2.44
183	BNP20210716_28058_A_24643	LT	XT4_UDN5318	TACTCTGTTA	XT4_UDN7318	TACTAACACA	0.81	5.24
184	BNP20210716_28061_A_24692	LT	XT3_UDN5227	CGTTCAGCCT	XT3_UDN7227	AATATGAAGC	0.67	2.95
185	BNP20210716_28064_A_24500	LT	XT2_UDN5172	CATAACACCA	XT2_UDN7172	CAACCGGAGG	0.71	3.58
187	BNP20210802_31022_A_24572	LT	XT3_UDN5234	GACAGACAGG	XT3_UDN7234	GTCACCACAG	0.85	5.85
188	BNP20210802_31058_A_24587	LT	XT4_UDN5294	TGTGCTAACA	XT4_UDN7294	CGTGTATCTT	0.88	7.9
189	BNP20210802_202_17907	PT	XT1_UDN5089	CGTGTATCTT	XT1_UDN7089	GTCCGTAAGC	0.52	2.13
190	BNP20210802_202_17917	PT	XT1_UDN5082	CTCATAGCGA	XT1_UDN7082	ACCGTTACAA	0.69	3.76
191	BNP20210802_202_17918	PT	XT1_UDN5090	GAACCATGAA	XT1_UDN7090	ACTTCAAGCG	0.63	3.37
192	BNP20210802_202_17928	PT	XT1_UDN5083	AGACACATTA	XT1_UDN7083	TATGCCTTAC	0.67	3.36
193	BNP20210802_202_17929	PT	XT1_UDN5091	GGCCATCATA	XT1_UDN7091	TCAGAAGGCG	0.68	3.68
194	BNP20210802_202_17940	PT	XT1_UDN5084	GCGCGATGTT	XT1_UDN7084	ACAAGTGGAC	0.76	5.51
195	BNP20210802_202_17941	PT	XT1_UDN5092	ACATACTTCC	XT1_UDN7092	GCGTTGGTAT	0.74	5.19
196	BNP20210802_202_17942	PT	XT1_UDN5005	ACATTATCCT	XT1_UDN7005	GACGAGATTA	0.75	5.49
197	BNP20210802_202_17952	PT	XT1_UDN5093	TATGTGCAAT	XT1_UDN7093	ACATATCCAG	0.74	5.96
198	BNP20210802_202_17953	PT	XT1_UDN5006	GTCCACTTGT	XT1_UDN7006	AACATCGCGC	0.69	4.01
199	BNP20210803_28037_A_24718	LT	XT2_UDN5189	GGCAGTAGCA	XT2_UDN7189	TGCGGTGTTG	0.58	4.31
200	BNP20210803_28038_A_24727	LT	XT1_UDN5016	AAGACTATAG	XT1_UDN7016	CGGTTACGGC	0.49	1.81
201	BNP20210803_28047_A_24389	LT	XT3_UDN5245	ACTGCCTTAT	XT3_UDN7245	TGGTCTAGTG	0.85	5.77
202	BNP20210803_28054_A_24387	LT	XT1_UDN5058	TACTAGTCAA	XT1_UDN7058	CTCGCTTCGG	0.77	3.96
204	BNP20210803_28058_A_24989	LT	XT4_UDN5352	ATTAGTGGAG	XT4_UDN7352	ACGGAATGCG	0.73	3.03
205	BNP20210803_28060_A_24363	LT	XT3_UDN5237	GTCACCACAG	XT3_UDN7237	TAAGACCTAT	0.82	4.76
207	BNP20210803_28064_B_24618	LT	XT1_UDN5082	CTCATAGCGA	XT1_UDN7082	ACCGTTACAA	0.89	8.32
208	BNP20210803_28066_B_24839	LT	XT2_UDN5131	GAACAAGTAT	XT2_UDN7131	TCACACCGAA	0.88	7.57
209	BNP20210803_31004_A_24388	LT	XT1_UDN5028	TCGTATGCGG	XT1_UDN7028	ACCACGACAT	0.81	4.57
210	BNP20210803_201_17947	PT	XT1_UDN5053	AGCACATCCT	XT1_UDN7053	GGAATTGTAA	0.73	4.32
211	BNP20210803_201_17948	PT	XT1_UDN5061	AGGCATGTAG	XT1_UDN7061	TGGCTAATCA	0.73	3.33
212	BNP20210803_201_17959	PT	XT1_UDN5054	TTCCGTCGCA	XT1_UDN7054	GCATAAGCTT	0.67	3.7
213	BNP20210803_201_17969	PT	XT1_UDN5047	CGGTGGCGAA	XT1_UDN7047	GTCCTGGATA	0.74	4.14
214	BNP20210803_201_17970	PT	XT1_UDN5055	CTTAACCACT	XT1_UDN7055	CTGAGGAATA	0.68	3.38
215	BNP20210803_201_17971	PT	XT1_UDN5063	TTGGCTCCGC	XT1_UDN7063	ATTGCGCGGT	0.76	4.81
216	BNP20210803_201_17975	PT	XT1_UDN5095	ATGTAGACAA	XT1_UDN7095	GTATTCCACC	0.74	4.71
217	BNP20210803_201_17980	PT	XT1_UDN5048	TAACAATAGG	XT1_UDN7048	CAGTGGCACT	0.63	3.03
218	BNP20210803_201_17981	PT	XT1_UDN5056	GCCTCGGATA	XT1_UDN7056	AACGCACGAG	0.63	3.09
219	BNP20210803_201_17982	PT	XT1_UDN5064	AACTGATACT	XT1_UDN7064	TGGCGCGAAC	0.62	2.91

ID	sample	CS	adapter_p5	tag_p5_5to3	adapter_p7	tag_p7_5to3	cov	depth
220	BNP20210803_203_17900	PT	XT1_UDN5025	GGCGAGATGG	XT1_UDN7025	AACCATAGAA	0.58	2.35
221	BNP20210803_203_17901	PT	XT1_UDN5033	GTCGATTACA	XT1_UDN7033	TGATTATACG	0.69	3.45
222	BNP20210803_203_17910	PT	XT1_UDN5026	AATAGAGCAA	XT1_UDN7026	GGTTGCGAGG	0.72	3.92
223	BNP20210803_203_17911	PT	XT1_UDN5034	ACTAGCCGTG	XT1_UDN7034	CAGCCGCGTA	0.7	3.46
224	BNP20210803_203_17921	PT	XT1_UDN5019	GGTTGCCTCT	XT1_UDN7019	CCATCATTAG	0.71	3.76
225	BNP20210803_203_17922	PT	XT1_UDN5027	TCAATCCATT	XT1_UDN7027	TAAGCATCCA	0.68	3.23
226	BNP20210803_203_17923	PT	XT1_UDN5035	AAGTTGGTGA	XT1_UDN7035	GGTAACTCGC	0.68	3.31
227	BNP20210803_203_17932	PT	XT1_UDN5020	CGCACATGGC	XT1_UDN7020	GATAGGCCGA	0.69	3.44
228	BNP20210803_203_17933	PT	XT1_UDN5028	TCGTATGCGG	XT1_UDN7028	ACCACGACAT	0.7	3.59
229	BNP20210803_203_17934	PT	XT1_UDN5036	TGGCAATATT	XT1_UDN7036	ACCGGCCGTA	0.76	4.91
230	BNP20210812_31002_A_25052	LT	XT4_UDN5339	CCGCTTAGCT	XT4_UDN7339	TCACTCATGT	0.7	2.79
231	BNP20210812_31004_A_24656	LT	XT1_UDN5065	GTAAGGCATA	XT1_UDN7065	TAATGTGTCT	0.83	4.94
232	BNP20210812_31004_A_24735	LT	XT2_UDN5131	GAACAAGTAT	XT2_UDN7131	TCACACCGAA	0.87	8.01
233	BNP20210812_31005_A_24872	LT	XT4_UDN5374	TTATGCGCCT	XT4_UDN7374	GTGGTTGAAG	0.81	4.91
235	BNP20210812_31016_A_24875	LT	XT4_UDN5357	TGGTATACCA	XT4_UDN7357	TGCGTCCAGG	0.8	4.13
236	BNP20210812_31022_B_24673	LT	XT1_UDN5021	GGCCTGTCCT	XT1_UDN7021	ATGGTTGACT	0.87	7.02
237	BNP20210812_31064_A_24980	LT	XT4_UDN5379	TACACGCTCC	XT4_UDN7379	CAGTATCAAT	0.88	7.1
238	BNP20210813_28038_A_24711	LT	XT1_UDN5038	TACCATCCGT	XT1_UDN7038	GTGCAGACAG	0.83	5.09
240	BNP20210813_28058_A_24368	LT	XT3_UDN5267	GCTACATTAG	XT3_UDN7267	TCGCCGGTTA	0.77	3.42
241	BNP20210813_28060_A_24577	LT	XT3_UDN5253	GACGTTCGCG	XT3_UDN7253	GGTATTGAGA	0.7	2.78
242	BNP20210813_28063_A_24551	LT	XT3_UDN5281	AACGTTACAT	XT3_UDN7281	CAGAGTGATA	0.68	2.76
243	BNP20210813_28064_A_24760	LT	XT4_UDN5384	GGTGGAATAC	XT4_UDN7384	CTTAACCACT	0.83	5.26
244	BNP20210822_28038_A_24830	LT	XT3_UDN5223	GCTATGCGCA	XT3_UDN7223	GGTTATGCTA	0.83	5.41
245	BNP20210824_28047_A_24790	LT	XT2_UDN5158	CCTGCTTGGT	XT2_UDN7158	AACCGCATCG	0.83	5.98
246	BNP20210826_31002_A_24719	LT	XT2_UDN5159	GACGAACAAT	XT2_UDN7159	CTAGTCCGGA	0.83	5.14
247	BNP20210826_31004_B_24933	LT	XT2_UDN5114	GTTAATCTGA	XT2_UDN7114	TCCAATTCTA	0.74	3.54
248	BNP20210826_31005_A_24953	LT	XT1_UDN5060	ACAGTTCCAG	XT1_UDN7060	TTACCTGGAA	0.85	5.58
249	BNP20210826_31064_A_24669	LT	XT4_UDN5312	TCTCGGACGA	XT4_UDN7312	ACTTCCTAGC	0.73	3.01
250	BNP20210923_31002_A_24766	LT	XT1_UDN5032	GAACATACGG	XT1_UDN7032	ACAGTGTATG	0.84	5.8
251	BNP20210923_31016_A_24354	LT	XT2_UDN5159	GACGAACAAT	XT2_UDN7159	CTAGTCCGGA	0.77	4.67
252	BNP20210923_31064_A_24605	LT	XT4_UDN5310	CTCGACTCCT	XT4_UDN7310	AAGAGAGGTG	0.63	3.02
253	BNP20210924_28050_A_25023	LT	XT1_UDN5063	TTGGCTCCGC	XT1_UDN7063	ATTGCGCGGT	0.63	2.26
254	BNP20210924_28057_A_24931	LT	XT1_UDN5049	CTGGTACACG	XT1_UDN7049	AGTGTTGCAC	0.77	4.18
255	FOR20210517_447_24319	PT	XT4_UDN5301	GAATTGAGTG	XT4_UDN7301	GCTCTCGTTG	0.84	5.19
256	FOR20210517_447_24320	PT	XT4_UDN5292	CGGTGACACC	XT4_UDN7292	TGGCAATATT	0.79	4.23
257	FOR20210517_447_24326	PT	XT3_UDN5262	TCCTAGGAAG	XT3_UDN7262	CATGGTCTAA	0.86	6.65
258	FOR20210517_447_24371	PT	XT3_UDN5235	TGTACTTGTT	XT3_UDN7235	ATTAGTGGAG	0.83	5.29
259	FOR20210517_447_24374	PT	XT1_UDN5005	ACATTATCCT	XT1_UDN7005	GACGAGATTA	0.75	3.94
260	FOR20210517_447_24394	PT	XT1_UDN5022	CTGTGTTAGG	XT1_UDN7022	TATTGCGCTC	0.81	4.95
261	FOR20210517_447_24416	PT	XT2_UDN5140	CGGTTATTAG	XT2_UDN7140	CCTTCACGTA	0.84	5.61
262	FOR20210517_447_24476	PT	XT3_UDN5286	ACCAAGTTAC	XT3_UDN7286	CCTTACTATG	0.85	6.95
263	FOR20210517_447_24568	PT	XT3_UDN5278	CCGTGGCCTT	XT3_UDN7278	ACTTGTCCAC	0.58	1.77
264	FOR20210517_447_24592	PT	XT3_UDN5208	GTATCGGCCG	XT3_UDN7208	TTATCCGATC	0.85	6.45
265	FOR20210517_447_24795	PT	XT2_UDN5103	TTGTAGTGTA	XT2_UDN7103	ACATAACGGA	0.83	5.38
266	FOR20210517_447_24835	PT	XT4_UDN5366	CCTTACTATG	XT4_UDN7366	GCGCAGAGTA	0.65	2.35
267	FOR20210517_447_24909	PT	XT2_UDN5099	CGGACAGTGA	XT2_UDN7099	GCGTGTGAGA	0.65	2.7
268	FOR20210517_447_24982	PT	XT3_UDN5282	CGGCAAGCTC	XT3_UDN7282	GGCGAATTCT	0.57	1.7
269	FOR20210517_447_25053	PT	XT4_UDN5329	AGGTTGCAGG	XT4_UDN7329	CGGCAAGCTC	0.74	3.28
270	FOR20210517_448_24325	PT	XT4_UDN5299	TATCATGAGA	XT4_UDN7299	AGTGAGTGAA	0.83	6.37
271	FOR20210517_448_24430	PT	XT1_UDN5054	TTCCGTCGCA	XT1_UDN7054	GCATAAGCTT	0.81	4.6
272	FOR20210517_448_24482	PT	XT4_UDN5361	CTGTGAGCTA	XT4_UDN7361	GAAGGTACAC	0.69	2.73
273	FOR20210517_448_24521	PT	XT2_UDN5113	ACCGGCTCAG	XT2_UDN7113	CTTGTAATTC	0.81	5.1
274	FOR20210517_448_24537	PT	XT4_UDN5319	GCGACTCGAT	XT4_UDN7319	TAGGTCGTTG	0.65	2.35
275	FOR20210517_448_24799	PT	XT3_UDN5222	GAGTCTCTCC	XT3_UDN7222	GTAGTAATAG	0.86	6.48
276	FOR20210517_448_24820	PT	XT3_UDN5204	GGAGTCGCGA	XT3_UDN7204	CTTCAGTTAC	0.7	2.86
277	FOR20210517_448_24852	PT	XT3_UDN5217	TCAGTTAATG	XT3_UDN7217	GTTGATAGTG	0.88	8.19
278	FOR20210517_448_24891	PT	XT2_UDN5147	GACCGCTGTG	XT2_UDN7147	TAAGGAACGT	0.76	3.61

ID	sample	CS	adapter_p5	tag_p5_5to3	adapter_p7	tag_p7_5to3	cov	depth
279	FOR20210517_448_25028	PT	XT3_UDN5279	GGATATATCC	XT3_UDN7279	TGTACTTGTT	0.49	1.48
280	FOR20210517_448_25046	PT	XT3_UDN5260	ACCGCGCAAT	XT3_UDN7260	CAATGGCGCC	0.45	1.26
281	FOR20210517_448_25054	PT	XT1_UDN5003	TATAGTAGCT	XT1_UDN7003	CGTCTCATAT	0.87	6.96
282	FOR20210526_446_24350	TT	XT4_UDN5378	GGAGTAGATT	XT4_UDN7378	AGAACCGCGG	0.87	6.78
283	FOR20210526_446_24351	TT	XT3_UDN5212	TAAGACCTAT	XT3_UDN7212	GTGCGGTAAG	0.82	5.15
284	FOR20210526_446_24552	TT	XT4_UDN5309	GGCTTAATTG	XT4_UDN7309	CTTGTCTTAA	0.79	4.16
285	FOR20210526_446_24606	TT	XT2_UDN5105	TGTGATGTAT	XT2_UDN7105	ACGATTGCTG	0.84	5.59
286	FOR20210526_446_24610	TT	XT3_UDN5206	CGTAATTAAC	XT3_UDN7206	ACAGTTCCAG	0.88	8.38
287	FOR20210526_446_24621	TT	XT4_UDN5381	CTCAAGGCCG	XT4_UDN7381	ATGAGAACCA	0.67	2.95
288	FOR20210526_446_24629	TT	XT3_UDN5273	GAGTGTGCCG	XT3_UDN7273	GTATCATTGG	0.68	2.91
289	FOR20210526_446_24701	TT	XT3_UDN5205	AACGCCAGAG	XT3_UDN7205	AGTCCGAGGA	0.85	5.15
290	FOR20210526_446_24731	TT	XT4_UDN5295	CCAGAAGTAA	XT4_UDN7295	ATTCATTGCA	0.83	5.16
291	FOR20210526_446_24850	TT	XT4_UDN5343	ATTCATTGCA	XT4_UDN7343	CGGCGTAAGA	0.81	4.9
292	FOR20210526_446_24950	TT	XT4_UDN5364	ACTGCAGCCG	XT4_UDN7364	AGCATTAACT	0.3	0.77
293	FOR20210526_446_24976	TT	XT1_UDN5081	TCGTCTGACT	XT1_UDN7081	TGTCGCTGGT	0.87	7.17
294	FOR20210526_446_25030	TT	XT3_UDN5197	CTGACCGGCA	XT3_UDN7197	ACAACCAGGA	0.84	5.39
295	FOR20210526_446_25045	TT	XT4_UDN5298	TTAGGCTTAC	XT4_UDN7298	CTCGACTCCT	0.84	5.06
296	FOR20210526_446_25055	TT	XT2_UDN5160	TGGCGGTCCA	XT2_UDN7160	GCTCCGTCAC	0.86	6.5
297	FOR20210526_451_24458	TT	XT3_UDN5271	AGTTAAGAGC	XT3_UDN7271	GAGACATAAT	0.73	3
298	FOR20210526_451_24557	TT	XT4_UDN5321	CCTCTTCGAA	XT4_UDN7321	CTAGCGTCGA	0.81	4.66
299	FOR20210526_451_24622	TT	XT2_UDN5124	TATGGCTCGA	XT2_UDN7124	GGTAACGCAG	0.87	7.62
300	FOR20210526_451_24647	TT	XT4_UDN5315	TCAGGTCAAC	XT4_UDN7315	CCTTAGTGCC	0.81	4.44
301	FOR20210526_451_24650	TT	XT1_UDN5053	AGCACATCCT	XT1_UDN7053	GGAATTGTAA	0.8	4.49
302	FOR20210526_451_24720	TT	XT3_UDN5268	TACGAATCTT	XT3_UDN7268	AGACTCTCTT	0.84	5.7
303	FOR20210526_451_24771	TT	XT4_UDN5313	ACCACGTCTG	XT4_UDN7313	GTGCTATTAA	0.63	2.18
304	FOR20210526_451_24990	TT	XT4_UDN5332	ATTGACACAT	XT4_UDN7332	GCAACAGGTG	0.74	3.86
305	FOR20210610_446_24342	TT	XT2_UDN5184	CAACGTCAGC	XT2_UDN7184	ATACCTGGAT	0.51	2.14
306	FOR20210610_446_24349	TT	XT4_UDN5360	AAGGCCACCT	XT4_UDN7360	ATCCTTGTCG	0.55	2
307	FOR20210610_446_24447	TT	XT4_UDN5335	CTCTGACGTG	XT4_UDN7335	CCGGAATCAT	0.82	4.63
308	FOR20210610_446_24452	TT	XT2_UDN5098	TTAAGTTGTG	XT2_UDN7098	GAATTGAGTG	0.89	7.52
309	FOR20210610_446_24512	TT	XT4_UDN5306	CGAGACCAAG	XT4_UDN7306	AACATACCTA	0.84	4.79
310	FOR20210610_446_24562	TT	XT2_UDN5187	CTAATGTCTT	XT2_UDN7187	GTGTGGCGCT	0.83	5.12
311	FOR20210610_446_24574	TT	XT2_UDN5165	AGGCCAGACA	XT2_UDN7165	CGAAGGTTAA	0.62	2.39
312	FOR20210610_446_24732	TT	XT4_UDN5343	ATTCATTGCA	XT4_UDN7343	CGGCGTAAGA	0.82	4.46
313	FOR20210610_446_24892	TT	XT2_UDN5186	CGCCATACCT	XT2_UDN7186	ACCAAGTTAC	0.86	6.55
314	FOR20210610_446_24896	TT	XT4_UDN5338	TGAACGCAAC	XT4_UDN7338	GTTGCAGTTG	0.65	2.78
315	FOR20210610_446_24937	TT	XT4_UDN5383	AATCCTTAGG	XT4_UDN7383	CAAGTTCATA	0.76	3.86
316	FOR20210610_446_24942	TT	XT4_UDN5363	AGAAGCCAAT	XT4_UDN7363	AGGCCAGACA	0.88	7.45
317	FOR20210610_446_24995	TT	XT4_UDN5377	ACGCTTGGAC	XT4_UDN7377	GTTGTACTCA	0.89	7.56
318	FOR20210610_451_24411	TT	XT4_UDN5325	TAGACAATCT	XT4_UDN7325	AAGCAGATAT	0.56	1.85
319	FOR20210610_451_24429	TT	XT3_UDN5276	CCTAGAGTAT	XT3_UDN7276	TCCTAGGAAG	0.8	3.89
320	FOR20210610_451_24486	TT	XT2_UDN5125	CTCGTGCGTT	XT2_UDN7125	TCCACGGCCT	0.83	4.83
321	FOR20210610_451_24541	TT	XT2_UDN5106	GAGCGCAATA	XT2_UDN7106	TTCTACAGAA	0.82	5.24
322	FOR20210610_451_24566	TT	XT4_UDN5346	TTCCGACATT	XT4_UDN7346	TTCCTCCTTA	0.6	1.95
323	FOR20210610_451_24591	TT	XT4_UDN5358	GCTCTCGTTG	XT4_UDN7358	AGGTGCGTAA	0.82	4.65
324	FOR20210610_451_24616	TT	XT3_UDN5283	TCTTGGCTAT	XT3_UDN7283	AGTGGTCAGG	0.84	5.24
325	FOR20210610_451_24676	TT	XT2_UDN5134	TCCAATTCTA	XT2_UDN7134	CATAACACCA	0.87	6.76
326	FOR20210610_451_24739	TT	XT4_UDN5307	TGCTGGACAT	XT4_UDN7307	GTGCTAGGTG	0.78	3.94
327	FOR20210610_451_24787	TT	XT4_UDN5292	CGGTGACACC	XT4_UDN7292	TGGCAATATT	0.78	3.87
328	FOR20210610_451_24925	TT	XT2_UDN5111	TGTTGTTCGT	XT2_UDN7111	CCTTGTTAAT	0.73	3.65
329	FOR20210610_451_24946	TT	XT2_UDN5146	ATTCCGCTAT	XT2_UDN7146	AATTGCTGCG	0.86	6.09
330	FOR20210610_451_24979	TT	XT2_UDN5135	TGAGACAGCG	XT2_UDN7135	ACAGAGGCCA	0.36	0.95
331	FOR20210610_451_24994	TT	XT2_UDN5143	TTCCAGGTAA	XT2_UDN7143	TTCATCCAAC	0.86	6.77
332	FOR20210610_451_25013	TT	XT3_UDN5255	CACGGATTAT	XT3_UDN7255	ACGAGACTGA	0.6	1.9
333	FOR20210804_447_17949	PT	XT1_UDN5069	TCTGTGTGGA	XT1_UDN7069	TGGAGTACTT	0.76	4.49
334	FOR20210804_447_17950	PT	XT1_UDN5077	CGTTGCTTAC	XT1_UDN7077	TCTGGTATCC	0.71	3.76
335	FOR20210804_447_17951	PT	XT1_UDN5085	CATGAGTACT	XT1_UDN7085	TGGTACCTAA	0.75	5.1

ID	sample	CS	adapter_p5	tag_p5_5to3	adapter_p7	tag_p7_5to3	cov	depth
336	FOR20210804_447_17960	PT	XT1_UDN5070	GGAATTCCAA	XT1_UDN7070	GTATTGACGT	0.74	4.61
337	FOR20210804_447_17961	PT	XT1_UDN5078	TGACTACATA	XT1_UDN7078	CATTAGTGCG	0.48	1.68
338	FOR20210804_447_17962	PT	XT1_UDN5086	ACGTCAATAC	XT1_UDN7086	TTGGAATTCC	0.68	3.64
339	FOR20210804_447_17972	PT	XT1_UDN5071	AAGCGCGCTT	XT1_UDN7071	CTTGTACACC	0.68	3.81
340	FOR20210804_447_17973	PT	XT1_UDN5079	CGGCCTCGTT	XT1_UDN7079	ACGGTCAGGA	0.68	3.5
341	FOR20210804_447_17983	PT	XT1_UDN5072	TGAGCGTTGT	XT1_UDN7072	ACACAGGTGG	0.69	4.09
342	FOR20210804_447_17984	PT	XT1_UDN5080	CAAGCATCCG	XT1_UDN7080	GGCAAGCCAG	0.68	3.71
343	FOR20210804_448_17902	PT	XT1_UDN5041	GACAACTGAA	XT1_UDN7041	ACTCGGCAAT	0.72	3.3
344	FOR20210804_448_17903	PT	XT1_UDN5049	CTGGTACACG	XT1_UDN7049	AGTGTTGCAC	0.58	2.33
345	FOR20210804_448_17904	PT	XT1_UDN5057	CGTCGACTGG	XT1_UDN7057	TCTATCCTAA	0.48	1.52
346	FOR20210804_448_17912	PT	XT1_UDN5042	AGTGGTCAGG	XT1_UDN7042	GTCTAATGGC	0.6	2.29
347	FOR20210804_448_17913	PT	XT1_UDN5050	TCAACGTGTA	XT1_UDN7050	GACACCATGT	0.62	2.75
348	FOR20210804_448_17914	PT	XT1_UDN5058	TACTAGTCAA	XT1_UDN7058	CTCGCTTCGG	0.62	3.15
349	FOR20210804_448_17924	PT	XT1_UDN5043	TTCTATGGTT	XT1_UDN7043	CCATCTCGCC	0.63	2.58
350	FOR20210804_448_17925	PT	XT1_UDN5051	ACTGTTGTGA	XT1_UDN7051	CCTGTCTGTC	0.67	3.1
351	FOR20210804_448_17935	PT	XT1_UDN5044	AATCCGGCCA	XT1_UDN7044	CTGCGAGCCA	0.58	2.18
352	FOR20210804_448_17936	PT	XT1_UDN5052	GTGCGTCCTT	XT1_UDN7052	TGATGTAAGA	0.74	4.03
353	FOR20210804_450_17943	PT	XT1_UDN5013	ATCACGAAGG	XT1_UDN7013	CTTGCCATTA	0.67	3.14
354	FOR20210804_450_17944	PT	XT1_UDN5021	GGCCTGTCCT	XT1_UDN7021	ATGGTTGACT	0.63	2.68
355	FOR20210804_450_17954	PT	XT1_UDN5014	CGGCTCTACT	XT1_UDN7014	GAAGCGGCAC	0.72	4.18
356	FOR20210804_450_17955	PT	XT1_UDN5022	CTGTGTTAGG	XT1_UDN7022	TATTGCGCTC	0.69	3.67
357	FOR20210804_450_17963	PT	XT1_UDN5094	GATTAAGGTG	XT1_UDN7094	TCATAGATTG	0.74	4.66
358	FOR20210804_450_17964	PT	XT1_UDN5007	TGGAACAGTA	XT1_UDN7007	CTAGTGCTCT	0.65	3.54
359	FOR20210804_450_17965	PT	XT1_UDN5015	GAATGCACGA	XT1_UDN7015	TCCATTGCCG	0.58	2.21
360	FOR20210804_450_17966	PT	XT1_UDN5023	TAAGGAACGT	XT1_UDN7023	ACGCCTTGTT	0.73	4.41
361	FOR20210804_450_17976	PT	XT1_UDN5008	CCTTGTTAAT	XT1_UDN7008	GATCAAGGCA	0.67	3.82
362	FOR20210804_450_17977	PT	XT1_UDN5024	CTAACTGTAA	XT1_UDN7024	TTCTACATAC	0.73	5.14
363	FOR20210818_447_24318	PT	XT4_UDN5323	GGTAAGATAA	XT4_UDN7323	ACTAGAACTT	0.82	5.06
364	FOR20210818_447_24375	PT	XT2_UDN5115	CGGCTAACGT	XT2_UDN7115	AGAGCTGCCT	0.84	6.69
365	FOR20210818_447_24404	PT	XT2_UDN5101	TGGTGCCTGG	XT2_UDN7101	ACATGCATAT	0.76	4.26
366	FOR20210818_447_24526	PT	XT4_UDN5297	ACTAGAACTT	XT4_UDN7297	TCTAGTCTTC	0.86	5.65
367	FOR20210818_447_24633	PT	XT2_UDN5161	CTTCAGTTAC	XT2_UDN7161	AGATGGAATT	0.85	5.93
368	FOR20210818_447_24635	PT	XT4_UDN5305	TCTCCATTGA	XT4_UDN7305	TGTGATGTAT	0.86	7.46
369	FOR20210818_447_24649	PT	XT2_UDN5150	TATAGATTCG	XT2_UDN7150	GTATTCTCTA	0.75	4.33
370	FOR20210818_447_24678	PT	XT3_UDN5268	TACGAATCTT	XT3_UDN7268	AGACTCTCTT	0.75	3.34
371	FOR20210818_447_24844	PT	XT2_UDN5164	AGGATAAGTT	XT2_UDN7164	CTGGTACACG	0.82	4.87
372	FOR20210818_448_24327	PT	XT2_UDN5170	TGGTACTGAT	XT2_UDN7170	TTGGTGGTGC	0.81	4.91
373	FOR20210818_448_24707	PT	XT3_UDN5216	TGCTAACTAT	XT3_UDN7216	AGCGCTTCGG	0.6	2.98
374	FOR20210818_448_24740	PT	XT2_UDN5136	ACGCTAATTA	XT2_UDN7136	TGGTGCCTGG	0.74	4.65
375	FOR20210818_448_24762	PT	XT2_UDN5190	TTAGGATAGA	XT2_UDN7190	GATTAAGGTG	0.71	3.79
376	FOR20210818_448_24879	PT	XT4_UDN5308	GATGGTATCG	XT4_UDN7308	CATACTTGAA	0.73	3.87
377	FOR20210818_448_25065	PT	XT2_UDN5100	GCACTACAAC	XT2_UDN7100	TCTCCATTGA	0.73	3.21
378	FOR20210818_450_24380	PT	XT3_UDN5233	CAGGTGTTCA	XT3_UDN7233	AAGTCTTGTA	0.76	3.48
379	FOR20210818_450_24382	PT	XT1_UDN5083	AGACACATTA	XT1_UDN7083	TATGCCTTAC	0.86	6.47
380	FOR20210818_450_24470	PT	XT2_UDN5118	TAACCGCCGA	XT2_UDN7118	GAACAAGTAT	0.82	4.76
381	FOR20210818_450_24491	PT	XT3_UDN5288	AACTAACGTT	XT3_UDN7288	TAATCGGTAC	0.71	3.03
382	FOR20210818_450_24626	PT	XT3_UDN5236	CTCTAAGTAG	XT3_UDN7236	TGCTAACTAT	0.85	6.21
383	FOR20210818_450_24680	PT	XT2_UDN5169	CAATCTATGA	XT2_UDN7169	CCAACAACAT	0.88	8.42
384	FOR20210818_450_24847	PT	XT2_UDN5137	TATATTCGAG	XT2_UDN7137	TAGGAACCGG	0.73	3.27
385	FOR20210818_450_24938	PT	XT3_UDN5244	TCCGCAAGGC	XT3_UDN7244	TTGAGAGGAT	0.87	6.69
386	FOR20210818_450_24945	PT	XT3_UDN5224	ATCGCATATG	XT3_UDN7224	ACAATAGAGT	0.85	6.25
387	FOR20210818_450_24987	PT	XT4_UDN5311	ATACACAGAG	XT4_UDN7311	TGCACGAGAA	0.86	6.62
388	KAL20210519_461_24343	TT	XT4_UDN5362	TCACAGATCG	XT4_UDN7362	TTGGCCAGGT	0.63	2.43
389	KAL20210519_461_24457	TT	XT4_UDN5333	CAGCCGATTG	XT4_UDN7333	CAAGGTGACG	0.73	3.05
390	KAL20210519_461_24704	TT	XT3_UDN5233	CAGGTGTTCA	XT3_UDN7233	AAGTCTTGTA	0.9	10.72
391	KAL20210519_461_24726	TT	XT1_UDN5036	TGGCAATATT	XT1_UDN7036	ACCGGCCGTA	0.83	5.28
392	KAL20210519_461_24827	TT	XT4_UDN5330	TAATACGGAG	XT4_UDN7330	GAAGCTAGCT	0.83	5.14

ID	sample	CS	adapter_p5	tag_p5_5to3	adapter_p7	tag_p7_5to3	cov	depth
393	KAL20210519_461_24831	TT	XT2_UDN5110	TGGTTAAGAA	XT2_UDN7110	ACGCTAATTA	0.89	8.4
394	KAL20210519_461_24832	TT	XT4_UDN5326	CAATGCTGAA	XT4_UDN7326	GCCAGATCCA	0.83	5.64
395	KAL20210519_461_24887	TT	XT4_UDN5347	TGGCACGACC	XT4_UDN7347	TGTGTAAGCT	0.81	5.01
396	KAL20210519_461_25050	TT	XT4_UDN5313	ACCACGTCTG	XT4_UDN7313	GTGCTATTAA	0.85	5.65
397	KAL20210519_461_25060	TT	XT4_UDN5380	TCCGATAGAG	XT4_UDN7380	TCCATAATCC	0.65	2.43
398	KAL20210519_482_24321	PT	XT4_UDN5327	GTCACGGTGT	XT4_UDN7327	TTGGATTCAA	0.72	3.74
399	KAL20210519_482_24383	PT	XT2_UDN5168	TTGCTTGTAT	XT2_UDN7168	GATTGTCATA	0.83	5.85
400	KAL20210519_482_24436	PT	XT2_UDN5148	TAGGAACCGG	XT2_UDN7148	CTATACGCGG	0.4	1.07
401	KAL20210519_482_24451	PT	XT3_UDN5213	TATACCATGG	XT3_UDN7213	GATATCCTAA	0.79	4.68
402	KAL20210519_482_24505	PT	XT3_UDN5238	TCTACATACC	XT3_UDN7238	TGGTTAAGAA	0.69	2.77
403	KAL20210519_482_24506	PT	XT1_UDN5092	ACATACTTCC	XT1_UDN7092	GCGTTGGTAT	0.77	4.55
404	KAL20210519_482_24623	PT	XT3_UDN5201	GATCTCTGGA	XT3_UDN7201	GAACTCGGTT	0.58	1.98
405	KAL20210519_482_24836	PT	XT3_UDN5236	CTCTAAGTAG	XT3_UDN7236	TGCTAACTAT	0.77	3.69
406	KAL20210519_482_25018	PT	XT2_UDN5128	AACCGCATCG	XT2_UDN7128	CGGTTATTAG	0.76	3.94
407	KAL20210519_483_24417	PT	XT4_UDN5289	TAGAGTTGGA	XT4_UDN7289	GGAATTGTTC	0.81	4.53
408	KAL20210519_483_24481	PT	XT4_UDN5362	TCACAGATCG	XT4_UDN7362	TTGGCCAGGT	0.58	1.92
409	KAL20210519_483_24549	PT	XT4_UDN5345	AATTCGATCG	XT4_UDN7345	ACTAATTCAG	0.87	6.39
410	KAL20210519_483_24599	PT	XT3_UDN5210	GTTATATGGC	XT3_UDN7210	TATAGTAGCT	0.67	2.7
411	KAL20210519_483_24615	PT	XT3_UDN5239	CACGTTAGGC	XT3_UDN7239	ACTCTTCCTT	0.67	2.58
412	KAL20210519_483_24757	PT	XT3_UDN5197	CTGACCGGCA	XT3_UDN7197	ACAACCAGGA	0.85	6.66
413	KAL20210519_483_24874	PT	XT3_UDN5231	AGTCAACCAT	XT3_UDN7231	ACGGCCGTCA	0.74	3.62
414	KAL20210519_483_24955	PT	XT2_UDN5105	TGTGATGTAT	XT2_UDN7105	ACGATTGCTG	0.73	3.9
415	KAL20210519_483_25029	PT	XT3_UDN5203	TTAATAGACC	XT3_UDN7203	GTAGCATACT	0.47	1.29
416	KAL20210519_483_25036	PT	XT3_UDN5202	CAGGCGCCAT	XT3_UDN7202	AGTTATCACA	0.59	2.26
417	KAL20210519_488_24322	PT	XT4_UDN5376	AGTATACGGA	XT4_UDN7376	GGACGTCTTG	0.85	6.65
418	KAL20210519_488_24379	PT	XT1_UDN5068	AACCTAGCAC	XT1_UDN7068	CACGGAACAA	0.79	4.3
419	KAL20210519_488_24403	PT	XT2_UDN5119	CTCCGTGCTG	XT2_UDN7119	AATTGGCGGA	0.64	2.27
420	KAL20210519_488_24544	PT	XT3_UDN5230	GCTACTATCT	XT3_UDN7230	CAGATACCAC	0.66	3.01
421	KAL20210519_488_24553	PT	XT3_UDN5221	CCATGTGTAG	XT3_UDN7221	TACCGAACTA	0.67	2.68
422	KAL20210519_488_24575	PT	XT2_UDN5156	GGCGCCAATT	XT2_UDN7156	TGAATATTGC	0.65	2.63
423	KAL20210519_488_24772	PT	XT3_UDN5229	CACGTCCACC	XT3_UDN7229	AGTTAAGAGC	0.63	2.3
424	KAL20210519_488_25010	PT	XT2_UDN5123	TAGGTTCTCT	XT2_UDN7123	TTCCTGTACG	0.66	2.35
425	KAL20210520_461_24344	TT	XT2_UDN5178	CTGGATATGT	XT2_UDN7178	CGCGACGATC	0.74	3.69
426	KAL20210520_461_24346	TT	XT4_UDN5381	CTCAAGGCCG	XT4_UDN7381	ATGAGAACCA	0.5	1.62
427	KAL20210520_461_24507	TT	XT1_UDN5064	AACTGATACT	XT1_UDN7064	TGGCGCGAAC	0.81	4.39
428	KAL20210520_461_24513	TT	XT3_UDN5257	CTCTGTATAC	XT3_UDN7257	AGATTGTTAC	0.78	3.92
429	KAL20210520_461_24538	TT	XT3_UDN5250	GGATCCGCAT	XT3_UDN7250	CCGAACGTTG	0.78	3.81
430	KAL20210520_461_24594	TT	XT1_UDN5078	TGACTACATA	XT1_UDN7078	CATTAGTGCG	0.83	4.67
431	KAL20210520_461_24662	TT	XT2_UDN5133	ATACCTGGAT	XT2_UDN7133	CGGCCTCGTT	0.74	3.84
432	KAL20210520_461_24666	TT	XT3_UDN5277	TAGGAAGACT	XT3_UDN7277	TCACAGATCG	0.75	3.97
433	KAL20210520_461_24716	TT	XT2_UDN5166	CCTTGAACGG	XT2_UDN7166	ATCGCATATG	0.88	7.53
434	KAL20210520_461_24756	TT	XT3_UDN5208	GTATCGGCCG	XT3_UDN7208	TTATCCGATC	0.81	4.5
435	KAL20210520_461_24776	TT	XT4_UDN5341	CGTATAATCA	XT4_UDN7341	ATCGTCGCTC	0.87	7.12
436	KAL20210520_461_24812	TT	XT4_UDN5293	GCGTTGGTAT	XT4_UDN7293	GAATGCACGA	0.82	4.24
437	KAL20210520_461_24843	TT	XT2_UDN5109	GTAGCCATCA	XT2_UDN7109	TAATTCTACC	0.88	8.07
438	KAL20210520_461_24897	TT	XT2_UDN5152	ATTCCTATTG	XT2_UDN7152	GACCGCTGTG	0.85	6.27
439	KAL20210520_461_24922	TT	XT3_UDN5226	GACCGGAGAT	XT3_UDN7226	AGATATGGCG	0.79	3.97
440	KAL20210520_461_24951	TT	XT4_UDN5365	AACATCTAGT	XT4_UDN7365	ATTACTCACC	0.79	3.61
441	KAL20210520_461_25000	TT	XT3_UDN5196	TTGACCAATG	XT3_UDN7196	CCATCCACGC	0.83	4.59
442	KAL20210520_461_25006	TT	XT4_UDN5351	TCTGGAATTA	XT4_UDN7351	TGAAGTAAGT	0.85	5.15
443	KAL20210520_461_25049	TT	XT2_UDN5134	TCCAATTCTA	XT2_UDN7134	CATAACACCA	0.76	3.45
444	KAL20210520_461_25061	TT	XT4_UDN5354	CGTTCGGAAC	XT4_UDN7354	ACACAGCGCT	0.79	4.07
445	KAL20210614_379_24520	TT	XT3_UDN5194	GTGTTACCGG	XT3_UDN7194	CTTGGCCTCG	0.78	4.35
446	KAL20210614_379_24672	TT	XT1_UDN5059	ATAGACCGTT	XT1_UDN7059	CTGTTGGTCC	0.77	3.88
447	KAL20210614_379_24677	TT	XT2_UDN5179	GGCCAATAAG	XT2_UDN7179	GCCTCGGATA	0.86	6.09
448	KAL20210614_379_24684	TT	XT2_UDN5174	TCTCTAGATT	XT2_UDN7174	GACGAACAAT	0.54	2.04
449	KAL20210614_379_24721	TT	XT4_UDN5353	GACTATATGT	XT4_UDN7353	GTGTGATATC	0.87	6.5

ID	sample	CS	adapter_p5	tag_p5_5to3	adapter_p7	tag_p7_5to3	cov	depth
450	KAL20210614_379_24775	TT	XT3_UDN5285	GTTCCGCAGG	XT3_UDN7285	CTCGTTATCA	0.81	5.88
451	KAL20210614_379_24882	TT	XT4_UDN5324	AACGAGCCAG	XT4_UDN7324	CACCTCTTGG	0.76	3.47
452	KAL20210614_379_24904	TT	XT3_UDN5250	GGATCCGCAT	XT3_UDN7250	CCGAACGTTG	0.71	3.38
453	KAL20210614_379_24958	TT	XT3_UDN5232	CGAGGCGGTA	XT3_UDN7232	GTAATTACTG	0.62	2.93
454	KAL20210614_381_24337	TT	XT3_UDN5258	GCAACAGGTG	XT3_UDN7258	TCTACCGCTG	0.74	3.32
455	KAL20210614_381_24345	TT	XT2_UDN5169	CAATCTATGA	XT2_UDN7169	CCAACAACAT	0.54	1.92
456	KAL20210614_381_24442	TT	XT4_UDN5348	GCCACAGCAC	XT4_UDN7348	GTGGCTGGTT	0.6	1.95
457	KAL20210614_381_24465	TT	XT4_UDN5384	GGTGGAATAC	XT4_UDN7384	CTTAACCACT	0.78	3.44
458	KAL20210614_381_24498	TT	XT3_UDN5232	CGAGGCGGTA	XT3_UDN7232	GTAATTACTG	0.78	3.59
459	KAL20210614_381_24503	TT	XT4_UDN5297	ACTAGAACTT	XT4_UDN7297	TCTAGTCTTC	0.88	7.94
460	KAL20210614_381_24567	TT	XT4_UDN5305	TCTCCATTGA	XT4_UDN7305	TGTGATGTAT	0.4	1.09
461	KAL20210614_381_24781	TT	XT3_UDN5246	TACGCACGTA	XT3_UDN7246	AGTGGATAAT	0.82	4.82
462	KAL20210614_381_24794	TT	XT4_UDN5326	CAATGCTGAA	XT4_UDN7326	GCCAGATCCA	0.47	1.49
463	KAL20210614_381_24868	TT	XT1_UDN5013	ATCACGAAGG	XT1_UDN7013	CTTGCCATTA	0.66	2.62
464	KAL20210614_382_24340	TT	XT4_UDN5334	TCTCACGCGT	XT4_UDN7334	ACCAGTCATT	0.64	2.69
465	KAL20210614_382_24341	TT	XT4_UDN5337	AAGGCCTTGG	XT4_UDN7337	CCACCTTACA	0.53	1.82
466	KAL20210614_382_24347	TT	XT3_UDN5243	GACATTGTCA	XT3_UDN7243	GAACCATGAA	0.49	1.4
467	KAL20210614_382_24483	TT	XT3_UDN5269	TAGGAGCGCA	XT3_UDN7269	GCTCGCCTAC	0.71	2.76
468	KAL20210614_382_24611	TT	XT4_UDN5380	TCCGATAGAG	XT4_UDN7380	TCCATAATCC	0.86	6.37
469	KAL20210614_382_24667	TT	XT4_UDN5352	ATTAGTGGAG	XT4_UDN7352	ACGGAATGCG	0.82	4.53
470	KAL20210614_382_24786	TT	XT2_UDN5175	CGCGAGCCTA	XT2_UDN7175	CCACTGGTCC	0.5	1.68
471	KAL20210614_382_24837	TT	XT1_UDN5026	AATAGAGCAA	XT1_UDN7026	GGTTGCGAGG	0.86	6.66
473	KAL20210812_482_24399	PT	XT3_UDN5243	GACATTGTCA	XT3_UDN7243	GAACCATGAA	0.85	6.17
474	KAL20210812_482_24406	PT	XT2_UDN5120	CATTCCAGCT	XT2_UDN7120	GGCCTGTCCT	0.61	2.15
475	KAL20210812_482_24427	PT	XT3_UDN5234	GACAGACAGG	XT3_UDN7234	GTCACCACAG	0.58	1.88
476	KAL20210812_482_24580	PT	XT4_UDN5320	CTAGGCAAGG	XT4_UDN7320	ATGCCGACCG	0.84	5.53
477	KAL20210812_482_24648	PT	XT3_UDN5205	AACGCCAGAG	XT3_UDN7205	AGTCCGAGGA	0.83	5.18
478	KAL20210812_482_24724	PT	XT2_UDN5180	ATTACTCACC	XT2_UDN7180	TGAGACAGCG	0.67	2.82
479	KAL20210812_482_24977	PT	XT3_UDN5217	TCAGTTAATG	XT3_UDN7217	GTTGATAGTG	0.77	3.63
480	KAL20210812_482_24999	PT	XT3_UDN5266	GTATAGCTGT	XT3_UDN7266	GATATAACAG	0.57	1.81
481	KAL20210812_482_25062	PT	XT1_UDN5041	GACAACTGAA	XT1_UDN7041	ACTCGGCAAT	0.83	5.33
482	KAL20210812_483_24377	PT	XT1_UDN5052	GTGCGTCCTT	XT1_UDN7052	TGATGTAAGA	0.84	5.13
483	KAL20210812_483_24450	PT	XT3_UDN5229	CACGTCCACC	XT3_UDN7229	AGTTAAGAGC	0.84	5.9
484	KAL20210812_483_24514	PT	XT2_UDN5143	TTCCAGGTAA	XT2_UDN7143	TTCATCCAAC	0.84	6.84
485	KAL20210812_483_24593	PT	XT1_UDN5073	ATCATAGGCT	XT1_UDN7073	CCTGCGGAAC	0.89	7.31
486	KAL20210812_483_24625	PT	XT1_UDN5002	CTACAAGATA	XT1_UDN7002	AGGTCAGATA	0.88	7.43
487	KAL20210812_483_24733	PT	XT3_UDN5206	CGTAATTAAC	XT3_UDN7206	ACAGTTCCAG	0.79	3.92
488	KAL20210812_483_24805	PT	XT3_UDN5262	TCCTAGGAAG	XT3_UDN7262	CATGGTCTAA	0.76	3.55
489	KAL20210812_483_24910	PT	XT4_UDN5317	CACTTAATCT	XT4_UDN7317	GGAGATTAGT	0.87	7.36
490	KAL20210812_483_24920	PT	XT4_UDN5293	GCGTTGGTAT	XT4_UDN7293	GAATGCACGA	0.27	0.86
491	KAL20210812_488_24466	PT	XT4_UDN5369	ACACAATATC	XT4_UDN7369	GTTATATGGC	0.77	3.73
492	KAL20210812_488_24484	PT	XT3_UDN5275	ATTAATACGC	XT3_UDN7275	CCGCTTAGCT	0.76	3.65
493	KAL20210812_488_24499	PT	XT3_UDN5218	GTGACCTTGA	XT3_UDN7218	AATAGAGCAA	0.78	3.8
494	KAL20210812_488_24560	PT	XT4_UDN5350	AGCTCTCAAG	XT4_UDN7350	CACGTTAGGC	0.75	3.2
495	KAL20210812_488_24725	PT	XT3_UDN5222	GAGTCTCTCC	XT3_UDN7222	GTAGTAATAG	0.8	4.21
496	KAL20210812_488_24736	PT	XT3_UDN5228	TTACTTCCTC	XT3_UDN7228	TAGCGCTAGT	0.88	7.96
497	KAL20210812_488_24745	PT	XT4_UDN5370	TGGAGGTAAT	XT4_UDN7370	CACTCGCACT	0.87	6.86
498	KAL20210812_488_24754	PT	XT3_UDN5274	CTAGTCCGGA	XT3_UDN7274	AATAGGCCTC	0.71	3
499	KAL20210812_488_24800	PT	XT4_UDN5357	TGGTATACCA	XT4_UDN7357	TGCGTCCAGG	0.88	6.87
500	KAL20210812_488_24944	PT	XT4_UDN5318	TACTCTGTTA	XT4_UDN7318	TACTAACACA	0.76	3.53
501	SUM20210514_432_24522	PT	XT2_UDN5149	AGCGGTGGAC	XT2_UDN7149	ATTCAGAATC	0.85	6.36
502	SUM20210514_432_24670	PT	XT2_UDN5128	AACCGCATCG	XT2_UDN7128	CGGTTATTAG	0.83	5.83
503	SUM20210514_432_24686	PT	XT3_UDN5224	ATCGCATATG	XT3_UDN7224	ACAATAGAGT	0.81	4.27
504	SUM20210514_432_24779	PT	XT3_UDN5259	GGTAACGCAG	XT3_UDN7259	AACGGTATGA	0.71	2.78
505	SUM20210514_432_24915	PT	XT3_UDN5195	AGATTGTTAC	XT3_UDN7195	GTCTCGTGAA	0.55	1.98
506	SUM20210514_432_25031	PT	XT1_UDN5050	TCAACGTGTA	XT1_UDN7050	GACACCATGT	0.77	3.69
507	SUM20210514_433_24398	PT	XT1_UDN5090	GAACCATGAA	XT1_UDN7090	ACTTCAAGCG	0.77	3.83

ID	sample	CS	adapter_p5	tag_p5_5to3	adapter_p7	tag_p7_5to3	cov	depth
508	SUM20210514_433_24413	PT	XT3_UDN5271	AGTTAAGAGC	XT3_UDN7271	GAGACATAAT	0.78	4.35
509	SUM20210514_433_24539	PT	XT2_UDN5178	CTGGATATGT	XT2_UDN7178	CGCGACGATC	0.81	5.07
510	SUM20210514_433_24755	PT	XT3_UDN5207	ACGAGACTGA	XT3_UDN7207	CCGCATATTC	0.58	1.93
511	SUM20210514_433_24824	PT	XT4_UDN5306	CGAGACCAAG	XT4_UDN7306	AACATACCTA	0.87	8.18
512	SUM20210514_442_24384	PT	XT1_UDN5057	CGTCGACTGG	XT1_UDN7057	TCTATCCTAA	0.76	3.55
513	SUM20210514_442_24561	PT	XT3_UDN5263	TTGAGCCTAA	XT3_UDN7263	ATACTGTGTG	0.77	3.72
514	SUM20210514_442_24597	PT	XT4_UDN5296	CTTATACCTG	XT4_UDN7296	TCCTTCATAG	0.71	3.02
515	SUM20210514_442_24609	PT	XT3_UDN5255	CACGGATTAT	XT3_UDN7255	ACGAGACTGA	0.74	3.67
516	SUM20210514_442_24780	PT	XT3_UDN5285	GTTCCGCAGG	XT3_UDN7285	CTCGTTATCA	0.73	3.22
517	SUM20210514_442_24921	PT	XT4_UDN5303	TTGAAGCAGA	XT4_UDN7303	GAGTCTCTCC	0.57	1.86
518	SUM20210514_457_24443	PT	XT3_UDN5249	CAGCGGACAA	XT3_UDN7249	TGCTGGACAT	0.65	2.62
519	SUM20210514_457_24462	PT	XT2_UDN5124	TATGGCTCGA	XT2_UDN7124	GGTAACGCAG	0.82	4.48
520	SUM20210514_457_24571	PT	XT2_UDN5107	ATCTTACTGT	XT2_UDN7107	TATTGCGTTC	0.85	5.89
521	SUM20210514_457_24681	PT	XT1_UDN5019	GGTTGCCTCT	XT1_UDN7019	CCATCATTAG	0.87	6.93
522	SUM20210514_457_24700	PT	XT3_UDN5244	TCCGCAAGGC	XT3_UDN7244	TTGAGAGGAT	0.58	1.92
523	SUM20210514_457_24928	PT	XT3_UDN5252	ACATAACGGA	XT3_UDN7252	TAGTCACAAC	0.55	2.24
524	SUM20210514_462_24316	PT	XT4_UDN5295	CCAGAAGTAA	XT4_UDN7295	ATTCATTGCA	0.86	6.36
525	SUM20210514_462_24531	PT	XT2_UDN5184	CAACGTCAGC	XT2_UDN7184	ATACCTGGAT	0.83	5.54
526	SUM20210514_462_24603	PT	XT4_UDN5340	CACCGAGGAA	XT4_UDN7340	GACTGGTTGC	0.84	4.75
527	SUM20210514_462_24811	PT	XT3_UDN5198	TCTCATCAAT	XT3_UDN7198	AGCAGAATTA	0.62	2.74
528	SUM20210514_462_25015	PT	XT2_UDN5163	CGCGCCTAGA	XT2_UDN7163	GATAACAAGT	0.83	5.69
529	SUM20210514_462_25019	PT	XT4_UDN5300	CTCACACAAG	XT4_UDN7300	GAAGCGGACC	0.82	5.03
530	SUM20210607_457_17945	PT	XT1_UDN5037	GATCACCGCG	XT1_UDN7037	TGTAATCGAC	0.68	3.38
531	SUM20210607_457_17946	PT	XT1_UDN5045	CCATAAGGTT	XT1_UDN7045	CGTTATTCTA	0.73	4.39
532	SUM20210607_457_17956	PT	XT1_UDN5030	CTTATGGAAT	XT1_UDN7030	CCACCAGGCA	0.69	3.5
533	SUM20210607_457_17957	PT	XT1_UDN5038	TACCATCCGT	XT1_UDN7038	GTGCAGACAG	0.67	3.73
534	SUM20210607_457_17958	PT	XT1_UDN5046	ATCTCTACCA	XT1_UDN7046	AGATCCATTA	0.66	2.89
535	SUM20210607_457_17967	PT	XT1_UDN5031	GCTTACGGAC	XT1_UDN7031	GTGACACGCA	0.65	2.93
536	SUM20210607_457_17968	PT	XT1_UDN5039	GCTGTAGGAA	XT1_UDN7039	CAATCGGCTG	0.65	3.18
537	SUM20210607_457_17978	PT	XT1_UDN5032	GAACATACGG	XT1_UDN7032	ACAGTGTATG	0.72	3.6
538	SUM20210607_457_17979	PT	XT1_UDN5040	CGCACTAATG	XT1_UDN7040	TATGTAGTCA	0.66	2.68
539	SUM20210607_457_17986	PT	XT1_UDN5096	CACATCGGTG	XT1_UDN7096	CCTCCGTCCA	0.56	2.18
540	SUM20210607_462_17905	PT	XT1_UDN5065	GTAAGGCATA	XT1_UDN7065	TAATGTGTCT	0.61	2.67
541	SUM20210607_462_17906	PT	XT1_UDN5073	ATCATAGGCT	XT1_UDN7073	CCTGCGGAAC	0.6	2.58
542	SUM20210607_462_17915	PT	XT1_UDN5066	AATTGCTGCG	XT1_UDN7066	ATACCAACGC	0.74	4.22
543	SUM20210607_462_17916	PT	XT1_UDN5074	TGTTAGAAGG	XT1_UDN7074	TTCATAAGGT	0.49	1.72
544	SUM20210607_462_17926	PT	XT1_UDN5059	ATAGACCGTT	XT1_UDN7059	CTGTTGGTCC	0.66	3.16
545	SUM20210607_462_17927	PT	XT1_UDN5075	GATGGATGTA	XT1_UDN7075	CTCTGCAGCG	0.66	2.96
546	SUM20210607_462_17937	PT	XT1_UDN5060	ACAGTTCCAG	XT1_UDN7060	TTACCTGGAA	0.76	4.38
547	SUM20210607_462_17938	PT	XT1_UDN5068	AACCTAGCAC	XT1_UDN7068	CACGGAACAA	0.63	2.9
548	SUM20210607_462_17939	PT	XT1_UDN5076	ACGGCCGTCA	XT1_UDN7076	CTGACTCTAC	0.65	2.81
549	SUM20210608_65027_A_24747	LT	XT4_UDN5371	CCTTCACGTA	XT4_UDN7371	ACCGGCTCAG	0.7	3.55
550	SUM20210608_65028_A_24564	LT	XT4_UDN5320	CTAGGCAAGG	XT4_UDN7320	ATGCCGACCG	0.84	5.32
551	SUM20210608_65029_A_24409	LT	XT4_UDN5312	TCTCGGACGA	XT4_UDN7312	ACTTCCTAGC	0.81	4.97
552	SUM20210608_65034_B_25057	LT	XT2_UDN5139	ACAATAGAGT	XT2_UDN7139	ATAGGTATTC	0.89	8.54
553	SUM20210608_66022_A_24829	LT	XT1_UDN5023	TAAGGAACGT	XT1_UDN7023	ACGCCTTGTT	0.77	4.04
554	SUM20210608_66053_A_24473	LT	XT4_UDN5300	CTCACACAAG	XT4_UDN7300	GAAGCGGACC	0.85	5.38
555	SUM20210608_432_17897	PT	XT1_UDN5001	TCGTGGAGCG	XT1_UDN7001	GAACTGAGCG	0.17	0.5
556	SUM20210608_432_17898	PT	XT1_UDN5009	GTTGATAGTG	XT1_UDN7009	GACTGAGTAG	0.42	1.3
557	SUM20210608_432_17899	PT	XT1_UDN5017	TCGGCAGCAA	XT1_UDN7017	GAGAATGGTT	0.6	2.4
558	SUM20210608_432_17908	PT	XT1_UDN5002	CTACAAGATA	XT1_UDN7002	AGGTCAGATA	0.58	2.66
559	SUM20210608_432_17909	PT	XT1_UDN5010	ACCAGCGACA	XT1_UDN7010	AGTCAGACGA	0.67	3.38
560	SUM20210608_432_17919	PT	XT1_UDN5003	TATAGTAGCT	XT1_UDN7003	CGTCTCATAT	0.62	3.05
561	SUM20210608_432_17920	PT	XT1_UDN5011	CATACACTGT	XT1_UDN7011	CCGTATGTTC	0.64	3.17
562	SUM20210608_432_17930	PT	XT1_UDN5004	TGCCTGGTGG	XT1_UDN7004	ATTCCATAAG	0.58	2.23
563	SUM20210608_432_17931	PT	XT1_UDN5012	GTGTGGCGCT	XT1_UDN7012	GAGTCATAGG	0.65	3.02
564	SUM20210608_432_17985	PT	XT1_UDN5088	ATCCGTAAGT	XT1_UDN7088	GGAGCGTGTA	0.68	3.73

ID	sample	CS	adapter_p5	tag_p5_5to3	adapter_p7	tag_p7_5to3	cov	depth
565	SUM20210625_65023_B_24533	LT	XT2_UDN5144	CATGTAGAGG	XT2_UDN7144	CAATTGGATT	0.84	5.8
566	SUM20210625_65023_B_24862	LT	XT1_UDN5033	GTCGATTACA	XT1_UDN7033	TGATTATACG	0.82	4.86
567	SUM20210625_65023_C_24397	LT	XT2_UDN5137	TATATTCGAG	XT2_UDN7137	TAGGAACCGG	0.86	6.21
568	SUM20210625_65023_C_24547	LT	XT2_UDN5190	TTAGGATAGA	XT2_UDN7190	GATTAAGGTG	0.89	8.57
569	SUM20210625_65023_C_24885	LT	XT1_UDN5008	CCTTGTTAAT	XT1_UDN7008	GATCAAGGCA	0.85	6.06
570	SUM20210625_65023_D_24493	LT	XT1_UDN5069	TCTGTGTGGA	XT1_UDN7069	TGGAGTACTT	0.71	2.93
571	SUM20210625_65023_E_24438	LT	XT2_UDN5110	TGGTTAAGAA	XT2_UDN7110	ACGCTAATTA	0.9	10
572	SUM20210625_65023_E_24532	LT	XT2_UDN5171	TTCATCCAAC	XT2_UDN7171	GCGAACGCCT	0.87	7.31
573	SUM20210625_65023_E_25056	LT	XT1_UDN5001	TCGTGGAGCG	XT1_UDN7001	GAACTGAGCG	0.78	3.83
574	SUM20210625_66001_A_25026	LT	XT2_UDN5127	TGTTCGCATT	XT2_UDN7127	CAACGTCAGC	0.67	2.72
575	SUM20210625_66004_A_24642	LT	XT1_UDN5011	CATACACTGT	XT1_UDN7011	CCGTATGTTC	0.89	8.4
576	SUM20210625_66006_A_24804	LT	XT4_UDN5338	TGAACGCAAC	XT4_UDN7338	GTTGCAGTTG	0.83	4.66
577	SUM20210625_66006_A_24916	LT	XT2_UDN5120	CATTCCAGCT	XT2_UDN7120	GGCCTGTCCT	0.6	2.33
578	SUM20210625_66006_A_25002	LT	XT2_UDN5126	CCAGTTGGCA	XT2_UDN7126	GATACCTCCT	0.84	6.01
579	SUM20210625_66006_B_24751	LT	XT3_UDN5251	TGCGGTGTTG	XT3_UDN7251	ATTAATACGC	0.86	6.36
580	SUM20210625_66006_B_24993	LT	XT2_UDN5132	ACGATTGCTG	XT2_UDN7132	AACGTTACAT	0.85	6.68
581	SUM20210625_66006_C_24540	LT	XT2_UDN5174	TCTCTAGATT	XT2_UDN7174	GACGAACAAT	0.9	9.12
582	SUM20210625_66006_D_24508	LT	XT2_UDN5106	GAGCGCAATA	XT2_UDN7106	TTCTACAGAA	0.74	3.67
583	SUM20210625_66006_E_25009	LT	XT2_UDN5183	GGCGAATTCT	XT2_UDN7183	GCTGTAGGAA	0.84	5.61
584	SUM20210625_66007_B_24586	LT	XT3_UDN5199	GGACCAACAG	XT3_UDN7199	CAGTCGTGCG	0.81	4.78
585	SUM20210625_66011_A_24619	LT	XT4_UDN5339	CCGCTTAGCT	XT4_UDN7339	TCACTCATGT	0.88	7.5
586	SUM20210625_66021_A_24637	LT	XT2_UDN5182	TTGTCAACTT	XT2_UDN7182	TCCAAGAATT	0.49	1.64
587	SUM20210625_66048_A_24627	LT	XT4_UDN5309	GGCTTAATTG	XT4_UDN7309	CTTGTCTTAA	0.85	5.99
588	SUM20210625_66061_A_24437	LT	XT2_UDN5145	GATTGTCATA	XT2_UDN7145	GGCCATCATA	0.86	6.11
589	SUM20210625_66062_A_24475	LT	XT3_UDN5266	GTATAGCTGT	XT3_UDN7266	GATATAACAG	0.77	3.73
590	SUM20210707_65002_A_24441	LT	XT4_UDN5344	TCATGTCCTG	XT4_UDN7344	GACATCAGCT	0.6	2.03
591	SUM20210707_65020_A_24608	LT	XT3_UDN5254	CATTCAACAA	XT3_UDN7254	CAAGATGCTT	0.77	3.36
592	SUM20210707_66008_A_24778	LT	XT4_UDN5316	AGTCCGAGGA	XT4_UDN7316	TGTACCGAAT	0.74	4.18
593	SUM20210707_66018_A_25032	LT	XT1_UDN5031	GCTTACGGAC	XT1_UDN7031	GTGACACGCA	0.76	3.62
594	SUM20210707_66018_A_25033	LT	XT2_UDN5102	TCCACGGCCT	XT2_UDN7102	CAGGCGCCAT	0.74	3.51
595	SUM20210707_66018_B_24391	LT	XT1_UDN5043	TTCTATGGTT	XT1_UDN7043	CCATCTCGCC	0.78	4.41
597	SUM20210707_66018_C_24431	LT	XT2_UDN5191	CGCAATCTAG	XT2_UDN7191	CAACATTCAA	0.82	5.27
598	SUM20210707_66018_C_24570	LT	XT1_UDN5009	GTTGATAGTG	XT1_UDN7009	GACTGAGTAG	0.62	2.42
599	SUM20210707_66018_C_24908	LT	XT1_UDN5089	CGTGTATCTT	XT1_UDN7089	GTCCGTAAGC	0.83	4.79
600	SUM20210707_66020_A_24435	LT	XT4_UDN5302	CGGATTATAT	XT4_UDN7302	GGACCTCAAT	0.54	1.67
601	SUM20210707_66057_A_24687	LT	XT2_UDN5167	CACCACCTAC	XT2_UDN7167	ATCATAGGCT	0.85	6.29
602	SUM20210707_66059_A_24352	LT	XT2_UDN5117	CCGAACGTTG	XT2_UDN7117	TCGGTCACGG	0.86	6.4
603	SUM20210720_65002_A_24894	LT	XT4_UDN5365	AACATCTAGT	XT4_UDN7365	ATTACTCACC	0.86	6.33
604	SUM20210720_65004_A_24582	LT	XT4_UDN5363	AGAAGCCAAT	XT4_UDN7363	AGGCCAGACA	0.35	0.9
605	SUM20210720_65006_A_24487	LT	XT4_UDN5322	TCATCCTCTT	XT4_UDN7322	TGCCTACGAG	0.79	3.91
606	SUM20210720_65007_A_24705	LT	XT4_UDN5328	GGTGTACAAG	XT4_UDN7328	ACTAGCCGTG	0.83	4.96
607	SUM20210720_65020_A_24792	LT	XT4_UDN5348	GCCACAGCAC	XT4_UDN7348	GTGGCTGGTT	0.87	6.98
608	SUM20210720_65023_B_24501	LT	XT1_UDN5079	CGGCCTCGTT	XT1_UDN7079	ACGGTCAGGA	0.61	1.9
609	SUM20210720_65023_B_24971	LT	XT2_UDN5133	ATACCTGGAT	XT2_UDN7133	CGGCCTCGTT	0.42	1.36
610	SUM20210720_65027_A_24966	LT	XT3_UDN5277	TAGGAAGACT	XT3_UDN7277	TCACAGATCG	0.59	1.87
611	SUM20210720_65029_A_24889	LT	XT4_UDN5321	CCTCTTCGAA	XT4_UDN7321	CTAGCGTCGA	0.69	3.08
612	SUM20210720_65044_A_25021	LT	XT3_UDN5235	TGTACTTGTT	XT3_UDN7235	ATTAGTGGAG	0.4	1.29
613	SUM20210720_65049_A_24708	LT	XT2_UDN5188	CAACCGGAGG	XT2_UDN7188	GGCAGTAGCA	0.75	3.65
614	SUM20210720_65050_A_24734	LT	XT1_UDN5006	GTCCACTTGT	XT1_UDN7006	AACATCGCGC	0.88	7.95
615	SUM20210720_65051_A_25016	LT	XT2_UDN5130	AGTGCCACTG	XT2_UDN7130	TCTTGGCTAT	0.86	6.49
616	SUM20210720_66001_A_24372	LT	XT3_UDN5275	ATTAATACGC	XT3_UDN7275	CCGCTTAGCT	0.69	2.47
617	SUM20210720_66005_A_24479	LT	XT4_UDN5332	ATTGACACAT	XT4_UDN7332	GCAACAGGTG	0.86	6.26
619	SUM20210720_66006_B_24395	LT	XT2_UDN5175	CGCGAGCCTA	XT2_UDN7175	CCACTGGTCC	0.83	5.02
622	SUM20210720_66007_A_25044	LT	XT4_UDN5371	CCTTCACGTA	XT4_UDN7371	ACCGGCTCAG	0.77	3.89
623	SUM20210720_66008_A_24460	LT	XT2_UDN5176	GATAAGCTCT	XT2_UDN7176	TGTTAGAAGG	0.63	4.72
624	SUM20210720_66011_A_24808	LT	XT4_UDN5368	GCCAGATCCA	XT4_UDN7368	GCAGGCTGGA	0.85	5.61
625	SUM20210720_66015_A_24661	LT	XT4_UDN5359	GTCTCGTGAA	XT4_UDN7359	GCAGCAACGA	0.38	1.04

ID	sample	CS	adapter_p5	tag_p5_5to3	adapter_p7	tag_p7_5to3	cov	depth
626	SUM20210720_66018_A_24421	LT	XT3_UDN5231	AGTCAACCAT	XT3_UDN7231	ACGGCCGTCA	0.69	2.76
627	SUM20210720_66018_B_24502	LT	XT2_UDN5098	TTAAGTTGTG	XT2_UDN7098	GAATTGAGTG	0.85	6.45
628	SUM20210720_66018_C_24712	LT	XT3_UDN5219	ACATGCATAT	XT3_UDN7219	CTAACTGTAA	0.8	5.42
629	SUM20210720_66020_A_24414	LT	XT2_UDN5148	TAGGAACCGG	XT2_UDN7148	CTATACGCGG	0.81	4.78
630	SUM20210720_66021_A_24853	LT	XT1_UDN5035	AAGTTGGTGA	XT1_UDN7035	GGTAACTCGC	0.85	5.78
631	SUM20210720_66023_A_24926	LT	XT4_UDN5373	GTTGCAGTTG	XT4_UDN7373	TGAACGCAAC	0.85	5.81
633	SUM20210720_66048_A_24816	LT	XT4_UDN5291	ACTCTACAGG	XT4_UDN7291	GACTTAGAAG	0.84	5.44
634	SUM20210720_66059_A_24569	LT	XT2_UDN5126	CCAGTTGGCA	XT2_UDN7126	GATACCTCCT	0.82	5.24
635	SUM20210720_66079_A_24802	LT	XT4_UDN5358	GCTCTCGTTG	XT4_UDN7358	AGGTGCGTAA	0.77	3.79
636	SUM20210802_65039_A_24688	LT	XT2_UDN5127	TGTTCGCATT	XT2_UDN7127	CAACGTCAGC	0.88	8.43
637	SUM20210802_66011_A_24743	LT	XT2_UDN5141	GATAACAAGT	XT2_UDN7141	GGCCAATAAG	0.83	5.53
638	SUM20210802_432_24315	PT	XT4_UDN5375	TCTCAGTACA	XT4_UDN7375	ACTGAATAGA	0.88	7.3
639	SUM20210802_432_24471	PT	XT4_UDN5369	ACACAATATC	XT4_UDN7369	GTTATATGGC	0.79	4.76
640	SUM20210802_432_24645	PT	XT2_UDN5163	CGCGCCTAGA	XT2_UDN7163	GATAACAAGT	0.62	2.17
641	SUM20210802_432_24744	PT	XT3_UDN5211	GCCTGCCATG	XT3_UDN7211	ACTCCGGTGG	0.67	2.85
642	SUM20210802_432_24934	PT	XT4_UDN5296	CTTATACCTG	XT4_UDN7296	TCCTTCATAG	0.76	3.2
643	SUM20210802_432_24964	PT	XT4_UDN5372	CTATACGCGG	XT4_UDN7372	ATAGACCGTT	0.83	5.59
644	SUM20210802_433_24434	PT	XT4_UDN5323	GGTAAGATAA	XT4_UDN7323	ACTAGAACTT	0.3	0.83
645	SUM20210802_433_24459	PT	XT3_UDN5248	CTGCACTTCA	XT3_UDN7248	GATCTCTGGA	0.47	1.42
646	SUM20210802_433_24876	PT	XT3_UDN5286	ACCAAGTTAC	XT3_UDN7286	CCTTACTATG	0.74	3.23
647	SUM20210802_433_24959	PT	XT2_UDN5122	ACCACACGGT	XT2_UDN7122	ACACAATATC	0.78	4.57
648	SUM20210802_433_25042	PT	XT4_UDN5345	AATTCGATCG	XT4_UDN7345	ACTAATTCAG	0.86	6.59
649	SUM20210802_442_24536	PT	XT2_UDN5145	GATTGTCATA	XT2_UDN7145	GGCCATCATA	0.58	2.15
650	SUM20210802_442_24717	PT	XT3_UDN5284	ACGGAATGCG	XT3_UDN7284	CATTCCAGCT	0.78	3.69
651	SUM20210802_442_24768	PT	XT4_UDN5340	CACCGAGGAA	XT4_UDN7340	GACTGGTTGC	0.83	5.22
652	SUM20210802_442_24788	PT	XT3_UDN5247	CGCTTGAAGT	XT3_UDN7247	GGCACGCCAT	0.87	7.24
653	SUM20210802_442_24960	PT	XT3_UDN5248	CTGCACTTCA	XT3_UDN7248	GATCTCTGGA	0.63	2.59
654	SUM20210802_457_24385	PT	XT2_UDN5099	CGGACAGTGA	XT2_UDN7099	GCGTGTGAGA	0.82	5.03
655	SUM20210802_457_24579	PT	XT3_UDN5242	GTAGAGTCAG	XT3_UDN7242	AGGTTGCAGG	0.77	4.35
656	SUM20210802_457_24646	PT	XT3_UDN5219	ACATGCATAT	XT3_UDN7219	CTAACTGTAA	0.42	1.15
657	SUM20210802_457_24764	PT	XT3_UDN5213	TATACCATGG	XT3_UDN7213	GATATCCTAA	0.81	4.04
658	SUM20210802_457_24963	PT	XT2_UDN5116	TCCAAGAATT	XT2_UDN7116	CTTCGCCGAT	0.89	7.91
659	SUM20210802_457_25014	PT	XT4_UDN5377	ACGCTTGGAC	XT4_UDN7377	GTTGTACTCA	0.76	3.48
660	SUM20210802_462_24576	PT	XT4_UDN5290	AGAGCACTAG	XT4_UDN7290	CCGGACCACA	0.69	2.58
661	SUM20210802_462_24614	PT	XT2_UDN5185	TCTTACATCA	XT2_UDN7185	GTTGGACCGT	0.68	2.98
662	SUM20210802_462_24653	PT	XT4_UDN5366	CCTTACTATG	XT4_UDN7366	GCGCAGAGTA	0.6	2.44
663	SUM20210802_462_24655	PT	XT3_UDN5194	GTGTTACCGG	XT3_UDN7194	CTTGGCCTCG	0.79	4.04
664	SUM20210802_462_24671	PT	XT3_UDN5196	TTGACCAATG	XT3_UDN7196	CCATCCACGC	0.75	4.23
665	SUM20210802_462_24685	PT	XT2_UDN5101	TGGTGCCTGG	XT2_UDN7101	ACATGCATAT	0.79	4.59
666	SUM20210804_462_17974	PT	XT1_UDN5087	GATACCTCCT	XT1_UDN7087	CCTCTACATG	0.63	3.19
667	SUM20210810_65023_A_24703	LT	XT1_UDN5072	TGAGCGTTGT	XT1_UDN7072	ACACAGGTGG	0.83	5.77
668	SUM20210825_65033_A_25037	LT	XT3_UDN5198	TCTCATCAAT	XT3_UDN7198	AGCAGAATTA	0.7	2.94
669	SUM20210825_65037_B_24807	LT	XT2_UDN5130	AGTGCCACTG	XT2_UDN7130	TCTTGGCTAT	0.85	6.13
670	SUM20210825_65039_B_24478	LT	XT2_UDN5132	ACGATTGCTG	XT2_UDN7132	AACGTTACAT	0.4	1.22
671	SUM20210825_65049_A_24490	LT	XT4_UDN5356	TACCACAATG	XT4_UDN7356	CAAGGCTATC	0.75	3.51
672	SUM20210825_65051_A_24864	LT	XT4_UDN5303	TTGAAGCAGA	XT4_UDN7303	GAGTCTCTCC	0.84	5.69
673	SUM20210825_65060_B_24863	LT	XT2_UDN5122	ACCACACGGT	XT2_UDN7122	ACACAATATC	0.79	4.52
674	SUM20210825_66007_A_24613	LT	XT4_UDN5331	CGAAGACGCA	XT4_UDN7331	ACAAGGATTG	0.8	4.58
675	SUM20210825_66008_A_24367	LT	XT3_UDN5202	CAGGCGCCAT	XT3_UDN7202	AGTTATCACA	0.77	3.6
676	SUM20210825_66019_A_24902	LT	XT4_UDN5329	AGGTTGCAGG	XT4_UDN7329	CGGCAAGCTC	0.87	7.3
677	SUM20210825_66021_A_24584	LT	XT3_UDN5272	TCGCGTATAA	XT3_UDN7272	AGCTGTTATA	0.76	3.7
678	SUM20210825_66033_A_24463	LT	XT4_UDN5355	TCGATACTAG	XT4_UDN7355	AGCGCGGTGA	0.81	5.27
679	SUM20210825_66045_A_24523	LT	XT2_UDN5129	CGAAGGTTAA	XT2_UDN7129	CGCGCCTAGA	0.78	4.4
680	SUM20210825_66048_A_24750	LT	XT1_UDN5004	TGCCTGGTGG	XT1_UDN7004	ATTCCATAAG	0.68	3.36
681	SUM20210825_66050_A_24729	LT	XT4_UDN5350	AGCTCTCAAG	XT4_UDN7350	CACGTTAGGC	0.8	4.47
682	SUM20210825_66051_A_24356	LT	XT2_UDN5165	AGGCCAGACA	XT2_UDN7165	CGAAGGTTAA	0.66	3.18
683	SUM20210825_66057_A_24826	LT	XT4_UDN5325	TAGACAATCT	XT4_UDN7325	AAGCAGATAT	0.59	2.68

ID	sample	CS	adapter_p5	tag_p5_5to3	adapter_p7	tag_p7_5to3	cov	depth
684	SUM20210825_66059_A_24859	LT	XT3_UDN5247	CGCTTGAAGT	XT3_UDN7247	GGCACGCCAT	0.38	1.04
685	SUM20210826_66062_A_24806	LT	XT3_UDN5281	AACGTTACAT	XT3_UDN7281	CAGAGTGATA	0.79	4.25
686	SUM20210922_65023_A_24530	LT	XT3_UDN5264	CCACCTGTGT	XT3_UDN7264	GCCGACAAGA	0.78	3.74
687	SUM20210922_65023_B_25064	LT	XT1_UDN5062	GCAAGTCTCA	XT1_UDN7062	AACACTGTTA	0.88	7.44
688	SUM20210922_65027_A_24858	LT	XT3_UDN5264	CCACCTGTGT	XT3_UDN7264	GCCGACAAGA	0.62	2.85
689	SUM20210922_65030_A_24355	LT	XT4_UDN5374	TTATGCGCCT	XT4_UDN7374	GTGGTTGAAG	0.85	6.36
690	SUM20210922_65037_B_24878	LT	XT2_UDN5109	GTAGCCATCA	XT2_UDN7109	TAATTCTACC	0.75	3.24
691	SUM20210922_65044_A_24370	LT	XT1_UDN5044	AATCCGGCCA	XT1_UDN7044	CTGCGAGCCA	0.75	3.28
692	SUM20210922_65050_A_24534	LT	XT4_UDN5331	CGAAGACGCA	XT4_UDN7331	ACAAGGATTG	0.86	6.05
693	SUM20210922_65051_A_24595	LT	XT4_UDN5367	GTGGCGAGAC	XT4_UDN7367	CGCCATACCT	0.86	6.27
694	SUM20210922_66006_A_24359	LT	XT3_UDN5223	GCTATGCGCA	XT3_UDN7223	GGTTATGCTA	0.77	3.44
695	SUM20210922_66006_B_24563	LT	XT1_UDN5017	TCGGCAGCAA	XT1_UDN7017	GAGAATGGTT	0.75	3.67
696	SUM20210922_66006_B_24854	LT	XT1_UDN5088	ATCCGTAAGT	XT1_UDN7088	GGAGCGTGTA	0.88	8.02
697	SUM20210922_66007_A_24848	LT	XT4_UDN5364	ACTGCAGCCG	XT4_UDN7364	AGCATTAACT	0.84	5.73
698	SUM20210922_66011_A_25058	LT	XT4_UDN5351	TCTGGAATTA	XT4_UDN7351	TGAAGTAAGT	0.86	6.79
699	SUM20210922_66015_A_24748	LT	XT4_UDN5336	TCGAATGGAA	XT4_UDN7336	TTGAGCCTAA	0.81	4.73
700	SUM20210922_66017_A_24357	LT	XT2_UDN5155	GCGCAGAGTA	XT2_UDN7155	ATTCCGCTAT	0.85	6.16
701	SUM20210922_66018_A_25008	LT	XT3_UDN5241	CTTCGAAGGA	XT3_UDN7241	TCCGCGTTCA	0.78	3.74
702	SUM20210922_66018_B_24893	LT	XT1_UDN5027	TCAATCCATT	XT1_UDN7027	TAAGCATCCA	0.85	6.15
703	SUM20210922_66033_A_24913	LT	XT2_UDN5121	GGTTATGCTA	XT2_UDN7121	TAGGTTCTCT	0.88	7.01
704	SUM20210922_66045_A_24358	LT	XT3_UDN5287	TGGCTCGCAG	XT3_UDN7287	AGAAGCCAAT	0.77	3.58
705	SUM20210922_66048_A_24884	LT	XT2_UDN5116	TCCAAGAATT	XT2_UDN7116	CTTCGCCGAT	0.85	6.23

Appendix B: Supplementary plots

(1) Quality Effects

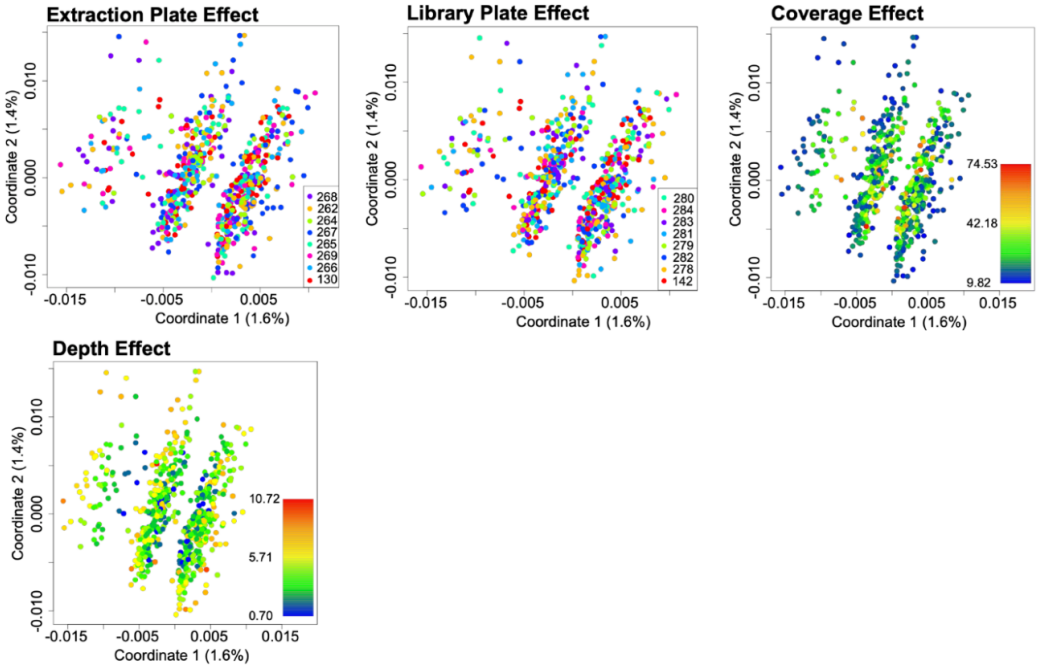

(2) Spatial Effects

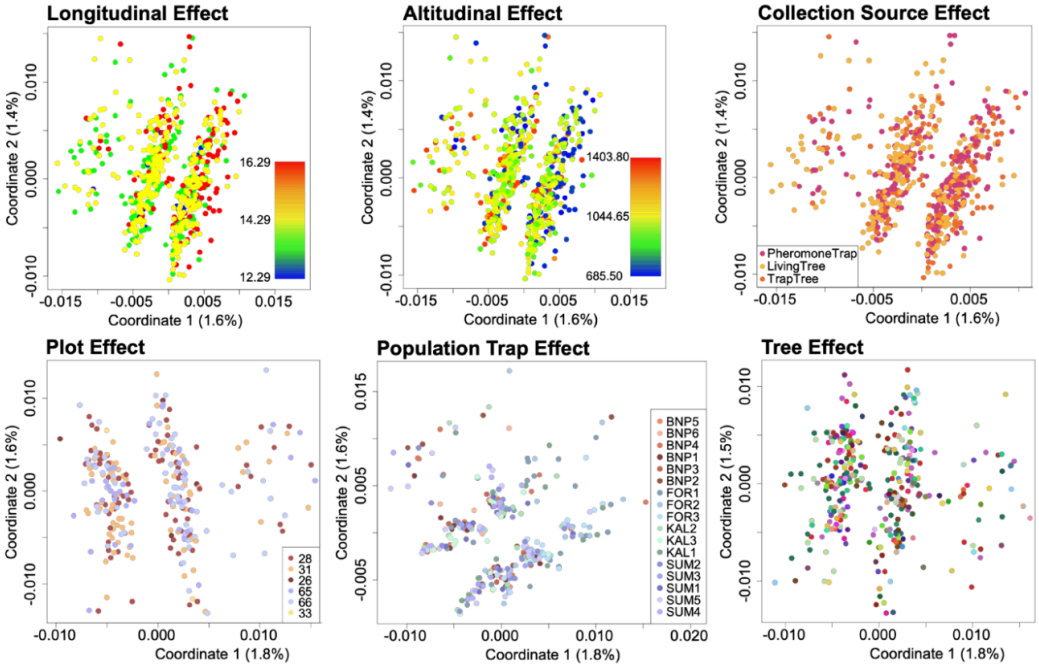

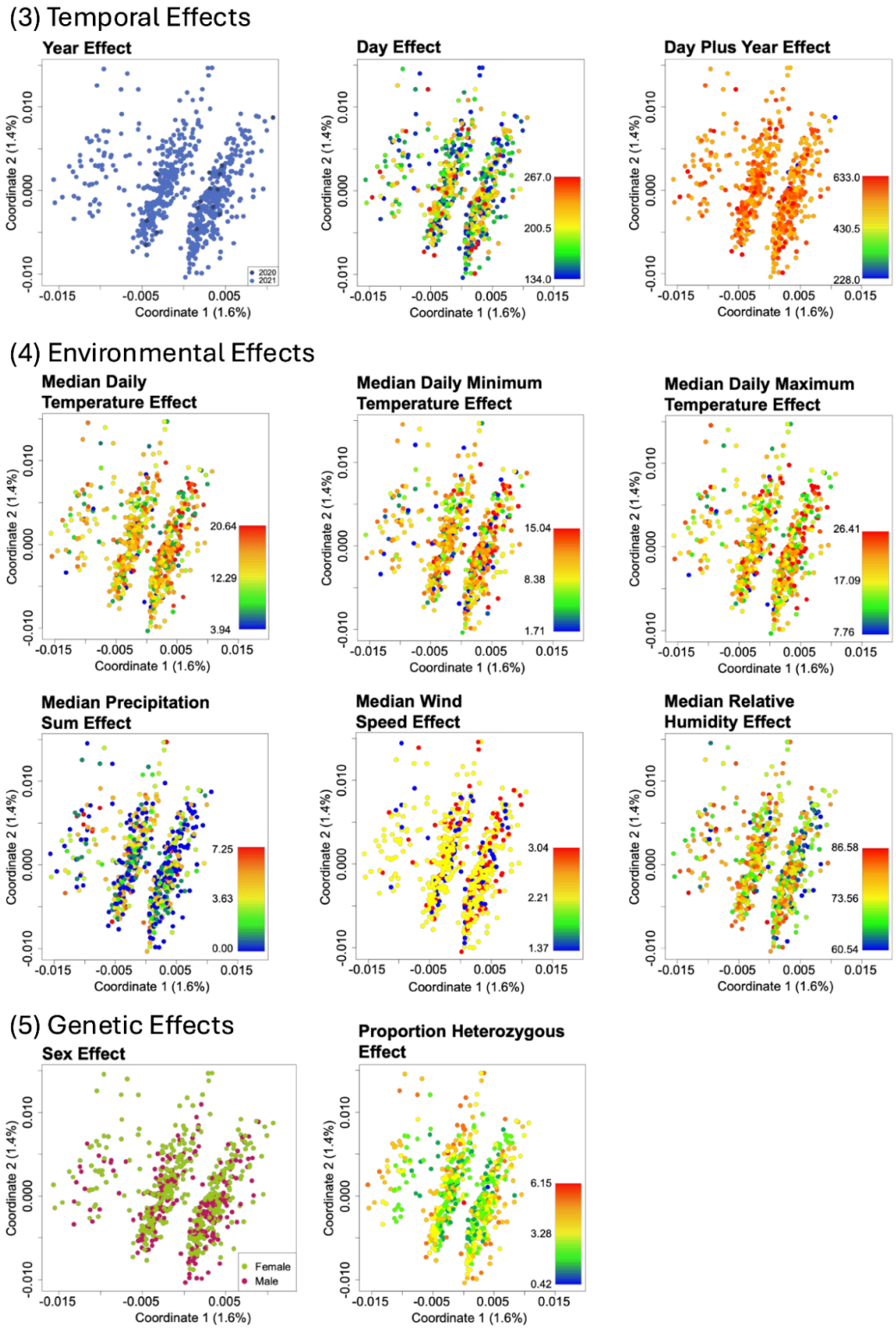

Figure 15: Supplementary MDS plots. MDS plots colored by (1) quality effects, (2) spatial effects, (3) temporal effects, (4) environmental effects, and (5) genetic effects. These illustrate that none of these factors account for the observed clustering (see main text, Figure 11).